

Lawrence Berkeley National Laboratory

Recent Work

Title

ELECTRON SPIN RESONANCE STUDIES OF RADICALS PRODUCED BY ELECTROLYSIS

Permalink

<https://escholarship.org/uc/item/540003c1>

Author

Talcott, Carolyn L.

Publication Date

1967-09-01

9.2

University of California Ernest O. Lawrence Radiation Laboratory

ELECTRON SPIN RESONANCE STUDIES OF RADICALS PRODUCED BY ELECTROLYSIS

Carolyn L. Talcott
(Ph.D. Thesis)

September 1967

RECEIVED
LAWRENCE
RADIATION LABORATORY
NOV 6 1967
LIBRARY AND
DOCUMENTS SECTION

TWO-WEEK LOAN COPY
*This is a Library Circulating Copy
which may be borrowed for two weeks.
For a personal retention copy, call
Tech. Info. Division, Ext. 5545*

Berkeley, California

UCRL-17743
9.2

DISCLAIMER

This document was prepared as an account of work sponsored by the United States Government. While this document is believed to contain correct information, neither the United States Government nor any agency thereof, nor the Regents of the University of California, nor any of their employees, makes any warranty, express or implied, or assumes any legal responsibility for the accuracy, completeness, or usefulness of any information, apparatus, product, or process disclosed, or represents that its use would not infringe privately owned rights. Reference herein to any specific commercial product, process, or service by its trade name, trademark, manufacturer, or otherwise, does not necessarily constitute or imply its endorsement, recommendation, or favoring by the United States Government or any agency thereof, or the Regents of the University of California. The views and opinions of authors expressed herein do not necessarily state or reflect those of the United States Government or any agency thereof or the Regents of the University of California.

UCRL-17743

UNIVERSITY OF CALIFORNIA
Lawrence Radiation Laboratory
Berkeley, California
AEC Contract No. W-7405-eng-48

ELECTRON SPIN RESONANCE STUDIES
OF RADICALS PRODUCED BY ELECTROLYSIS

Carolyn L. Talcott

(Ph. D. Thesis)

September 1967

TABLE OF CONTENTS (continued)

| | | |
|-------|--|----|
| 3. | NITROGEN HYPERFINE COUPLING PARAMETERS | 38 |
| 3.1 | Experimental Determination of the Parameters Q_N^N and Q_{CN}^N | 38 |
| 3.2 | Theoretical Calculation of the Parameters Q_N^N , Q_{CN}^N , and Q_{ON}^N | 42 |
| 3.2.1 | Format for the Calculation | 45 |
| 3.2.2 | Evaluation of Two Electron Integrals | 48 |
| 3.2.3 | Evaluation of Excitation Energies and of Magnitudes of Wave Functions at the Nitrogen Nucleus | 56 |
| 3.2.4 | Discussion of Results | 58 |
| 4. | THEORETICAL SPIN DENSITIES FOR NITROGEN HETEROCYCLIC RADICAL ANIONS | 62 |
| 4.1 | Unsubstituted Nitrogen Heterocyclics | 62 |
| 4.1.1 | McLachlan and Restricted Self Consistent Field Approximations | 62 |
| 4.1.2 | Unrestricted Self Consistent Field Approximation | 66 |
| 4.2 | Methyl-Substituted Pyridines: McLachlan Approximation... | 71 |
| 4.3 | Pyridine N-Oxides | 76 |
| 4.3.1 | McLachlan Approximation | 76 |
| 4.3.2 | Unrestricted Self Consistent Field Approximation | 78 |
| 4.3.3 | Theoretical Spin Densities Used to Determine the Parameters Q_N^N (Pyridine N-oxide) and Q_{ON}^N ... | 80 |
| 5. | NITROSOBENZENES | 83 |
| 5.1 | Assignment of the Ortho Proton Coupling Constants | 83 |
| 5.2 | Theoretical Spin Densities: McLachlan Approximation Including Alpha and Beta Effects | 87 |

TABLE OF CONTENTS (continued)

| | | |
|-----------------------|--|-----|
| 5.3 | The "Q" Effect: Theoretical Calculation of the Parameters Q_{CH}^H and Q_{OH}^H | 91 |
| 5.4 | Theoretical Spin Densities: McLachlan Approximation Assuming "Q" Effect | 93 |
| 5.5 | Solvent Effects | 94 |
| 5.6 | Theoretical Spin Densities: Unrestricted Self Consistent Field Approximations | 97 |
| ACKNOWLEDGMENTS | | 101 |
| APPENDICES | | |
| I. | Atomic Orbitals Used in Calculation of Spin Polarization Parameters | 102 |
| II. | Program USCFMO | 103 |
| III. | USCF Calculation of Spin Densities in the Pyridine- N-Oxide Radical Anion: Parameter Variation | 113 |
| IV. | McLachlan Approximate Spin Density for Nitrosobenzene Type Radical Anions: Parameter Variations | 115 |
| REFERENCES | | 118 |

ELECTRON SPIN RESONANCE STUDIES
OF RADICALS PRODUCED BY ELECTROLYSIS

Carolyn L. Talcott

Inorganic Materials Research Division, Lawrence Radiation Laboratory,
and Department of Chemistry,
University of California, Berkeley, California

ABSTRACT

The ESR spectra of the radical anions of pyridine, pyrimidine, and pyrazine in liquid ammonia were measured. The coupling constants obtained from these spectra allowed values of the quantities Q_N^N , Q_{CN}^N , and Q_{CH}^H to be determined without relying on calculated spin densities. The values found are: $Q_N^N = +27.3$ gauss, $Q_{CN}^N = -1.7$ gauss, and $Q_{CH}^H = -24.5$ gauss. Theoretical values for the parameters Q_N^N (pyridine, pyridine N-oxide, nitrosobenzene, and nitrobenzene), Q_{CN}^N , and Q_{ON}^N were calculated using configuration interaction in an MO framework.

The ESR spectra of several substituted pyridine radical anions in liquid ammonia are reported including: 4-picoline, 3,5-lutidine, pyridine N-oxide, 4-picoline N-oxide, and 2,6-lutidine N-oxide. A series of McLachlan type spin density calculations were carried out in order to determine values of the variable parameters appropriate for the various N-heterocyclic radical anions. Excellent agreement between experimental and calculated spin densities was obtained for the simple heterocyclics and for the methyl substituted pyridines. The parameters for the N-oxides were not as well determined. USCF calculations including an approximate doublet state projection operator were carried out for the unsubstituted N-heterocyclics and for pyridine N-oxide with the resulting spin densities slightly better than those calculated using

the McLachlan approximation.

The ESR spectra of the radical anions of nitrosobenzene in DMSO and THF and of ortho- and para-nitrosotoluene and 2-nitroso-m-xylene in liquid ammonia were measured. The values of the coupling constants determined for the methyl nitrosobenzenes corresponded to an assignment of the larger ortho proton coupling constant observed in the nitrosobenzene radical anion to the proton nearest the oxygen atom. This is consistent with the assignment predicted by including non-neighbor resonance integrals in the MO calculations of spin density distribution. An additional mechanism whereby the $1s_N$ electrons are polarized by spin density in the oxygen pi orbital was proposed and values of the parameters Q_{OHC}^H and Q_{CHO}^H were estimated using simple three center MO's.

McLachlan calculations for the nitrosobenzene radical anions were carried out using several models to account for the effects of restricted rotation. In each case it was found that several sets of parameters gave equally good predictions of the ring position spin densities, with wide variation of the predicted distribution in the nitroso group. USCF calculations were carried out for the nitrosobenzene radical anion and similar ambiguity in the choice of parameters was found. In the absence of non-neighbor integrals, the USCF wave functions predict a larger spin density in the ortho carbon atom which is further from the oxygen atom.

1. INTRODUCTION

There is a relation that allows for the correlation of two important quantities present in various fields of scientific study. In the author's experience this relation seems quite valid. The important quantities are theory and experiment, related as: $f(T) \times f(E) \sim \text{constant}$. In this expression $f(T)$ is a function of the amenability of a system to examination by theoretical techniques and $f(E)$ is the corresponding function of the experimental study of that system. This constant seems in fact to be a function of time and presents a challenge both to experimentalists and theoreticians to contribute to its increasing magnitude.

In the literature, there is a large and growing number of organic radical ions that have been studied in solution by electron spin resonance (ESR) spectroscopy. The greater part of these studies tend to treat the more complicated systems arising from such compounds as the fused ring and highly substituted aromatic compounds. Interest in the quantum mechanical treatment of conjugated pi electron systems has been notable since the time of Hückel. The study of molecules containing unpaired electrons has received much additional attention since the advent of the ESR studies of these molecules, although rigorous theoretical treatment has been limited to small fragments such as the hypothetical $\cdot\text{CH}$ radical.

Areas of interest common to both the theoretician and experimentalist are increasing as can be seen in the studies of such simple radicals as $\cdot\text{OH}$, $\cdot\text{NH}_2$, and $\cdot\text{CH}_3$ as well as the more complicated systems including the allyl radical, butadiene radical anion, and the much studied benzene molecule and its radical anion. Many molecules remain, however, that have received much theoretical attention but have defied experimental efforts.

With the development of a technique for production of radical anions by continuous electrolysis in liquid ammonia,¹ many avenues for exploration were opened. This work was undertaken in order to test the limits and capabilities of the liquid ammonia system with the hope of extending the limits of mutual theoretical and experimental study.

1.1 Summary of ESR and Theoretical Studies of Pi Conjugated Organic Radicals²

In 1953 Weissman³ and his co-workers reported the ESR spectra of radical anions formed by treating a number of aromatic compounds with sodium in unreactive ether solvents such as dimethoxyethane (DME) and tetrahydrofuran (THF). The surprising feature of the spectra was the complicated hyperfine structure observed for the radical anions of naphthalene, anthracene, naphthacene, and some nitro substituted benzenes. The suggestion that the hyperfine structure was due to interactions of the unpaired electron with the protons attached to the aromatic rings in the hydrocarbon cases was supported by work of Fraenkel and Venkataraman⁴ on some aromatic quinones and their methyl and deuterium substituted derivatives. The radicals were produced by known chemical methods and the use of a flow system to observe less stable radicals was proposed.

Weissman and others^{5a,b} then reported the ESR spectra of a large number of aromatic radical anions including the benzene radical anion,^{5b} produced by alkali metal reduction in ethers. They also observed the ESR spectra of the radical cations of many of these compounds formed by dissolving the parent molecules in concentrated sulfuric acid.^{5a}

Austen, et al.⁶ observed ESR signals from frozen dimethylformamide (DMF) solutions of anthracene, benzophenone, and anthraquinone. The samples were taken during polarographic experiments and corresponded to

the products of one electron reductions. A technique for electrolysis within the microwave cavity of an ESR spectrometer was later developed by Maki and Geske.⁷ This technique allowed for continuous production of radical anions while ESR spectra were being recorded. The electrolyses were carried out under polarographic conditions to insure production of the desired species. The spectrum of the nitrobenzene radical anion in acetonitrile was obtained with the resolution of more hyperfine lines than observed in earlier experiments. Further ESR studies of nitrobenzene radical anions generated electrolytically in aqueous solutions were carried out by Adams et al.⁸ who noted, that in contrast to previous general agreement among reports of the observed hyperfine patterns for aromatic hydrocarbons, there was a significant change in the spacing between lines attributed to interaction of the unpaired electron with the nitrogen nucleus. This effect was attributed to the difference in solvents.

Fraenkel et al.⁹ pointed out that complete and rapid reduction of the parent molecule was important in the production of well resolved spectra. They developed a method for electrolysis outside of the spectrometer using a cell with a large cathode surface area and designed so that the paramagnetic solution could be transferred to the spectrometer. Again the use of a rapid flow system for very unstable radicals was suggested. Additional advantages of the external production of radical ions included the possibility of observing color changes and the production of gases in the solutions being studied. Many nitriles were studied by this external electrolysis technique.

Interest in the nitrogen heterocyclic compounds arose rather quickly with the nearly simultaneous publications of Carrington and dos Santos Vlega¹⁰ and of Ward¹¹ reporting radical anions produced by alkali metal

reduction of various single and multiring, poly-nitrogen heterocyclic compounds and by Hauser¹² reporting electrolytic reduction of phenazine and diproto phenazine. Much work in this area followed and the recent article by Henning¹³ includes a review.

Extension of electrolytic reduction to aromatic hydrocarbons was first reported by Fraenkel, et al.¹⁴ in their studies of azulene and methyl substituted azulenes. The technique for electrolytic production of radical anions in liquid ammonia was developed by Levy and Myers.¹ Electrolysis in liquid ammonia differs from that in most other solvents because reduction by the solvated electron is a homogeneous reaction in contrast to the heterogeneous reduction that occurs at a controlled potential electrode. The use of sodium and other alkali metals in liquid ammonia to produce radical anions has been reported.¹⁵ The mechanisms for alkali metal or electrolytic reductions are similar. Electrolysis is not complicated by the presence of alkali cations, allows for variation of the electron concentration at will during an experiment, and provides for continuous production of the species being studied. Other methods of radical production commonly employed in ESR studies include photolysis in alcohol solutions,¹⁶ generation of hydroxyl radicals in the solution to be studied by the reaction of Tl^{+++} and H_2O_2 ,¹⁷ and reduction in alkaline solution of sodium dithionite.¹⁸

After noting the variety in available data and the many possible ways for obtaining them, the question that remains is: How can these data be most meaningfully interpreted? The interactions of magnetic species with one another and with external static magnetic fields are described by the following spin Hamiltonian.

$$N_{\text{spin}} = N_Z + N_{\text{DP}} + N_{\text{FC}} \quad (1)$$

$$N_Z = g_e \beta_e S \cdot H - g_x \beta_x I \cdot H \quad (1a)$$

$$N_{\text{DP}} = -g_e \beta_e g_x \beta_x (I \cdot S / r^3 - 3(I \cdot r)(S \cdot r) / r^5) \quad (1b)$$

$$N_{\text{FC}} = \frac{8\pi}{3} g_e \beta_e g_x \beta_x \sum_k \delta(r_{\text{xk}}) S(k) \cdot I \quad (1c)$$

N_Z (1a) is the Zeeman interaction between a magnetic moment and a static magnetic field, N_{DP} (1b) is the dipolar interaction between two magnetic moments, and N_{FC} (1c) is the Fermi contact interaction. The δ function in (1c) when multiplied by $S_z(k)$ implies that there must be electron spin density at the nucleus in order for N_{FC} to be non-zero. (For a discussion of notation see Carrington,^{2a} and additional discussions of spin Hamiltonians may be found in references 19-24.

In the high field limit, this Hamiltonian when applied to a system containing one electron and one nucleus and having spherical symmetry gives rise to the following energy levels:

$$E(M_S, M_I) = (g_e \beta_e M_S - g_x \beta_x M_I) H_z + A M_S M_I,$$

where M_S and M_I are the z components of the electron and nuclear spins, respectively and A is a constant determined by the Fermi contact Ham (1c). ESR transitions are those in which $\Delta M_S = 1$ and $\Delta M_I = 0$ and therefore the frequencies of the transitions observed in an ESR experiment are

$$h\nu(M_I) = g_e \beta_e H_z + A M_I. \quad (2)$$

Weissman²⁵ has shown that for molecules tumbling rapidly in solution the average value of N_{DP} is zero. This gives the molecule an average

spherical symmetry and to a good approximation the ESR spectra of most radicals in solution can be described by equations similar to (2).

The surprise encountered when hyperfine structure was observed in the ESR spectra of aromatic radical anions was due to the rather well established approximation that the sigma and the pi electrons of an aromatic molecule can be treated independently and that only the pi electrons need be considered explicitly in the study of most electronic properties.²⁶ With the odd electron moving in a pi type orbital, the contact term was expected to be zero for nuclei in the pi nodal plane. Once it was determined that the coupling was indeed due to protons attached to the carbon atoms rings, various methods of accounting for spin density at the proton nuclei were tried. Out of plane vibrations were ruled out by the lack of dependence of the coupling constant on the hydrogen isotopes' atomic weights and also by calculations which predicted the coupling to be orders of magnitude smaller than that observed.⁴ Polarization of the σ electrons, which results when sigma and pi electrons are allowed to interact, will also give unpaired electron density at the nucleus. The two common methods available to treat this polarization are: configurational mixing of sigma excited states with the ground state wave function and the removal of the restriction that electrons of different spin must occupy equivalent spatial orbitals when the electronic Hamiltonian is solved. The latter method results in wave functions that are not eigenfunctions of S^2 . Both methods depend on the inclusion of the electron-electron repulsion term $1/r_{ij}$ between sigma and pi parts of the wave function. Although the advantages of a single determinant wave function are lost, the configuration interaction (CI) technique seems to be the better of the two. The fact that the unrestricted solutions of the

electronic Hamiltonian are not eigenfunctions of S^2 has been discussed by many authors.²⁷⁻²⁹

The proton hyperfine interaction has been extensively studied.^{28,30-32} McConnell^{30a} proposed that the proton coupling constant is proportional to the unpaired electron density in the pi atomic orbital of the carbon atom to which the proton is bonded. This proportionality is expressed by

$$A(H) = Q_{CH}^H \rho, \quad (3)$$

where the symbol Q_{XY}^Z is taken to mean the polarization of s electrons on atom Z due to interaction of electrons in the XY bond with electron density in the pi orbital of atom X. The proposal was based on CI treatment of a CH fragment and was further verified by more thorough studies.^{30b,32} Applying this technique in the valence-bond frame work, Karplus and Fraenkel³³ arrived at a similar expression, Eq. (4), for the hyperfine coupling of an sp^2 hybridized C-13 atom.

$$A(C^{13}) = (S^C + \sum_{X_1} Q_{CX_1}^C) \rho_C + \sum_{X_1} Q_{X_1C}^C \rho_{X_1} \quad (4)$$

In Eq. (4) the carbon atom is bonded to atoms X_1 ($1 = 1,2,3$) and the symbol S^C represents the polarization of the 1s electrons whereas the Q 's represent polarization of 2s electrons.

McConnell's equation has proved to be a useful tool in correlating measured coupling constants with spin density calculations. These calculations vary in degree of sophistication and complexity, from the simplest Hückel molecular orbital (HMO) format³⁴ through McLachlan's approximate unrestricted self-consistent field (USCF) treatment³⁵ and from

open shell and closed shell SCF^{26,36,37} to the USCF calculations with projection of the appropriate spin states.³⁸ The degree of correlation of calculated spin densities with experimental spin densities is not in general a function of the degree of rigor involved in the calculation. Hückel theory, in fact, has often provided the best results.

Although the dipolar part of the spin Hamiltonian does not affect the energy of the ESR transitions, it has been shown that the anisotropy of the electronic g-value arising from spin-orbit coupling and the anisotropy of the electron-nuclear spin-spin interaction contribute to the widths of the individual hyperfine lines. The result is a linewidth function of the form:

$$T_2^{-1} = \alpha + \beta M_I + \gamma M_I^2$$

where β is a function of the rate of tumbling, the magnetic field, and the anisotropies of the g-value and of the electron-nuclear coupling; and γ is a function of the rate of tumbling and of the anisotropy in the electron-nuclear coupling all squared.³⁹ From this equation it is possible to determine the sign of a given coupling constant, since this sign determines whether the $+M_I$ component or the $-M_I$ component will appear at the high (or low) field end of the ESR spectrum. The sign of the nitrogen and carbon coupling constants have been determined in this manner in several cases.³⁹⁻⁴¹

In addition to the interest in the theoretical interpretation of data obtained from ESR spectra, much of the interest is often there for the chemistry. The study of paramagnetic intermediates in reaction mechanisms has been fruitful in a number of cases as is exemplified by the work of Russell and his co-workers.⁴²

The phenomenon of ion pairing has been known to ESR spectroscopists for some time⁴³ and data are available for a variety of radical anions. It is especially prominent in the alkali metal-ether solutions where additional hyperfine structure is observed due to spin density on the metal cation.⁴⁴ The magnitude of the coupling in the ion-pair is determined by such factors as solvent, temperature, and the nature of the ions.⁴⁵

Electron transfer processes involving paramagnetic species are well suited to ESR studies. Such simple processes as the transfer of an electron from an anion to the corresponding neutral molecule have recently been carried out on the stilbene-stilbene radical anion system.⁴⁶ If the rate and activation energy for such a reaction are known, inference about changes in conformation (or lack thereof) upon reduction can be made. Studies of electron transfer involving reduction of a neutral aromatic compound by the previously generated radical anion of a different compound have been carried out by Adams and co-workers⁴⁷ in order to obtain further information on oxidation-reduction reactions of aromatic systems.

Analysis of the ESR spectra of p-nitrobenzaldehyde and other para-substituted benzaldehydes and acetophenones⁴⁸ has shown that the number of unique proton coupling constants is greater than that expected for molecules having a 2-fold symmetry axis. The lower symmetry is due to restricted rotation of the aldehyde group. The effect of restricted rotation has also been observed in the spectra of the stilbene,⁴⁹ azobenzene,⁵⁰ and nitrosobenzene^{50,51} radical anions and in a number of iminoxy radicals.⁵² Other structural and conformational information such as the degree of planarity and type of bonding can be obtained from the magnitude and number of coupling constants.⁵³

1.2 Systems to be Considered

It was noted earlier that there has been considerable interest in the ESR spectra of radicals derived from nitrogen heterocyclic compounds. In particular, many attempts have been made to observe the ESR spectrum of the pyridine radical anion. Kuwata⁵⁴ reports the evolution of gas and the appearance of a single broad ESR line when pyridine is treated with sodium in tetrahydrofuran (THF). Voevodskii and Solodovnikov^{55,56} obtained a multi-lined ESR spectrum by reducing pyridine with potassium in dimethoxyethane (DME), but they did not analyze the hyperfine splitting. Others including Ward,^{11a} Markau and Maier,⁵⁷ and Carrington and dos Santos Viega¹⁰ have identified the ESR spectrum obtained, by reduction of pyridine with an alkali metal in THF or DME, as that of the 4,4'-dipyridyl radical anion. Similarly a spectrum of greater width and complexity than would be predicted has been observed when pyrimidine is treated with alkali metal in THF or DME.^{10,11b} The radical formed was not identified.

On the brighter side, Dodd and his co-workers⁵⁸ have reported the ultraviolet absorption (UV) spectra of the radical anions of pyridine, pyrimidine, pyrazine, pyridazine, and 4,4'-dipyridyl. These were formed by brief contact of a THF solution of the parent compound with a sodium mirror. Both the ESR⁵⁹ and UV⁶⁰ spectra of the 3,5-lutidine radical anion have been observed. In each case the parent compound was reduced by potassium or sodium in DME.

The N-oxides of aromatic amines have received much attention from chemists since the discovery of their remarkable chemical behavior. The reactions of the N-oxides are well characterized and various UV, IR, and

NMR spectroscopic studies have been carried out. To the author's knowledge no attempts have been made previously to produce the radical anions of these compounds. ESR offers a sensitive test of the electron distribution. The spectra of the radical anions would provide data for additional correlations with quantum mechanical predictions and new bonding situations would shed light on the nitrogen spin polarization problem.

The ESR spectrum of the nitrosobenzene radical anion in liquid ammonia and several other solvents has been reported.^{51,61-63} However, the interpretation of the effects of restricted rotation on the proton coupling constants remains ambiguous. A significant contribution would be made if it were possible to assign each ortho proton coupling constant according to the position of the proton relative to the oxygen atom. The observation that methyl group substitution tends to have little effect on the electron distribution in nitroso and nitrobenzenes, combined with the steric effects observed in methyl substituted nitrobenzenes, suggests that the ESR spectra of the appropriate combination of methyl substituted nitrosobenzenes would allow such an assignment to be made.

Additional studies of the effects of various solvents and of methods of reduction on the radical anion of nitrosobenzene should provide more information about the electron distribution and the hetero atom parameters necessary for molecular orbital calculations.

2. EXPERIMENTAL

2.1 Chemicals

2.1.1 Nitrogen Heterocyclics

Reagent grade pyridine was refluxed over BaO, distilled at atmospheric pressure onto CaH₂, and transferred in a vacuum line, after degassing, to a capillary tube of appropriate volume (2 to 8 μl). This sample could then be distilled into the electrolytic cell.

The remaining heterocyclic compounds were purchased from the Aldrich Chemical Company. Pyrimidine and pyrazine were used without further purification. 4-Picoline and 3,5-lutidine were stored over CaH₂, distilled once at atmospheric pressure and once in the vacuum line. Commercial pyridine N-oxide is a soupy solid and is about as hygroscopic as KOH pellets. It was dried for about a week over CaCl₂ in vacuo. No further purification was attempted. 4-Picoline N-oxide was recrystallized from benzene. The commercial 2,6-lutidine N-oxide was a brown highly viscous tar. It was stored overnight over BaO at about 100°C. Distillation at atmospheric pressure resulted in apparent decomposition, therefore the tar was vacuum distilled at room temperature and about 0.75 cc was collected in a liquid nitrogen trap after 24 hours. This sample was a clear colorless liquid at room temperature. Due to its low vapor pressure the lutidine N-oxide was transferred to the electrolytic cell with a microliter syringe.

2.1.2 Nitrosobenzene and Substituted Nitrosobenzenes

Nitrosobenzene from the Aldrich Chemical Company was recrystallized from 95% ethanol, dried over CaCl₂, and stored under refrigeration in a CaCl₂ desiccator. The methyl substituted nitrosobenzenes (o-nitrosotoluene,

p-nitrosotoluene, and 2-nitroso-m-xylene) were prepared from the corresponding nitro compounds by standard reduction procedures.^{64,65} The crude products were separated by steam distillation and further purification and storage was similar to that for nitrosobenzene.

2.1.3 Solvents and Electrolytes

Pure, dry dimethylsulfoxide (DMSO) was obtained from the technical grade solvent by its treatment with NaOH followed by distillation from molecular sieves. (The author appreciates the generous gifts of purified solvent from Mr. William Smyrl). Chromatographic grade tetrahydrofuran (THF) was refluxed over Na or K metal, distilled onto CaH₂, and transferred from the CaH₂ under vacuum. Reagent grade liquid ammonia was purchased from the Matheson Company and was used without further purification. Polarographic grade tetra-n-butylammonium perchlorate (TBAP) and tetra-n-methylammonium iodide (TMAI) were obtained from the Southwestern Analytical Company and were used without further purification.

2.2 General Procedure and Remarks Concerning Electrolysis in Liquid Ammonia

The ESR spectrometer and electrolysis cell used in all experiments have been previously described. An ammonia solution saturated with tetramethylammonium iodide and containing 10 to 100 micromoles of parent compound per 10 cc of solution was electrolyzed at about -75°C to produce each of the observed radical anions. Current was passed through the cell starting at 1 μ a and was gradually increased until an ESR signal could be observed. The current was then adjusted to maximize signal intensity and resolution. It was often necessary for the "solvated electron" concentration to be so great as to produce a single intense signal that appears slightly to the high field side of the center of the radical anion spectrum in several of the figures.

In the amine and amine-N-oxide spectra no M_I line width dependence was observed. The apparent variation in signal intensity between the high and low field extrema in some of the spectra presented is due to a change in radical concentration during the 20 to 30 minute period of the field sweep. It was often found that the best spectra were obtained under conditions of precarious and short lived dynamic balance among the concentrations of parent compound, radical anion, and "solvated electron" in the vicinity of the cathode. In contrast to pyridine and its derivatives, nitrosobenzene and methyl substituted nitrosobenzenes form very stable radical anions in liquid ammonia and can consequently be studied in the absence of a large excess in the solvated electron concentration. The coupling constants measured for the amine and amine-N-oxide radical anions with related data from other works are listed in Table I. The corresponding data for the nitrosobenzenes are listed in Table II. Results pertinent to each radical anion are discussed in the following sections.

2.3 Nitrogen Heterocyclic Radical Anions

2.3.1 Pyridine

The pyridine radical anion is first observed at $\sim 20 \mu\text{a}$ with a spectrum of 34 lines grouped in sets of 3 and 4. The number of lines observed is less than the theoretically possible 54 because the coupling constants $A(N)$ and $A(4)$ happen to be linearly dependent on $A(1)$ and $A(2)$. The individual line widths at this low current are about 0.5 gauss. When the current is gradually raised to a maximum of 240 μa (the maximum current was limited by the 110 volts available from the power supply and by the conductivity of the solution) there is an increase in signal intensity and decrease of line width to 0.15 gauss. After 45 minutes of continuous

Table I

Observed coupling constants for nitrogen heterocyclic radical anions in liquid ammonia

| Heterocyclic Compound ^a | Atom | Heterocyclic | N-Oxide |
|--|---------------------|---------------------|-----------|
| | | A (gauss) | A (gauss) |
| Pyridine | N | 6.28 | 10.82 |
| | H(2) | 3.55 | 3.04 |
| | H(3) | 0.82 | 0.47 |
| | H(4) | 9.70 | 8.61 |
| 4-Picoline (4-methylpyridine) | N | 5.67 | 9.89±0.3 |
| | H(2) | 3.80 | 3.35 |
| | H(3) | 0.60 | < 0.30 |
| | CH ₃ (4) | 11.38 | 9.89±0.3 |
| 3,5-Lutidine (3,5-dimethylpyridine) | N | 7.40 ^(b) | ---- |
| | H(2) | 3.19 | ---- |
| | CH ₃ (3) | 1.06 | ---- |
| | H(4) | 8.94 | ---- |
| 2,6-Lutidine (2,6-dimethylpyridine) | N | (c) | 9.85 |
| | CH ₃ (2) | ---- | 4.25 |
| | H(3) | ---- | 0.47 |
| | H(4) | ---- | 8.98 |
| Pyrazine (1,4-diazine) | N | 7.22 ^(d) | ---- |
| | H | 2.72 | ---- |
| Pyrimidine (1,3-diazine) | N | 3.26 | ---- |
| | H(2) | 0.72 | ---- |
| | H(4) | 9.78 | ---- |
| | H(5) | 1.31 | ---- |

(a) Rings numbered by standard convention. See, for example, Handbook of Chemistry and Physics, Chemical Rubber Publishing Co., Cleveland, Ohio.

(b) Reference 59a obtained 6.21, 3.41, 0.80 and 8.96, respectively, using alkali metal reduction in dimethoxyethane. Reference 59b obtained 6.12, 3.27, 0.92, and 8.70, respectively, under similar conditions.

(c) A spectrum has been obtained using 2,6-lutidine as the parent compound but we have been unable to assign it.

(d) References 10, 11, 13, and 68 have obtained quite similar values in a number of other solvents.

Table II
 Experimental coupling constants^(a) for Nitrosobenzene type radical anions

| Radical Anion | Reducing Medium | Coupling Constants (in Gauss) | | | |
|------------------------|--------------------------|-------------------------------|---|------------------|----------|
| | | A(N) | A(Ortho) ^(b) cis } trans } | A(Meta) | A(Para) |
| Nitroso- benzene | NH ₃ (c) | 7.97 | 3.99±.15 } 2.97 } | 1.05±.09 | 3.99±.15 |
| | DMSO | 7.60 | 3.82 } 2.77 } | 1.08 | 3.82 |
| | DMSO+ (d) tBuOK/tBuOH | 8.0 | 3.9 } 2.9 } | 1.1 | 3.9 |
| | THF | 8.0 | 4.0±.2 } 3.0 } | 1.1 | 4.0±.2 |
| | EtOH/Na (e) | 10.2 | 4.25 } 3.76 } | 1.26 | 3.76 |
| | p-Nitroso- toluene | | 8.21 | 3.94 } 3.04 } | 1.12 |
| O-Nitroso- toluene | NH ₃ | 7.66 | 4.05 } 2.20* } | 1.22 } 0.99 } | 4.05 |
| 2-Nitroso- m-xylene | | 7.52 | 3.18* | 1.14 | 4.21 |

(a) Unless otherwise noted data were obtained from this work.

(b) Assignments based on arguments cited in text.

(c) Ref. 61.

(d) Ref. 51.

(e) Ref. 62 and 51 obtained $A(o,P) = 4.02$, $A(o') = 3.65$ and Ref. 63 obtained $A(o,P) = 3.9$, $A(o') = 4.2$ under similar conditions.

(f) Starred quantities represent methyl group coupling constants.

Table I

Observed coupling constants for nitrogen heterocyclic radical anions in liquid ammonia

| Heterocyclic Compound ^a | Atom | Heterocyclic | N-Oxide |
|--|---------------------|---------------------|-----------|
| | | A (gauss) | A (gauss) |
| Pyridine | N | 6.28 | 10.82 |
| | H(2) | 3.55 | 3.04 |
| | H(3) | 0.82 | 0.47 |
| | H(4) | 9.70 | 8.61 |
| 4-Picoline (4-methylpyridine) | N | 5.67 | 9.89±0.3 |
| | H(2) | 3.80 | 3.35 |
| | H(3) | 0.60 | < 0.30 |
| | CH ₃ (4) | 11.38 | 9.89±0.3 |
| 3,5-Lutidine (3,5-dimethylpyridine) | N | 7.40 ^(b) | ---- |
| | H(2) | 3.19 | ---- |
| | CH ₃ (3) | 1.06 | ---- |
| | H(4) | 8.94 | ---- |
| 2,6-Lutidine (2,6-dimethylpyridine) | N | (c) | 9.85 |
| | CH ₃ (2) | ---- | 4.25 |
| | H(3) | ---- | 0.47 |
| | H(4) | ---- | 8.98 |
| Pyrazine (1,4-diazine) | N | 7.22 ^(d) | ---- |
| | H | 2.72 | ---- |
| Pyrimidine (1,3-diazine) | N | 3.26 | ---- |
| | H(2) | 0.72 | ---- |
| | H(4) | 9.78 | ---- |
| | H(5) | 1.31 | ---- |

(a) Rings numbered by standard convention. See, for example, Handbook of Chemistry and Physics, Chemical Rubber Publishing Co., Cleveland, Ohio.

(b) Reference 59a obtained 6.21, 3.41, 0.80 and 8.96, respectively, using alkali metal reduction in dimethoxyethane. Reference 59b obtained 6.12, 3.27, 0.92, and 8.70, respectively, under similar conditions.

(c) A spectrum has been obtained using 2,6-lutidine as the parent compound but we have been unable to assign it.

(d) References 10, 11, 13, and 68 have obtained quite similar values in a number of other solvents.

Table II
 Experimental coupling constants^(a) for Nitrosobenzene type radical anions

| Radical Anion | Reducing Medium | Coupling Constants (in Gauss) | | | |
|------------------------|--------------------------|-------------------------------|---|------------------|----------------------|
| | | A(N) | A(Ortho) ^(b) cis } trans } | A(Meta) | A(Para) |
| Nitroso- benzene | NH ₃ (c) | 7.97 | 3.99±.15 } 2.97 } | 1.05±.09 | 3.99±.15 |
| | DMSO | 7.60 | 3.82 } 2.77 } | 1.08 | 3.82 |
| | DMSO+ (d) tBuOK/tBuOH | 8.0 | 3.9 } 2.9 } | 1.1 | 3.9 |
| | THF | 8.0 | 4.0±.2 } 3.0 } | 1.1 | 4.0±.2 |
| | EtOH/Na (e) | 10.2 | 4.25 } 3.76 } | 1.26 | 3.76 |
| p-Nitroso- toluene | | 8.21 | 3.94 } 3.04 } | 1.12 | 4.28 ^{*(f)} |
| O-Nitroso- toluene | NH ₃ | 7.66 | 4.05 } 2.20* } | 1.22 } 0.99 } | 4.05 |
| 2-Nitroso- m-xylene | | 7.52 | 3.18* | 1.14 | 4.21 |

(a) Unless otherwise noted data were obtained from this work.

(b) Assignments based on arguments cited in text.

(c) Ref. 61.

(d) Ref. 51.

(e) Ref. 62 and 51 obtained $A(o,P) = 4.02, A(o') = 3.65$ and Ref. 63 obtained $A(o,P) = 3.9, A(o') = 4.2$ under similar conditions.

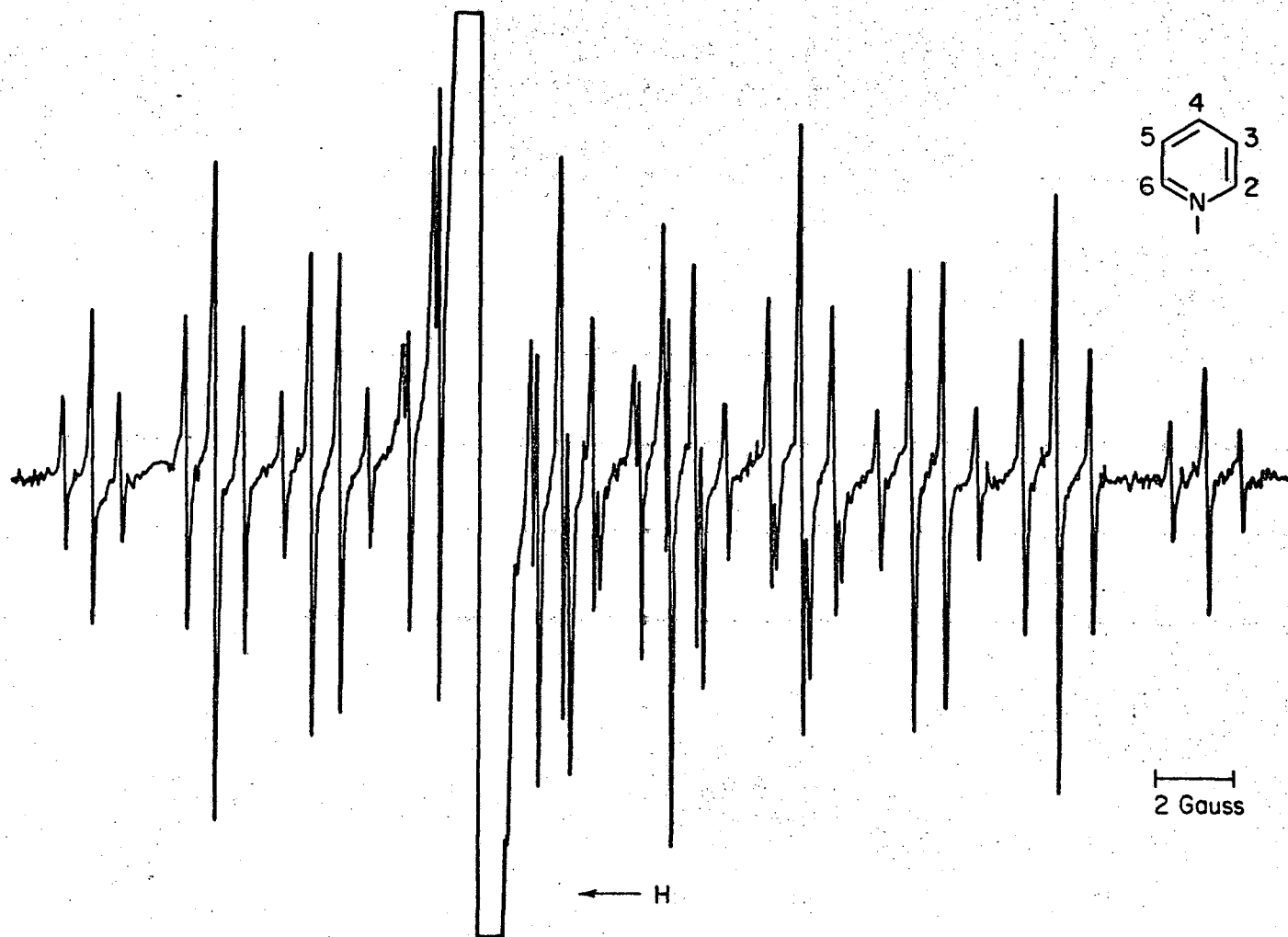
(f) Starred quantities represent methyl group coupling constants.

electrolysis at this current level the lines narrow further (80 milligauss or less) and additional splitting in some of the central lines is observed. This splitting corresponds to the actual linear independence of $A(4)$. A trace of the spectrum recorded under these conditions is shown in Fig. 1. Along with the increased resolution, at maximum current a 25% increase in conductivity is observed, then the signal begins to decay and is completely gone in 10 to 15 minutes. If the voltage is turned off the signal reappears and reaches a maximum intensity in about 5 minutes. It then decays with a "half-life" of 1 to 1.5 minutes. The "half-life" for decay at the $40 \mu\text{a}$ level is 0.75 minutes. All "half-lives" are taken as the time necessary for the signal to decrease to one-half its original intensity. Quantitative studies of decay rates were not undertaken.

It should be pointed out that current levels quoted are only qualitatively reproducible. The exact values depend on such factors as solute concentration and presence of traces of O_2 , water, and other impurities. The exact values are mentioned only to give an idea of the type of experiment performed.

2.3.2 4-Picoline (4-Methylpyridine)

4-Picoline behaves in much the same way as pyridine in liquid ammonia. Reduction is observed at about $15 \mu\text{a}$. There is a similar increase in radical concentration and decrease in line width as the current is increased. The spectrum as shown in Fig. 2 consists of 81 out of the theoretically possible 108 lines. The strong central line, not expected in a radical containing an odd number of equivalent protons, is due to the accidental equality $A(\text{CH}_3) = 2A(\text{N})$. Continued electrolysis at maximum current results in decay and eventual disappearance of the signal. After the voltage is turned off the signal attains maximum strength within



MUB-13101

Fig. 1 The ESR spectrum of the radical anion of pyridine in liquid ammonia near -75°C . The strong line is due to the "solvated electrons" present in the system under steady state electrolysis.

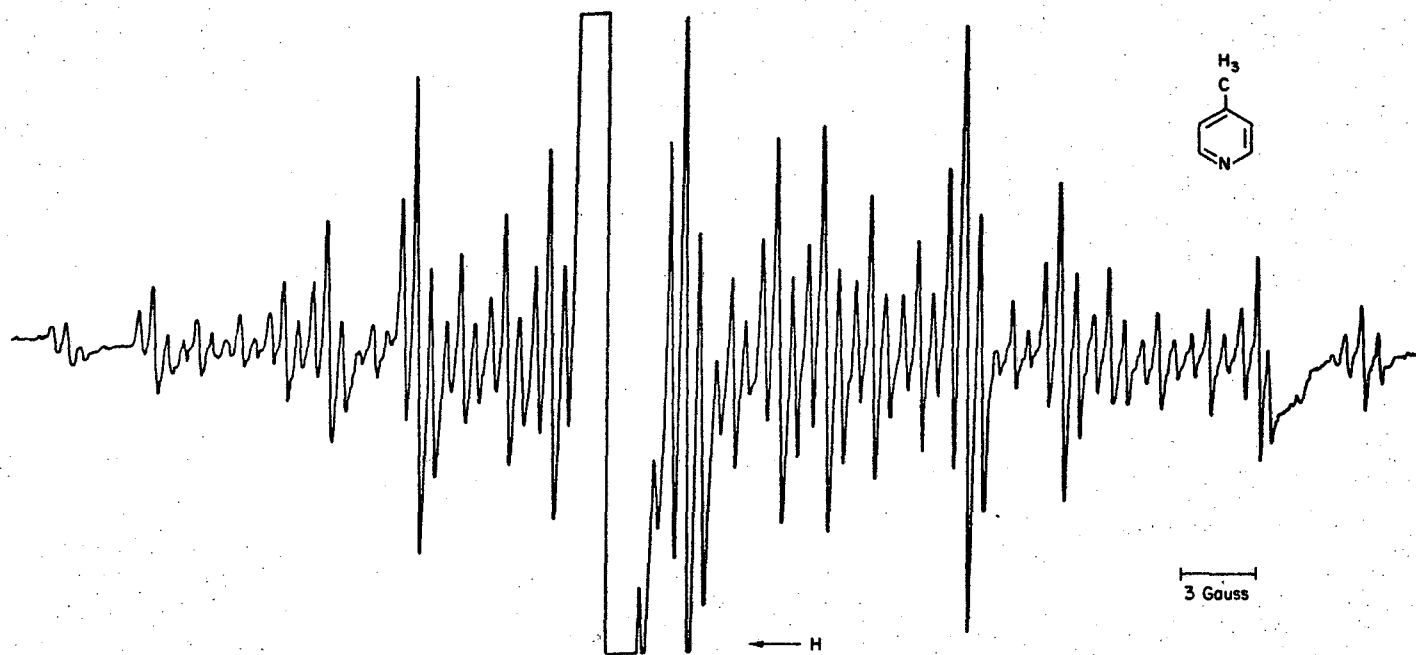


Fig. 2 The ESR spectrum of the radical anion of 4-picoline. The intensity variations from one end of this spectrum to the other are largely due to variations with time.

MUB:13102

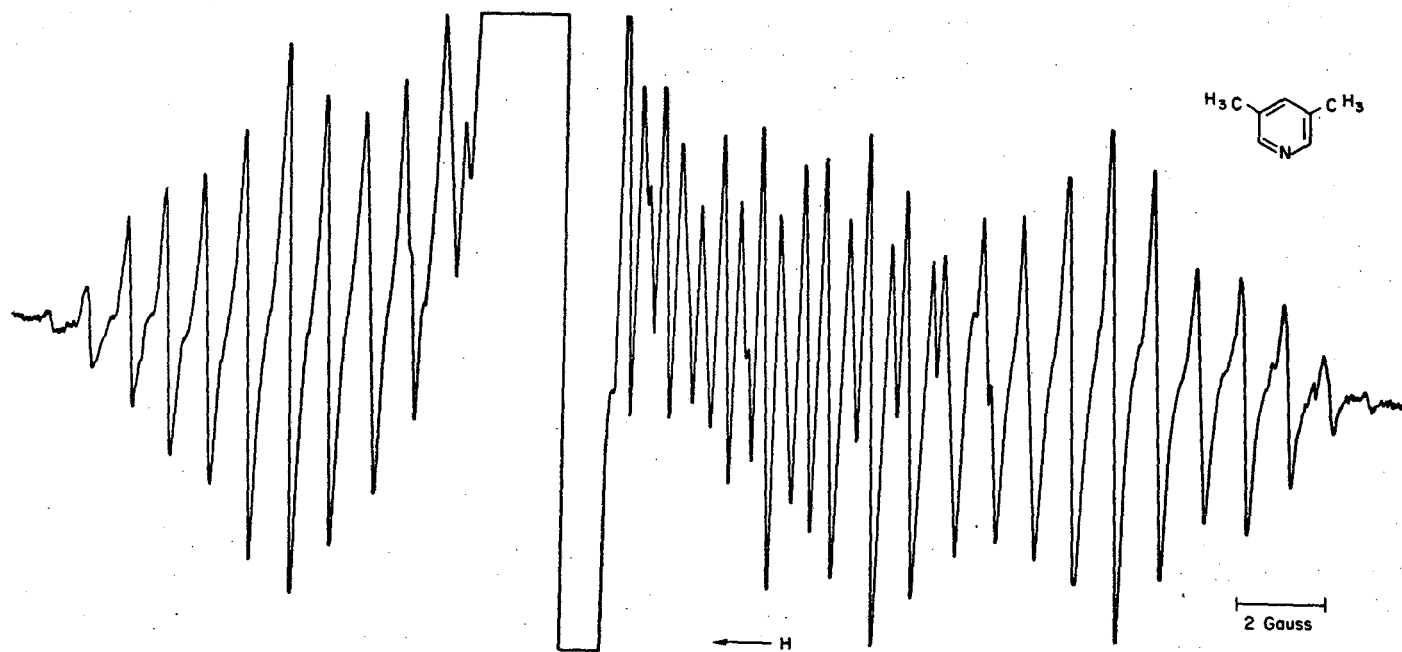
5 to 8 minutes and decays with a 1 minute "half-life".

2.3.3 3,5-Lutidine (3,5-Dimethylpyridine)

The 3,5-lutidine radical anion was prepared in order to compare results obtained in liquid ammonia with those obtained by chemical reduction.^{59a,b} A signal is observed at 20 to 25 μ a and the best spectrum, shown in Fig. 3, is obtained at approximately 70 μ a. This current is significantly less than the corresponding values for the pyridine and 4-picoline radical anions. The line width varied from 0.5 to 0.2 gauss, but could not be further reduced. Only 50 of the 126 possible lines are resolved due to the fairly broad lines and the near equalities $A(N) \cong 7 A(CH_3)$ and $A(2) \cong 3A(CH_3)$. Continued electrolysis at or above 70 μ a causes the signal to decrease and the conductivity to increase. The signal grows back when the voltage is shut off and then decays with a 4 minute "half-life". The observations indicate that the 3,5-lutidine radical anion is somewhat more stable than the pyridine or picoline radical anions. The difference in the hyperfine coupling constants as measured in the two solvent systems (Table I) was at first surprising, especially considering the good agreement in the case of pyrazine radical anion measured in a wide variety of systems. This point will be discussed in section 4.2.

2.3.4 Pyrazine (1,4-Diazine)

The pyrazine radical anion was also prepared in order to form a basis for comparing results obtained in liquid ammonia with those obtained using other techniques.^{10,11,13,45,59a,60,100} An observable quantity of radical anion is formed when only 1 μ a of current is passed through the solution. The best signal is obtained at 7 to 10 μ a. The signal intensity decreased when the current is raised above 10 μ a but returns to the



MU 813104

Fig. 3 The ESR spectrum of the radical anion of 3,5-lutidine.

original level if the current is reduced or set to zero. The pyrazine radical anion is quite stable in liquid ammonia with no noticeable decay of its signal after two hours at zero current.

2.3.5 Pyrimidine (1,3-Diazine)

In contrast to pyrazine, pyrimidine radical anion is not observed until the current is raised to 20 μ a. Between 20 and 100 μ a the spectrum consists of nine broad lines which begin to show additional splitting as the 100 μ a level is approached. Continued electrolysis at 125 μ a produces a well resolved spectrum as shown in Fig. 4a that consists of eleven equally spaced quartets.

The four lines of equal intensity can be assigned to the two non-equivalent protons in positions numbered 2 and 5. Eleven equally spaced lines of relative intensities 1:2:3:4:5:6:5:4:3:2:1 can be generated in two ways from two equivalent nitrogen nuclei and two equivalent hydrogen nuclei: a) if the observed spacing is equal to $|A(H)|$ and $A(N) = 2|A(H)|$ or, b) if the observed spacing is equal to $A(N)$ and $|A(H)| = 3A(N)$. The equalities are probably not exact and should be written: a) $A(N) = 2|A(H)| + \delta \cdot |A(H)|$ or, b) $|A(H)| = 3A(N) + \delta \cdot A(N)$, where the term $\delta \cdot A$ is too small ($\lesssim 1/3$ line width) to cause observable splitting but may be detected in the distortion of the hyperfine lines. Table III shows the statistical relative intensities and expected positions of the hyperfine components for each set ($M_I(N)$, $M_I(H)$) for both cases. It is seen that four of the eleven lines in each case are made up of overlapping lines corresponding to different values of ($M_I(N)$, $M_I(H)$). If the centers of the two components are not coincident, the observed line will appear to be broadened. On the basis of the observed

Table III

Positions of hyperfine components for alternate assignments of the pyrimidine radical anion ESR spectrum

| line ^(a) | $M_I(N)$ | $M_I(H)$ | $ H-H_0 /A$ ^(b) | i ^(c) |
|---------------------|----------|----------|----------------------------|--------------------|
| 1a | ± 2 | ∓ 1 | $5 + 2\delta$ | 1 |
| 1b | ± 2 | ∓ 1 | $5 + \delta$ | 1 |
| 2a | ± 2 | 0 | $4 + 2\delta$ | 2 |
| 2b | ± 1 | ∓ 1 | $4 + \delta$ | 2 |
| 3a } } | ± 2 | ± 1 | $3 + 2\delta$ | 1 |
| | ± 1 | ∓ 1 | $3 + \delta$ | 2 |
| 3b | 0 | ∓ 1 | $3 + \delta$ | 3 |
| 4a | ± 1 | 0 | $2 + \delta$ | 4 |
| 4b } } | ∓ 1 | ∓ 1 | $2 + \delta$ | 2 |
| | ± 2 | 0 | 2 | 2 |
| 5a } } | ± 1 | ± 1 | $1 + \delta$ | 2 |
| | 0 | ∓ 1 | 1 | 3 |
| 5b } } | ∓ 2 | ∓ 1 | $1 + \delta$ | 1 |
| | ± 1 | 0 | 1 | 4 |
| 6a,b | 0 | 0 | 0 | 6 |

(a) Observed lines numbered from extreme's to center of spectrum.

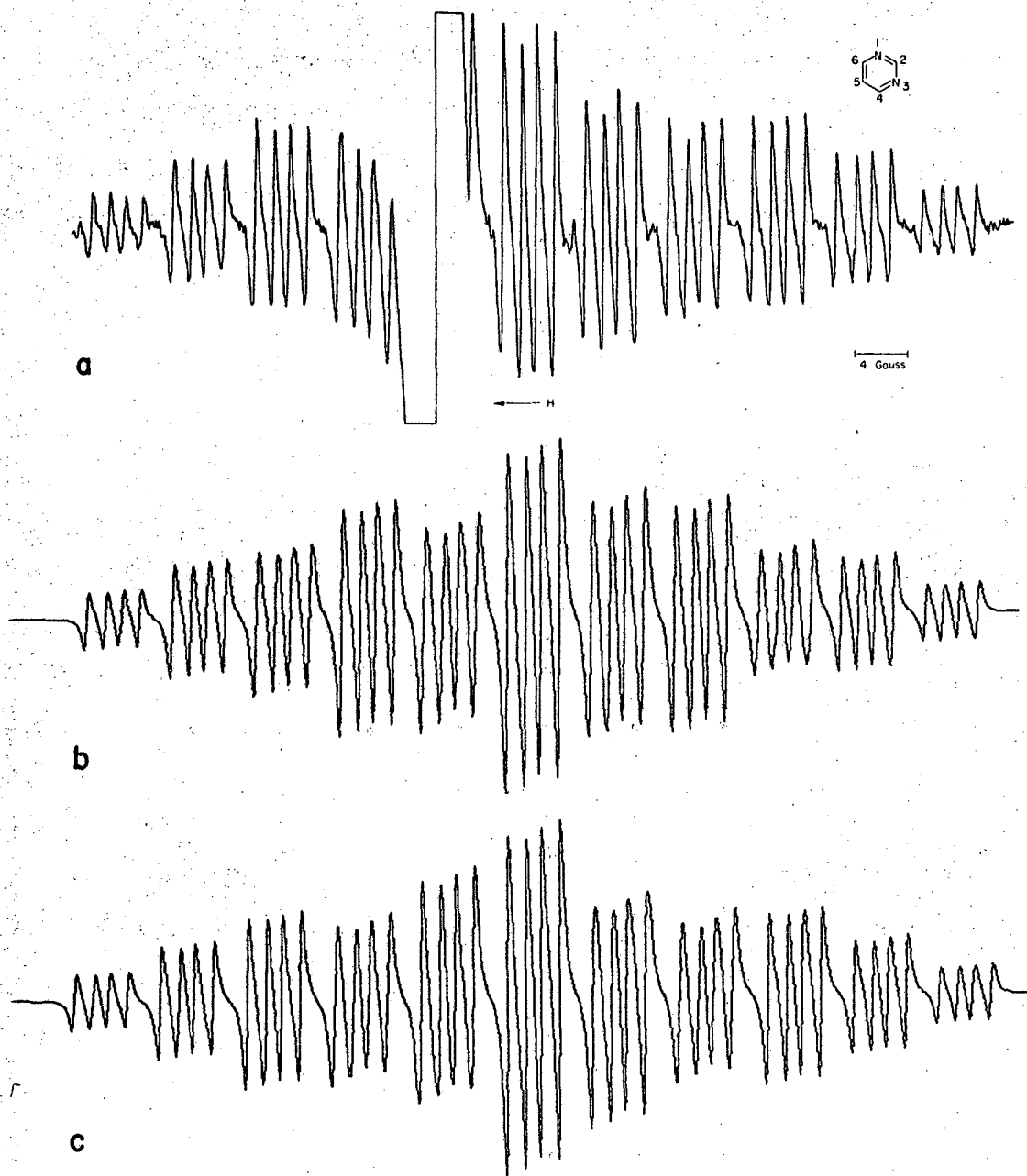
a $\Rightarrow |A(H)| = A$ the average separation between centers of quartets and $A(N) = -3A - \delta \cdot A$.

b $\Rightarrow A(N) = A$ and $A(H) = -3A - \delta \cdot A$.

(b) $|H-H_0|$ is the distance from center of spectrum.

(c) i is the relative intensity of the component.

$i = \text{multiplicity of } M_I(N) \cdot \text{multiplicity of } M_I(H)$.



XBL672-833

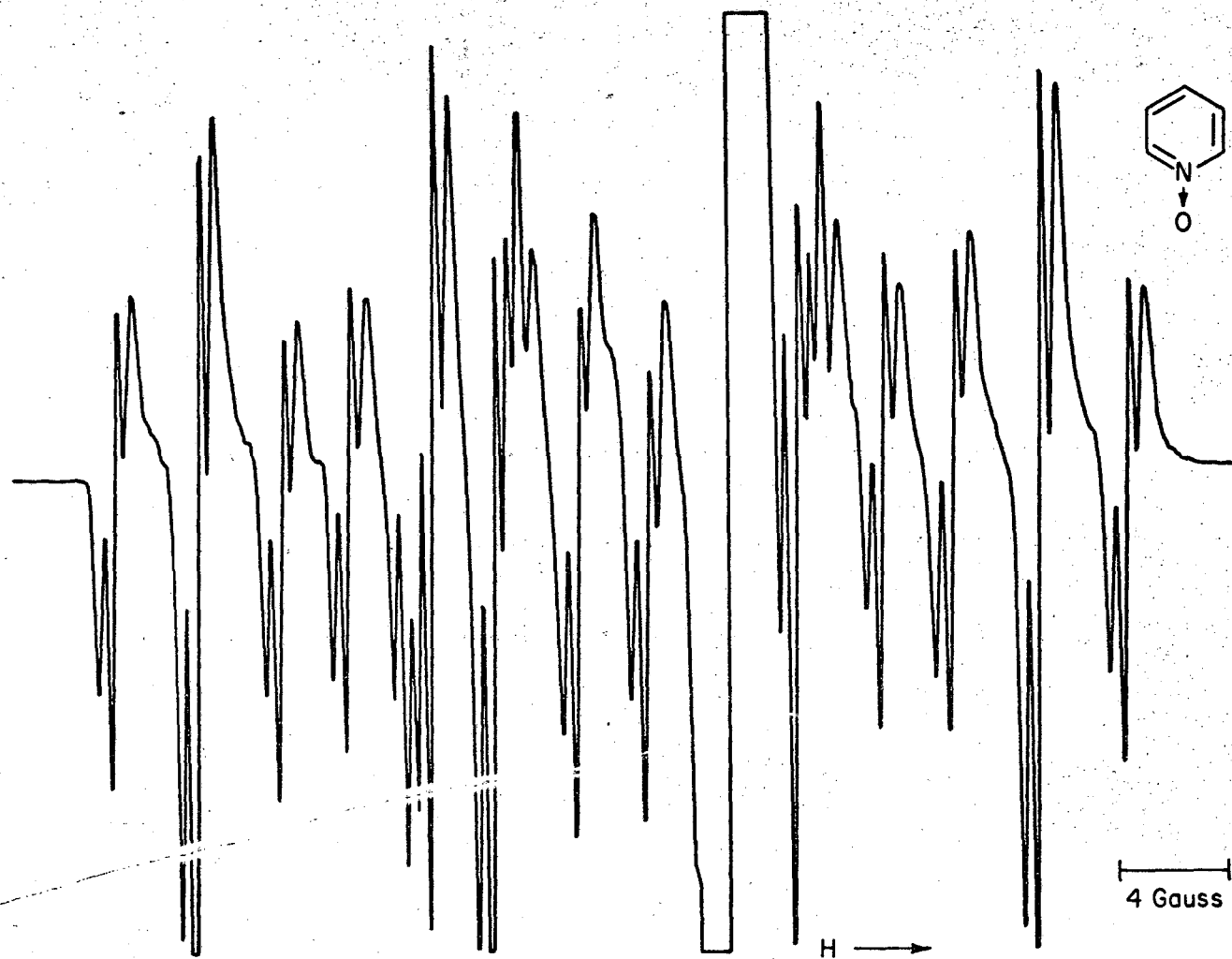
Fig. 4 (a) The ESR spectrum of the radical anion of pyrimidine.
(b) The calculated spectrum with $A(N) = 2A(4) \pm 0.15$ gauss.
(c) The calculated spectrum with $A(N) = 1/3 A(4) \pm 0.18$ gauss.
Note the improved intensities in this case.

deviations of the 4th and 5th groups of lines from the predicted intensity ratios, the above assignment (b), where $|A(H)| = 3A(N)$, was determined to be the correct one. Figures 4b and 4c show the calculated spectra for both cases which further confirm the assignment.

Increasing the current above the 125 μ a level resulted in a decrease of signal strength. Original intensity was restored when the current was dropped back to 125 μ a. After several hours of electrolysis new lines began to appear toward the center of the spectrum indicating the formation of a new species. This second spectrum was not intense enough to analyze or identify.

2.3.6 Pyridine N-Oxide

The radical anion is produced in an observable quantity at a current level as low as 2 μ a. This is in part due to a high concentration of parent compound (about ten times that of most of the other compounds run). The spectrum consists of 14 lines each about 1 gauss wide. After several hours of electrolysis at maximum current (150 μ a), these lines resolve into triplets with a line width of 0.20 to 0.25 gauss. This spectrum is shown in Fig. 5. Eventually the conductivity of the solution increases and the radical decays. The signal grows back when the voltage is turned off and then decays with a "half life" of 2 minutes. Prolonged electrolysis results in the growth of additional sharp lines toward the center of the spectrum. The separation of these lines is the same as for the corresponding lines in the pyridine radical anion spectrum. It has been previously observed that chemical reduction of pyridine N-oxide in liquid ammonia yields both pyridine and 4,4'-dipyridyl.⁶⁶



MUB13106

Fig. 5 The ESR spectrum of the radical anion of pyridine N-oxide.

2.3.7 4-Picoline N-Oxide

A signal is observed at 5 μ a that consists of six triplets with a line width of about one gauss. Increasing the current to 100 μ a has no effect on the line width or resolution. Several attempts including prolonged electrolysis at various current levels and variation in parent compound concentration failed to resolve the expected small triplet splittings or to resolve the near equality $A(N) \sim A(CH_3)$. Continued electrolysis at currents greater than 100 μ a yielded a new spectrum which could be identified as that of the 4-picoline radical anion. Comparison with computed spectra indicate that it is reasonable to assume a small unresolved triplet splitting of 0.25 to 0.30 gauss and a difference of up to 0.5 gauss in the values of $A(N)$ and $A(CH_3)$. It was not possible to decide which of the two is larger. The spectrum is shown in Fig. 6.

2.3.8 2,6-Lutidine N-Oxide

A signal is observed at 5 to 10 μ a that consists of eighteen lines having a line width of \sim 1 gauss. It was necessary to electrolyze at maximum current (180 μ a) for several hours before further splitting could be resolved. The spectrum is shown in Fig. 7. No decay of signal, increase in conductivity or production of 2,6-lutidine was observed at maximum current.

2.4 Nitrosobenzene Type Radical Anions

2.4.1 Methyl Substituted Nitrosobenzenes

Strong ESR signals are observed at only 2 μ a of current for the ortho and para nitrosotoluenes (o,p NOT). The signals improved with increasing current to about 10 μ a. At higher current, the signals began to decrease and a single broad line with a g -value and total width about equal to that of the resolved spectrum appeared. Line width dependence

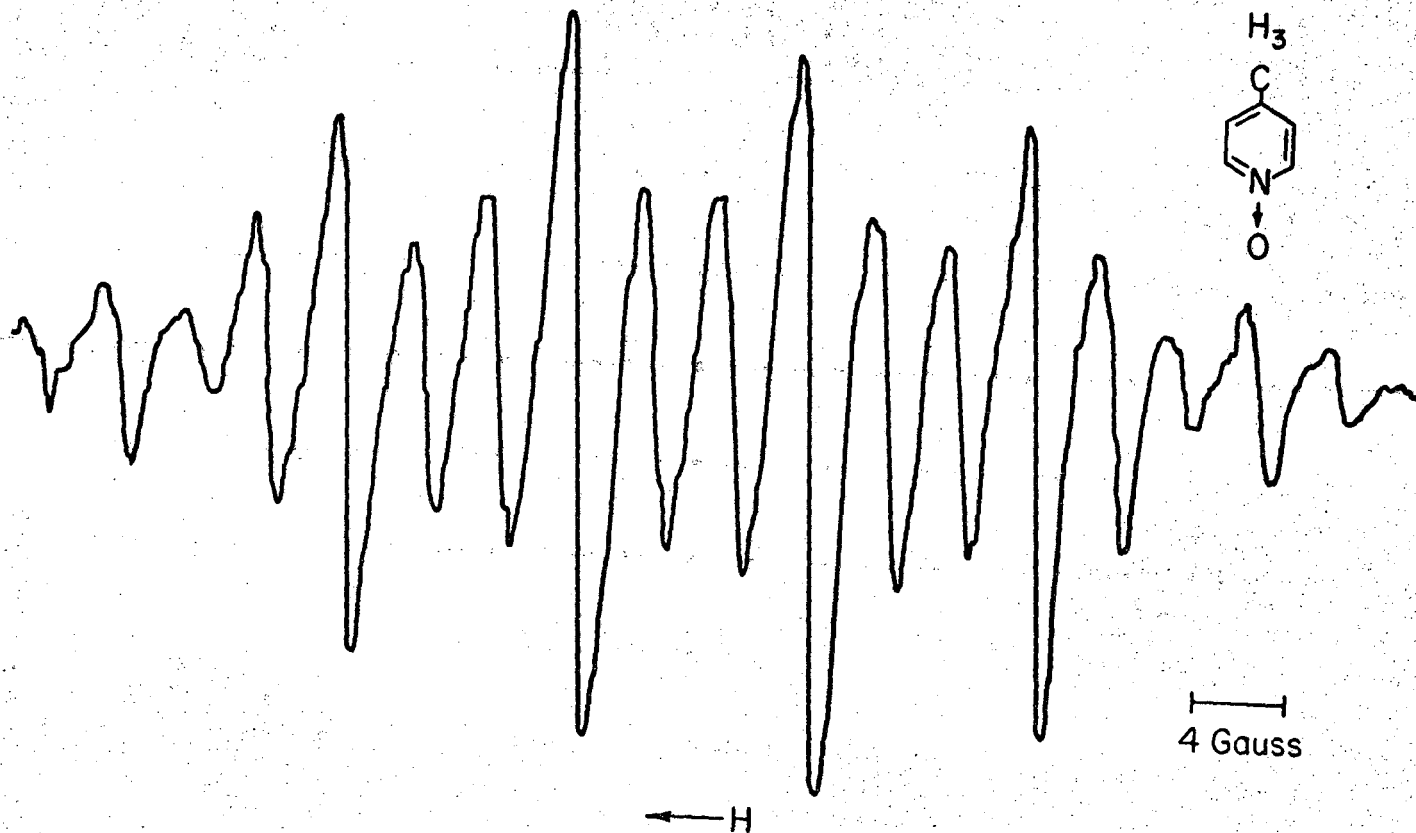


Fig. 6 The best ESR spectrum obtained for the radical anion of 4-picoline N-oxide.

MUB13107

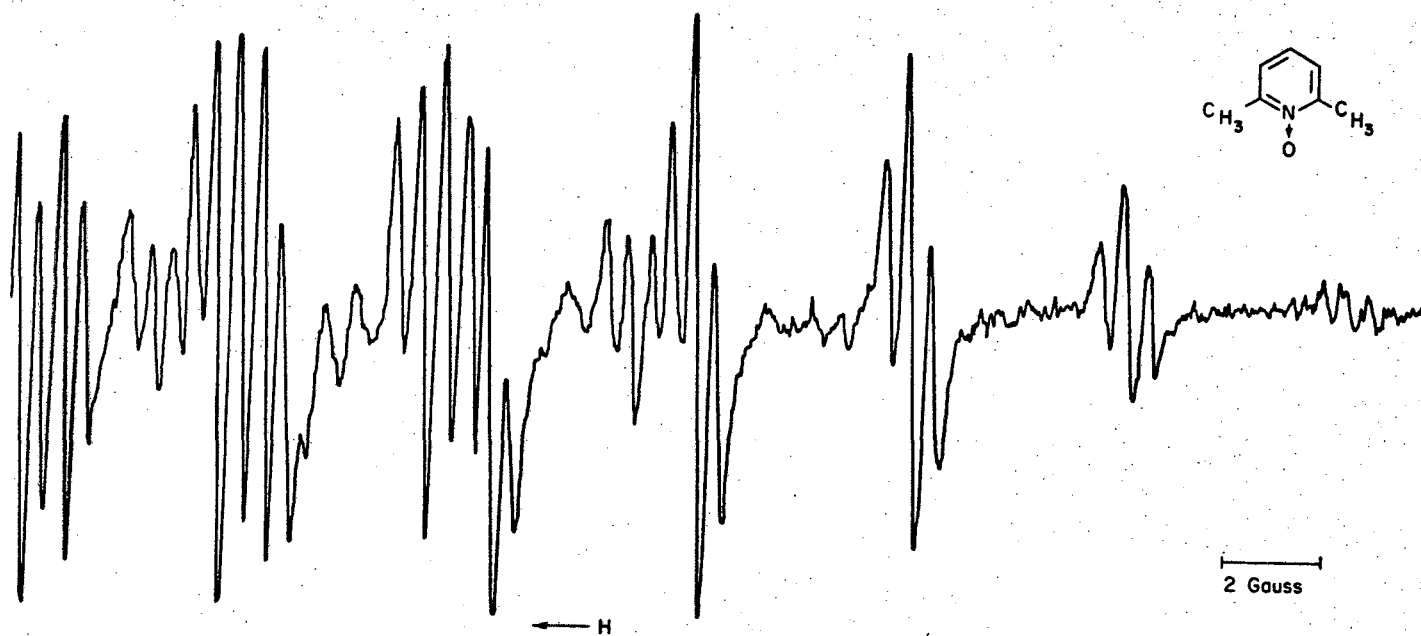


Fig. 7 One-half of the ESR spectrum of the radical anion of 2,6-lutidine N-oxide

MUB 13108

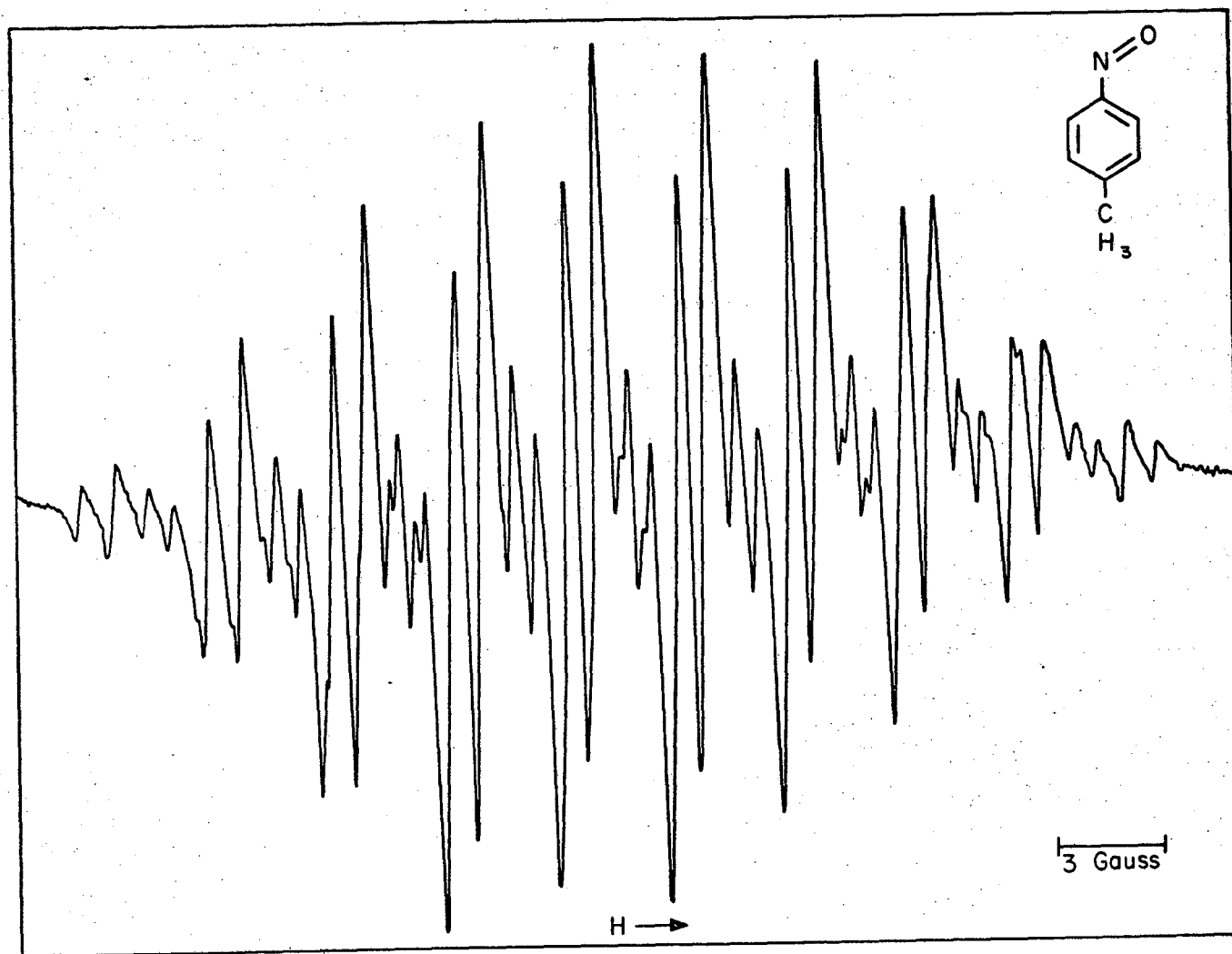
on the quantum number $M_I(N)$ was noted for both of the NOT radical anions. The ratio of the observed intensities of the outer equally probable hyperfine components were averaged over a number of traces with the result that $I(\text{high field})/I(\text{low field}) = 0.83$. The same result was found for either molecule.

2-Nitroso-m-xylene (NOX) did not reduce appreciably until a current level of 10 μa was reached. The sample appeared to contain some nitroxylene impurity. As a result three well separated groups of lines were superposed on the nitroso spectrum. The higher g-value of the nitro radical anion causes about a 2 gauss down-field shift from that of the nitroso radical anion at 9.0 Gc. When the solution containing the two radicals was allowed to sit for 6 hours with no current passing through the cell, the ESR signals assigned to the nitrosoxylene remained and the signal assigned to the nitroxylene decayed. $M_I(N)$ line width dependence was again observed. The ratio of the high field to low field intensities was found to be 0.79 for NOX.

The spectra of the three methyl substituted nitrosobenzenes are shown in Figs. 8-10.

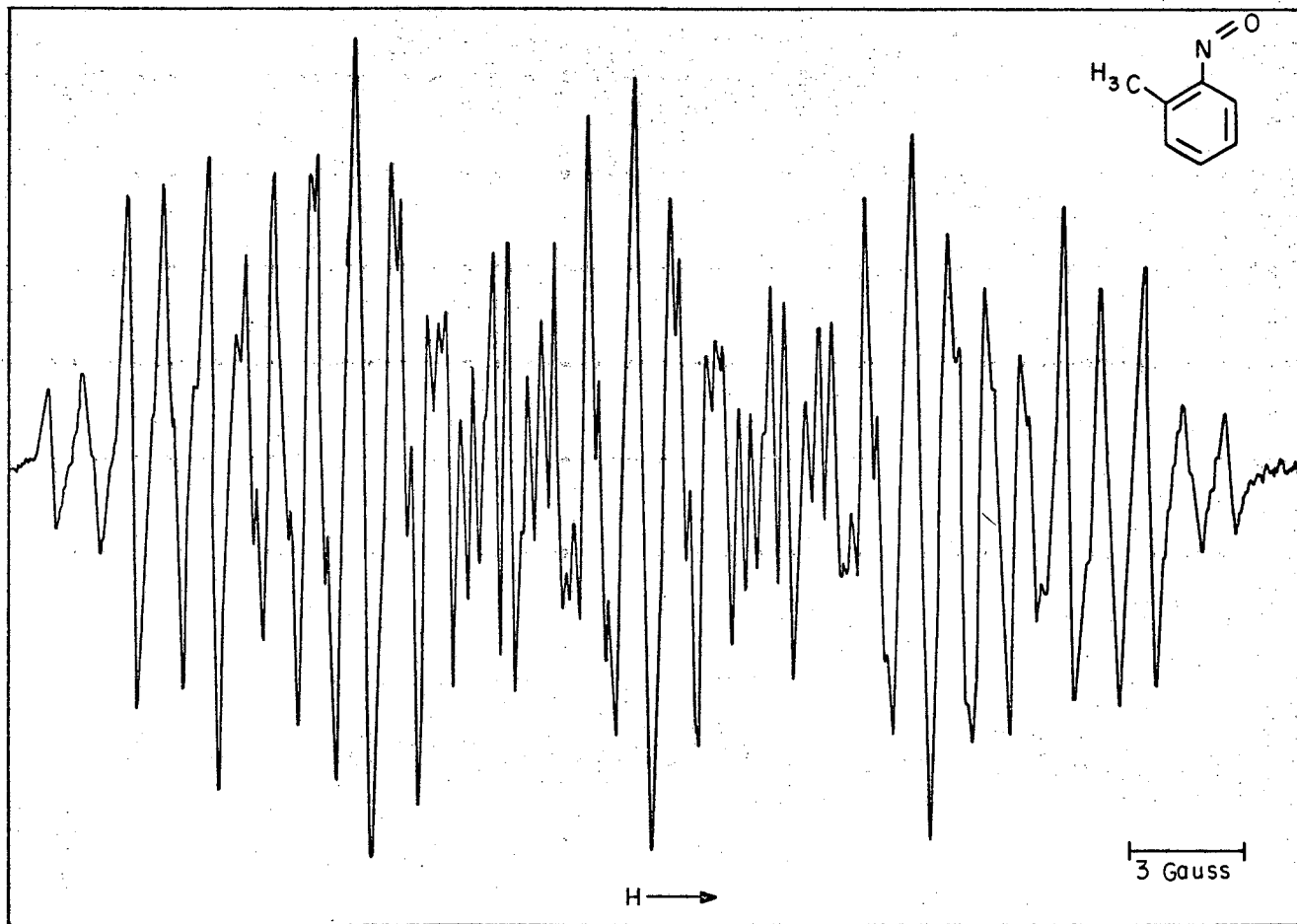
2.4.2 Nitrosobenzene

The radical anion of nitrosobenzene (ΦNO) was prepared in DMSO and in THF electrolytically using TBAP as the supporting electrolyte. For the DMSO experiment, 0.03 mmoles of nitrosobenzene and 0.5 mmoles of TBAP were dissolved in 10 ml of DMSO and put into the same electrolytic cell that was used for the ammonia experiments. The mixing and transfer were carried out in a nitrogen atmosphere. The solution was cooled and a vacuum applied in order to remove traces of oxygen. The best spectrum



XBL677-3460

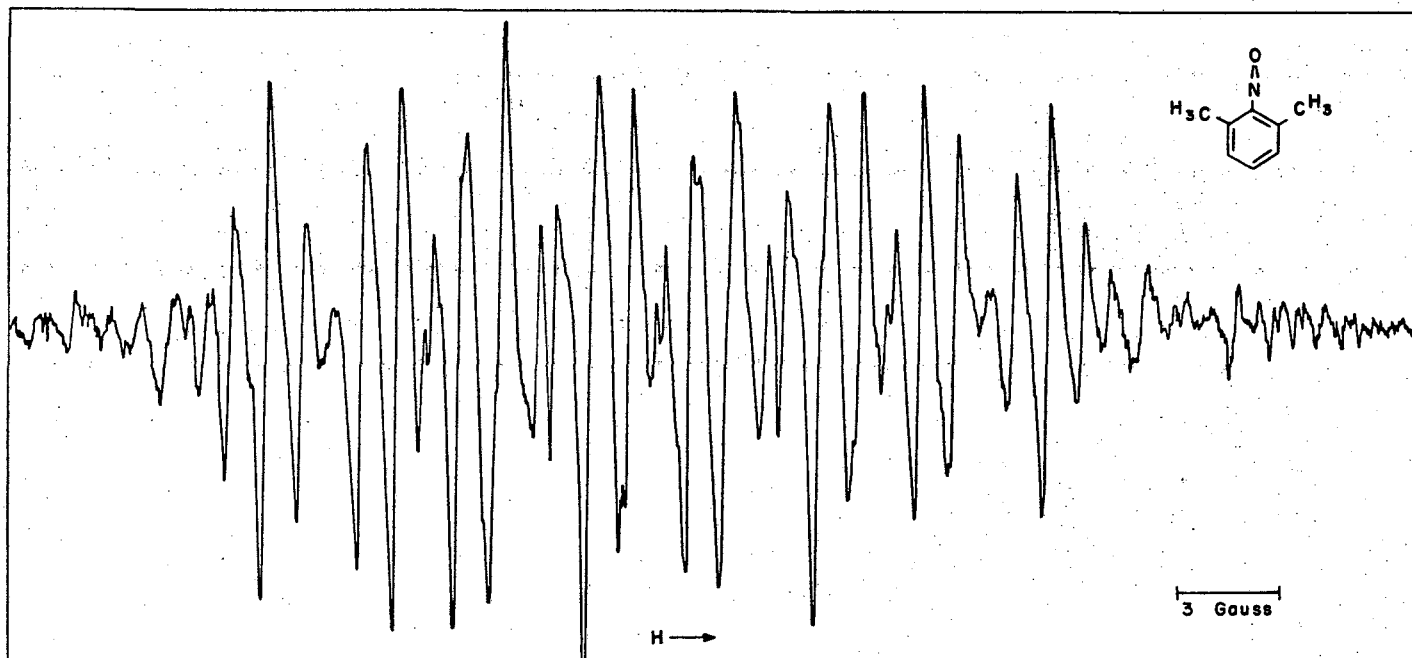
Fig. 8 The ESR spectrum of the radical anion of p-nitrosotoluene



-32-

XBL677-3459

Fig. 9 The ESR spectrum of the radical anion of o-nitrosotoluene



-33-

XBL677-3458

Fig. 10 The ESR spectrum of the radical anion of 2-nitroso-m-xylene

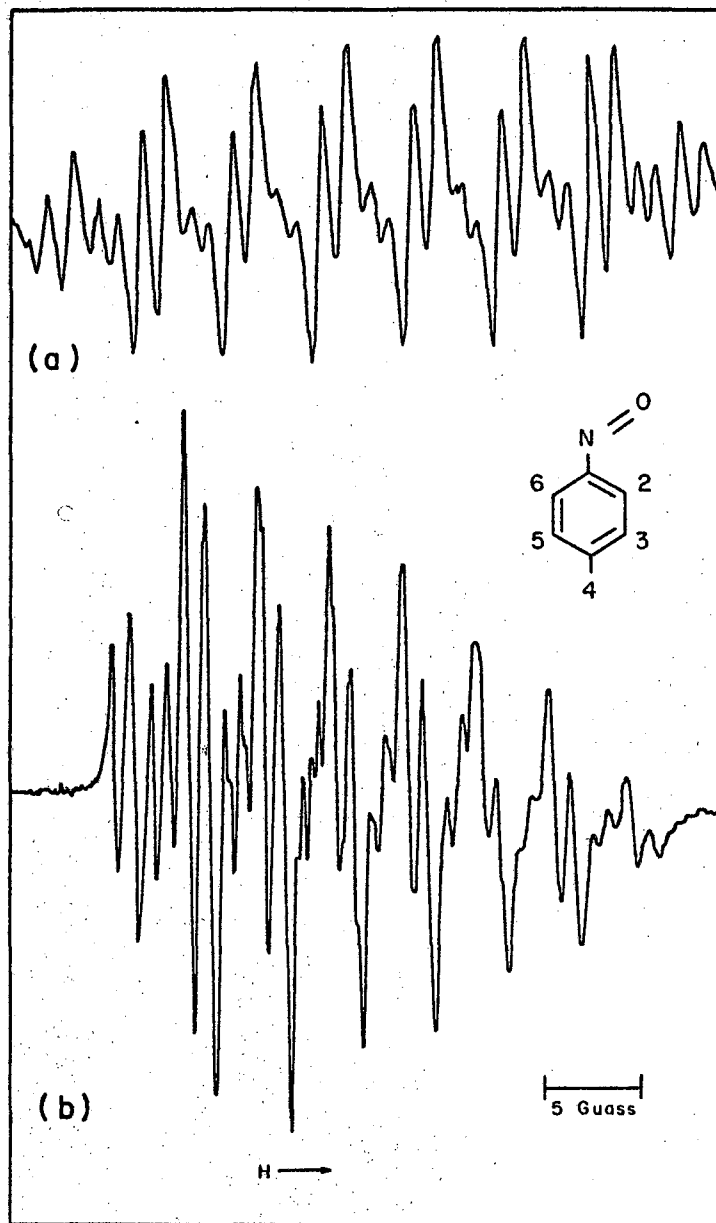
consisting of 30 lines was obtained in DMSO with about 2 volts across the platinum electrodes. The center line of the outermost 1:2:1 triplet is broadened due to a small nonequivalence of the two protons causing the triplet splitting.

For the THF experiment, the electrolysis cell containing 0.02 mmoles of nitrosobenzene and 1 mmole TBAP was evacuated and 10 ml of dry THF was distilled in. ESR signals were observed at 5.6 volts, however, it was found that an improved signal resulted when the voltage was raised to as much as 15 volts. At room temperature the spectrum in THF shows a very pronounced broadening of the high field lines. The ratio of intensities of low field to high field for equally probable lines is about 2 to 1. As the solution temperature is lowered slightly, the high field lines become broader until eventually the hyperfine structure is no longer discernible in the outer two groups. In the room temperature spectrum a difference of about 0.25 gauss in the strongest 1:2:1 triplet is resolved where some of the inner lines are not broadened by other overlap or other splittings.

In either DMSO or THF the radical begins to decay as soon as the voltage is turned off. This is in contrast to the liquid ammonia system in which the nitrosobenzene radical anions are quite stable.⁶¹ Figure 11a,b shows the spectra recorded in DMSO and THF.

2.5 Discussion of Phenomena Observed in Liquid Ammonia Electrolyses

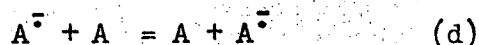
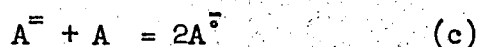
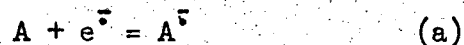
In the liquid ammonia electrolyses described above, most of the interesting reactions occur in a small area above the cathode (a platinum bead sealed in the bottom of a 4 mm quartz tube). The volume involved is roughly 2% of the total solution volume. The processes of interest



XBL 677-3698

Fig. 11 The ESR spectrum of the radical anion of nitrosobenzene (a) in DMSO (b) in THF

are equilibria of the sort:



where A represents the parent compound of interest and $e^{\cdot-}$ is the "solvated electron" in all of its possible forms. There are also the irreversible decay processes such as:



The products are in general unknown, but the importance of these processes is to cause additional decrease in concentrations of $A^{\cdot-}$ and A^{2-} . The concentration of $e^{\cdot-}$ can be controlled by adjusting the current passing through the electrolytic cell. The parent compound concentration at the cathode is determined variously by the initial concentration, the rate at which it is being used up and the rate of diffusion from the bulk solution into the cathode area. Constants for the equilibria (a) - (c) are functions of the reduction potentials and solvation energies of the species involved.

With preceding considerations as a guide, one can propose probable explanations of the phenomena observed during electrolyses of the various nitrogen heterocyclics. The decrease in radical anion concentration at higher current levels can be attributed to dianion formation. An increase in electron concentration coupled with an increase in the concentration of radical anion and/or a decrease in parent compound concentration in sufficient amount would favor reaction (b) instead of (a). The dianion

is also a likely species to yield the monoanion when the electron concentration is drastically reduced. The decay of the dianion could proceed either by (b) reversed or by (c). Both are possible depending upon the relative amount of A. Another question of interest concerns the formation of pyridine and picoline from the respective N-oxides. The high current level necessary to bring about the deoxygenation together with the proposal that prolonged electrolysis at a high current level results in the formation of the dianion suggest that the dianion is an intermediate in this process.

The width of the lines in an ESR spectrum can often give information about the processes going on in a solution. If the exchange reaction (d) took place with a frequency on the order of 10^6 sec^{-1} it would make a significant contribution to the line width of many organic radical anions (which typically have line widths of 0.1 to 1 mc). If the concentration of parent molecule were to decrease by a large factor the exchange rate would also drop and there would be a corresponding decrease in the line width of the spectrum. The decrease in line width in the spectra of radical anions in liquid ammonia observed at increasing current levels is evidence for a line width contribution of this sort.

3. NITROGEN HYPERFINE COUPLING PARAMETERS

3.1 Experimental Determination of the Parameters Q_N^N and Q_{CN}^N

The equation (Eq. 4) derived by Karplus and Fraenkel³³ for the interpretation of C-13 hyperfine coupling constants have been adapted to explain N-14 coupling in a variety of situations.^{13,67,68} For molecules in which the nitrogen atom is bonded to two carbon atoms the N-14 hyperfine splitting is to first order bilinear in ρ_N (the electron spin density on the nitrogen atom) and $\rho_C + \rho_C'$ (the electron spin densities on the carbon atoms bonded to the nitrogen) and can be written

$$A(N) = (S^N + 2Q_{NC}^N) \rho_N + Q_{CN}^N (\rho_C + \rho_C') \quad (5)$$

where S^N represents the contribution of nonbonding electrons including the $1s_N$ and the lone pair electrons. The constant Q_{NC}^N represents the contribution due to electrons associated with the carbon-nitrogen bonds. We shall replace the quantity $(S^N + 2Q_{NC}^N)$ by a single symbol Q_N^N since the two contributions are not separable in the present series of compounds. The quantity Q_N^N would have different components and hence a different numerical value if derived for a nitrogen atom in a different molecular framework and possibly in very different solvents.

There are many determinations of the parameters Q_N^N and Q_{CN}^N in the literature. These are summarized in Table IV. These calculations all involved data from molecules containing one or more positions of unknown spin density. The numbers presented are therefore dependent on the reliability of molecular orbital calculations and on an estimate of Q_{CH}^H , the parameter in McConnell's Eq. (3).

Table IV. Experimental determinations of nitrogen spin polarization parameters.


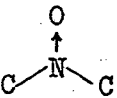
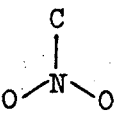
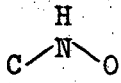

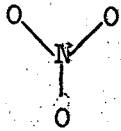
| Nitrogen Framework | Q_N^N | Q_{CN}^N | Q_{ON}^N | Data and Method | Reference |
|---|---------|--------------|-------------------|---|---------------------------------------|
| | | <u>Gauss</u> | | Radical Anions of: | |
| | +25±2 | ~0 | -- | pyrazine, 4,4'-dipyridyl, phenazine quinoxaline, tetraazaanthracene: | Carrington and dos Santos Veiga (10). |
| | +21 | +7 | -- | pyrazine, 4,4' dipyridyl | Ward (11) |
|  | +28.4 | -1.5 | -- | pyrazine, 3,5 lutidine: Q_{CH}^H & $Q_{CH_3}^{CH_3}$ | Atherton et. al. (59a) |
| | +19.1 | +9.1 | -- | pyrazine, 4,4'-dipyridyl 1,4- and 1,5-diazaphthylene | Henning (13) |
| | +30.9±2 | -2±4 | -- | pyrazine, phenazine | Stone and Maki (68) |
| | (a) | -4 | -- | 2,2' dipyrimidine | Geske (17) |
| | +27.3 | -1.7 | -- | pyridine, pyrazine, pyrimidine | This work (6) |
|  | +36 | -- | +1.38 to -0.98 | diphenylnitroxide solvent effect data | Ayscough and Sargent (62) |
| | ±50±8 | | ±65±25 | pyridine N-oxide, 4-picoline N-oxide, 2,6-lutidine N-oxide | This work |
|  | ±99 | -- | ±36 | substituted nitrobenzenes | Reiger and Fraenkel (67) |
| | -- | -- | +37 | solvent effect: p-substituted nitro benzenes | Pannell (82) |

Table IV. (Continued)

| Nitrogen Framework | Q_N^N | Q_{CN}^N | Q_{ON}^N | Data and Method | Reference |
|---|--|------------|--|--|---------------------------|
|  | + 25 | -- | -0.96 | monophenyl nitroxide: solvent effect | Ayscough and Sargent (62) |
|  | + 24 ^(c) + 18 ^(d) | -- | -2 ^(c) +9 ^(d) | nitroso benzene solvent effect | This work |
|  | -- | -- | -3.7 | NO ₃ $Q_{NO}^N = +7$ to 20 deduced from nitroxides, nitroaromatics and NO ₂ ⁻² | Gross and Symons (81) |

(a) Assumed value of Ref. 17.

(b) Using only Eqs. (6) and (7) and assuming that $A(3) < 0$ for pyridine which gives $Q_{CH}^H = -24.5$ gauss.

(c) Using "β" effect type calculation.

(d) Using "Q" effect type calculation.

Using only the coupling constants for the pyridine, pyrazine and pyrimidine radical anions it is possible to calculate values for Q_N^N and Q_{CN}^N , as well as to determine a value for Q_{CH}^H . The major assumption underlying this determination is the validity of Eqs. (3,5). The calculation involved the simultaneous solution of equations of the type:

$$A(N) = Q_N^N \left(1 - \sum_i A(i)/Q_{CH}^H\right) + Q_{CN}^N \left(\sum_s A(s)/Q_{CH}^H\right) \quad (6)$$

$$A(N) = 1/2 Q_N^N \left(1 - \sum_i A(i)/Q_{CH}^H\right) + Q_{CN}^N \left(\sum_s A(s)/Q_{CH}^H\right) \quad (7)$$

where i is summed over all carbon atoms in the ring and s is summed over the carbon atoms adjacent to the nitrogen atom in question. Equation (6) applies to the pyridine radical anion and Eq. (7) applies to the pyrazine and pyrimidine radical anions. The assumption that $\sum_j \rho_j = 1$ (j is summed over all atoms in the ring) is implicit in the derivation of Eqs. (6) and (7).

In these equations one must know the sign of each coupling constant while the ESR data only determine the magnitudes. It is well known that Q_{CH}^H is negative and the sign of $A(N)$ appears to be positive^{39,40} in most situations. In the case of the pyrimidine radical anion, simple Hückel theory places a node at carbons 2 and 5, but calculations using McLachlan USCF approximations yield a small negative spin density. It was assumed that $A(2)$ and $A(5)$ are positive for pyrimidine. The only other positions where the sign of A is questionable are the 3,5 positions of pyridine. Hückel and USCF type calculations give contradictory answers. If Eqs. (6) and (7) are solved assuming $A(3) > 0$ for pyridine one obtains $Q_N^N = +27.7$, $Q_{CN}^N = +6.4$ and $Q_{CH}^H = -17.5$ gauss.

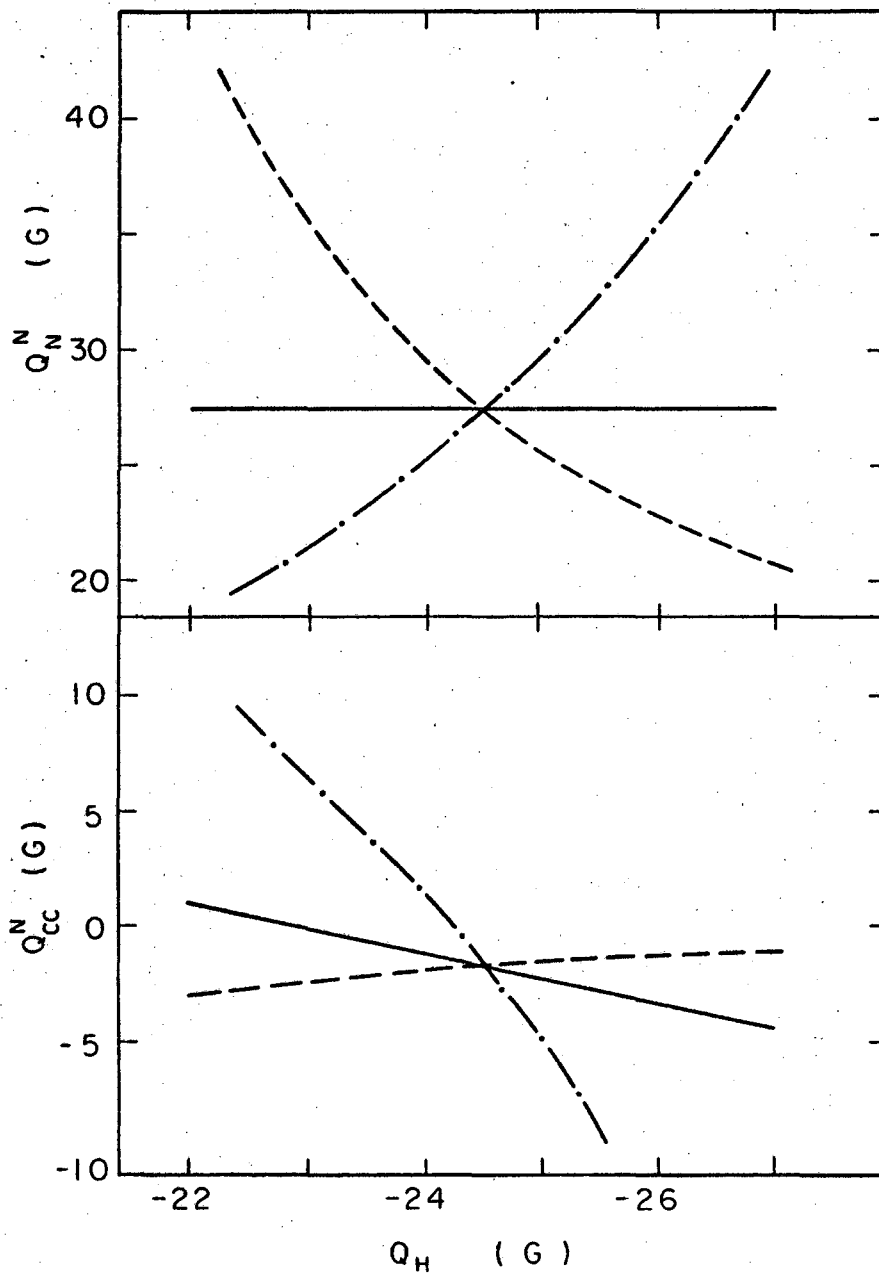
While the nitrogen Q values are reasonable, Q_{CH}^H is not. On the other hand, if $A(3) < 0$ for pyridine is assumed, then one obtains the values listed in Table II together with a very reasonable $Q_{CH}^H = -24.5$ gauss.

Additional insight into the probable errors, involved when one or more parameters must be estimated, is shown in Fig. 12. The three radical anions, pyridine, pyrazine, and pyrimidine are utilized in pairs in Eqs. (6) and (7) to solve for Q_N^N and Q_{CN}^N as a function of Q_{CH}^H . It can be seen that the pairs pyrimidine and pyrazine for Q_N^N and pyrimidine and pyridine for Q_{CN}^N give solutions which are largely independent of Q_{CH}^H . This increases the confidence within the accuracy of Eqs. (3) and (5), in the values of Q_N^N and Q_{CN}^N . A second pair, as shown in Fig. 12, selects with some precision the exact value of $Q_{CH}^H = -24.5$ gauss. The value of Q_{CN}^N is very close to zero and it confirms the approximate determinations of References 10, 59, 68, and 69. (Henning¹³ obtained the larger positive value for Q_{CN}^N using "corrected" Hückel spin densities.) Since the above determinations are essentially independent of any molecular orbital theory and are only a test of Eqs. (3) and (5), it would seem that the best possible values for Q_N^N and Q_{CN}^N for this type of nitrogen heterocyclic compound have now been established.

3.2 Theoretical Calculation of the Parameters

$$\underline{Q_N^N, Q_{CN}^N, \text{ and } Q_{ON}^N}$$

In addition to the variety of experimental determinations of the parameters Q_N^N and Q_{CN}^N that has been previously discussed, there are many and more diverse estimates of the parameters Q_{ON}^N and Q_N^N for molecules containing nitrogen oxygen bonds. (See Table IV.) The number of unknown



MUB14131

Fig. 12 The determination of Q values by pair-wise solution of Eqs. (3) and (4).

- Pyridine plus pyrimidine
- Pyrazine plus pyrimidine
- .-.- Pyridine plus pyrazine

quantities involved in the determination of nitrogen hyperfine coupling parameters increases when oxygen atoms are added to the system, and no additional data are available since the common oxygen isotope does not have a nuclear spin.

Since there appears to be no attempt at a systematic theoretical examination of the hyperfine coupling parameters of nitrogen other than in the $\cdot\text{NH}_2$ or $\cdot\text{NH}_3^+$ radicals, it seemed appropriate to attempt such a calculation. Four types of molecules were considered: pyridine, pyridine N-oxide, nitrosobenzene, and nitrobenzene. The usual approximation, that it is only necessary to consider the nitrogen atom and the 2 or 3 atoms to which it is bonded, was invoked.

The coupling constant $A(\bar{x})$ due to interaction of the unpaired electron with any magnetic nucleus \bar{x} , as measured in an ESR spectrum is equal to the separation between hyperfine lines corresponding to a difference of ± 1 in the nuclear magnetic quantum number $M_I(\bar{x})$. It can be seen from Eqs. (1c) and (2) that $A(\bar{x})$ can be expressed in terms of the ground state wave function ψ as follows

$$A(\bar{x}) = a(\bar{x})/2 \langle \psi | \sum_k \delta(r_{\bar{x}k}) S_z(k) / M_S | \psi \rangle \quad (8)$$

$$a(\bar{x}) = 16\pi/3 g_e \beta_e g_x \beta_x$$

M_S is the total electron z component of the ground state wave function:

$M_S = \langle \psi | \sum_k S_k(z) | \psi \rangle / \langle \psi | \psi \rangle$ and $\delta(r_{\bar{x}k})$ is the Dirac delta function of the distance between electron k and the nucleus \bar{x} . The term

$\langle \psi | \sum_k \delta(r_{\bar{x}k}) S_z(k) / M_S | \psi \rangle$ measures the electron spin density at the nucleus

\bar{x} .

3.2.1 Format for the Calculation

Calculation of $A(x)$ was carried out using LCAO-MO formalism. Slater type atomic orbitals, with and without orthogonalized 2s orbitals (STO and STO^\dagger) and hydrogen like orbitals (HO), were employed at various stages as will be indicated. The exact forms of these orbitals for nitrogen, carbon, and oxygen atoms are given in Appendix I. For each atom sp^2 hybridization with all angles equal to 120° was assumed. The internuclear distances assumed for the four molecules are shown in Fig. 13 (Appendix I). The nitrogen atomic orbitals, n_x, n_y, n_z , are the hybrid orbitals directed toward atoms s, y, and z (n_u is the orbital occupied by the lone pair in pyridine and nitrosobenzene) and c_n, ox_n are the carbon and oxygen hybrids directed toward the nitrogen atom. Bonding and antibonding orbitals (Eq.9)

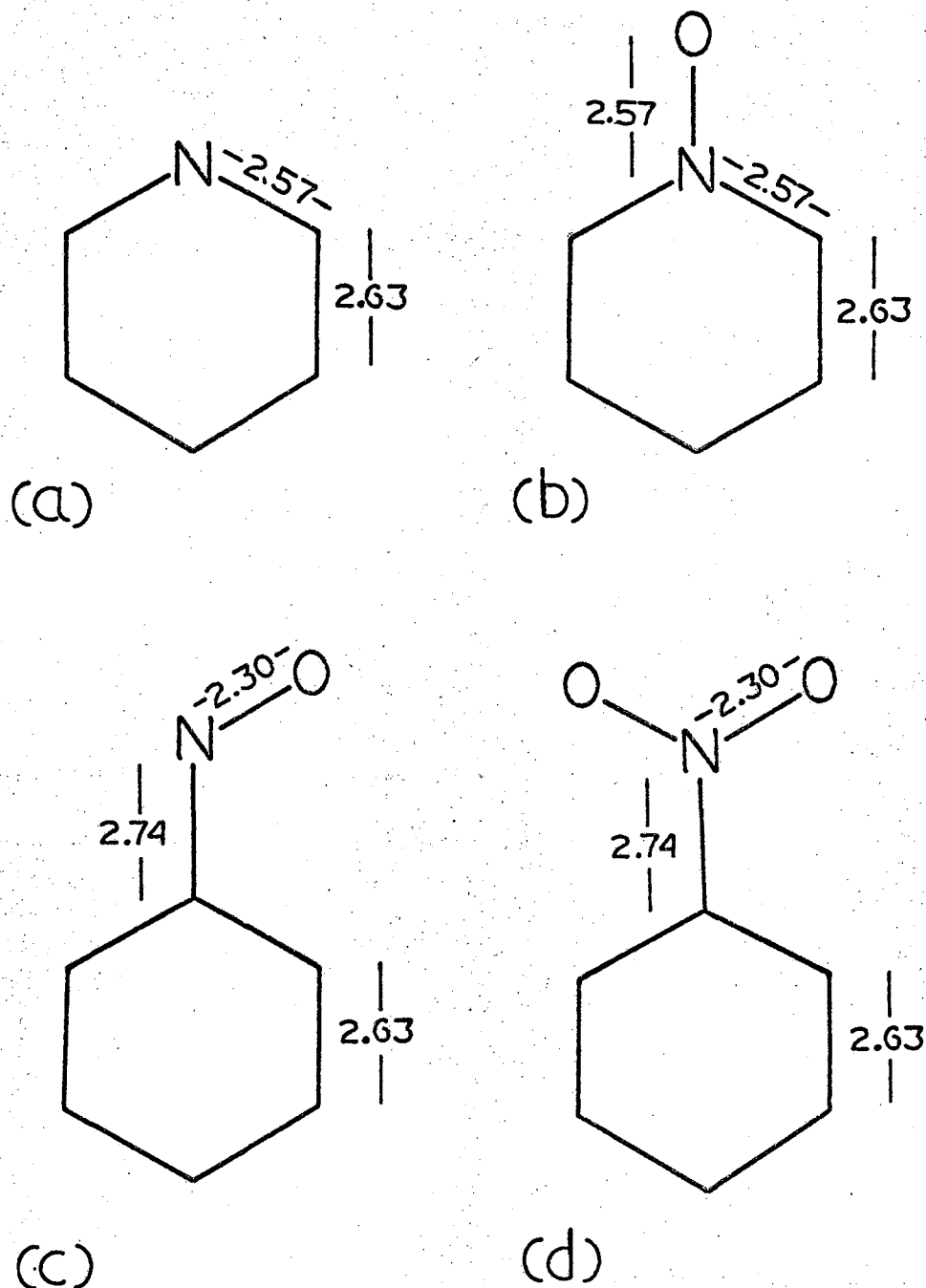
$$\sigma_{nx} = \frac{n_x + x_n}{(2+2S_{nx})^{1/2}} \quad \sigma_{nx}^* = \frac{n_x - x_n}{(2-2S_{nx})^{1/2}} \quad (9)$$

were formed from the atomic hybrids assuming purely covalent bonds. This reduces the complexity of the problem and the introduction of small amounts of ionic character does not appear to have significant effect on the results. S_{nx} is the overlap integral $\langle n_x | x_n \rangle$ between the orbitals n_x and x_n .

The zero order ground state wave function (Eq. 10) was taken to be an antisymmetrized product of spin orbitals.

$$\psi_0 = \left\| 1s_n \bar{1}s_n \sigma_n \bar{\sigma}_n \sigma_{na} \bar{\sigma}_{na} \sigma_{nb} \bar{\sigma}_{nb} \sigma_{nc} \bar{\sigma}_{nc} \pi_0 \right\| \quad (10)$$

The double vertical bars represent a Slater determinant, π_0 is the pi molecular orbital occupied by the odd electron, and the spin orbitals ϕ and $\bar{\phi}$ are functions with the spatial character described above, having



XBL 679-4946

Fig. 13 Geometries (a) Pyridine, (b) Pyridine-N-oxide, (c) Nitrosobenzene, (d) Nitrobenzene. Distances are in atomic units: 1 au = 0.529Å. All interior angles are assumed to be 120° except \angle CNO for nitrosobenzene which is taken as 116° in the USCF calculations.

eigenvalues of S_z equal to $\pm 1/2$, respectively. (For pyridine and nitrosobenzene σ_{nc} is replaced by n_u^* .)

Many authors have observed that the use of ψ_0 in Eq. (8) results in the prediction that $A(x) = 0$. Therefore, configuration interaction was employed using 1st order perturbation theory and the $1/r_{1j}$ term of the Hamiltonian to mix excited states with ψ_0 .

When only configurations involving single excitations of the type σ_x ($= \sigma_{nx}, n_u$ or $1s_n$) $\rightarrow \sigma_{ny}^*$ are considered, each excitation gives rise to two doublet states only one of which contributes to the spin density at the nucleus. By replacing the sigma part of the wave function, not involved in the excitation, by $\Sigma(x \rightarrow y)$ this doublet can be written:

$$\psi(x \rightarrow y) = \frac{1}{\sqrt{6}} \left\{ 2 \|\Sigma(x \rightarrow y) \sigma_x \sigma_{ny}^* \pi_0\| - \|\Sigma(x \rightarrow y) \bar{\sigma}_x \sigma_{ny}^* \pi_0\| - \|\Sigma(x \rightarrow y) \sigma_x \bar{\sigma}_{ny}^* \pi_0\| \right\} \quad (11)$$

The ground state wave function now becomes

$$\psi = \psi_0 - \sum_{(x \rightarrow y)} \frac{\left\langle \psi_0 \left| \frac{1}{r_{1j}} \right| \psi(x \rightarrow y) \right\rangle}{\Delta E(x \rightarrow y)} \psi(x \rightarrow y); \quad (12)$$

where $\Delta E(x \rightarrow y)$ is the excitation energy corresponding to the process

$\sigma_x \rightarrow \sigma_{ny}^*$.

By combining Eqs. (8) and (12) and writing π_0 in terms of the atomic pi orbitals $\pi_0 = \sum_j a_{0j} P_j$, the expression for $A(N)$ reduces to:

$$A(N) = a(N) \sum_{ij} \left(\rho_{ij} \sum_{\{x,y\}} Q_{ij}^N(x \rightarrow y) \right) \quad (13)$$

where:

$$Q_{ij}^N(x \rightarrow y) = \frac{\langle \sigma_x P_{\pi i} | \sigma_{ny}^* P_{\pi j} \rangle}{\Delta E(x \rightarrow y)} \left(\sigma_x(r_N = 0) \cdot \sigma_{ny}^*(r_N = 0) \right) \quad (14)$$

$$\rho_{ij} = a_{0i} a_{0j} \quad (14)$$

and

$$\langle \Phi_i \Phi_j | \Phi_k \Phi_l \rangle = \langle \Phi_i(1) \Phi_k(2) | \frac{1}{r_{12}} | \Phi_j(1) \Phi_l(2) \rangle$$

The calculation can now be divided into three parts; evaluation of the integrals $\langle \sigma_x P_{\pi i} | \sigma_{ny}^* P_{\pi j} \rangle$, estimation of the excitation energies $\Delta E(x \rightarrow y)$, and determination of the quantity $(\sigma_x(r_N = 0) \cdot \sigma_{ny}^*(r_N = 0))$. The results are shown in Table V and a discussion of the above problems follows.

3.2.2 Evaluation of Two Electron Integrals

It was necessary to determine the values for four sets of heteronuclear diatomic integrals: Pyridine N-C integrals ($r_{NC} = 2.57$ a.u.), Pyridine N-oxide N-O integrals ($r_{NO} = 2.57$ a.u.), Nitrosobenzene N-C integrals ($r_{NC} = 2.74$ a.u.), and Nitrosobenzene N-O integrals ($r_{NO} = 2.30$ a.u.). Hybrid integrals were approximated using Mulligan's adaptation of the Sklar approximation for heteronuclear diatomic molecules.^{70,71}

The approximation is formulated as follows:

$$\left\langle \begin{matrix} \alpha \phi_i & \alpha \phi_j \\ a & a \end{matrix} \middle| \begin{matrix} \alpha \phi_k & \beta \phi_l \\ a & b \end{matrix} \right\rangle = \frac{\left\langle \begin{matrix} \alpha \phi_k & \beta \phi_l \\ a & b \end{matrix} \right\rangle}{\left\langle \begin{matrix} \alpha \phi_k & \alpha \phi_l \\ a & b \end{matrix} \right\rangle} \left\langle \begin{matrix} \alpha \phi_i & \alpha \phi_j \\ a & a \end{matrix} \middle| \begin{matrix} \alpha \phi_k & \alpha \phi_l \\ a & b \end{matrix} \right\rangle \quad (15)$$

where $\alpha \phi_i$ is the atomic orbital (i) centered on atom (a) with orbital exponent (α). In cases where the overlap integral is zero, for example when $k = 2s$ and $l = P_{\pi}$, the overlap integral is replaced by the xz

Table V: Theoretical calculation of nitrogen spin polarization parameters.

Parts Ia-IVa: Contributions of excited configurations to Q values for specific molecules.^(a)
 Parts Ib-IVb: Determination of Q values.

| Part Ia: Pyridine | | | | | | |
|-------------------|-----------------|--|--|--|--|--|
| I | II | III | IV | V | VI | VII |
| σ_x | σ_{ny}^* | $\Delta E(\sigma_x \rightarrow \sigma_{ny}^*)$ | $\sigma_x(r_n=0) \cdot \sigma_{ny}^*(r_N=0)$ $\left. \begin{array}{l} \text{STO}^\dagger \\ \text{HO} \end{array} \right\}$ | $\langle \sigma_x P_{\pi N} \sigma_{ny}^* P_{\pi N} \rangle$ $Q_{NN}(\sigma_x \rightarrow \sigma_{ny}^*)$ $\left. \begin{array}{l} \text{STO}^\dagger \\ \text{HO} \end{array} \right\}$ | $\langle \sigma_x P_{\pi C} \sigma_{ny}^* P_{\pi C} \rangle$ $Q_{CC}(\sigma_x \rightarrow \sigma_{ny}^*)$ $\left. \begin{array}{l} \text{STO}^\dagger \\ \text{HO} \end{array} \right\}$ | $\langle \sigma_x P_{\pi O} \sigma_{ny}^* P_{\pi O} \rangle$ $Q_{OO}(\sigma_x \rightarrow \sigma_{ny}^*)$ $\left. \begin{array}{l} \text{STO}^\dagger \\ \text{HO} \end{array} \right\}$ |
| σ_{NC} | σ_{NC}^* | 1.44 | 1.205 0.543 | 0.0331 0.028 0.0125 | -0.0291 -0.024 -0.0108 | ----- ----- ----- |
| n_u | σ_{NC}^* | 0.25-0.30 | 2.36 1.06 | 0.00975 0.084 0.038 | -0.00423 -0.036 -0.016 | ----- ----- ----- |
| $1s_N$ | σ_{NC}^* | 16.8 | -17.45 -11.05 | 0.00985 -0.0102 -0.0065 | ----- ----- ----- | ----- ----- ----- |
| σ_{NC} | σ_{NC}^* | 1.73 | 1.205 0.543 | 0.0268 0.0187 0.0084 | -0.0015 -0.0010 -0.0005 | ----- ----- ----- |

Table V (continued)

Part IIa: Pyridine N-oxide

| I | II | III | IV | V | VI | VII |
|----------------------|------------------------|------|------------------|------------------------------|-------------------------------|-------------------------------|
| σ_{NC} | σ_{NC}^* | 1.44 | 1.205 0.543 | 0.0331 0.028 0.0125 | -0.0291 -0.024 -0.0108 | -0.0002 -0.0002 -0.0001 |
| σ_{NO} | σ_{NO}^* | 1.33 | 1.07 0.482 | 0.0398 0.032 0.014 | -0.0008 -0.0006 -0.0003 | -0.0457 -0.034 -0.017 |
| $1s_{\text{N}}$ | σ_{NC}^* | 16.8 | -17.45 -11.05 | 0.0098 -0.0102 -0.0065 | ----- ----- ----- | ----- ----- ----- |
| $1s_{\text{N}}$ | σ_{NO}^* | 15.6 | -14.7 - 9.33 | 0.013 -0.012 -0.0078 | ----- ----- ----- | ----- ----- ----- |
| σ_{NC} | σ_{NC}^* | 1.73 | 1.205 0.543 | 0.0268 0.019 0.0084 | -0.0015 -0.0010 -0.0005 | -0.0022 -0.0015 -0.0007 |
| σ_{NO} | σ_{NC}^* | 2.69 | 1.25 0.562 | 0.0147 0.0068 0.0031 | -0.0215 -0.010 -0.0045 | -0.0011 -0.0005 -0.0002 |
| σ_{NC} | σ_{NO}^* | 0.45 | 1.036 0.466 | 0.0334 0.077 0.035 | -0.0123 -0.028 -0.013 | -0.0011 -0.0025 -0.0011 |

Table V (Continued)

| I | II | III | IV | V | VI | VII |
|----------------------------------|------------------------|-----------|------------------|------------------------------|-------------------------------|-------------------------------|
| <u>Part IIIa: Nitrosobenzene</u> | | | | | | |
| σ_{NC} | σ_{NC}^* | 1.89 | 1.113 0.502 | 0.0367 0.022 0.010 | -0.0306 -0.018 -0.008 | 0.0003 0.0002 0.0001 |
| σ_{NO} | σ_{NO}^* | 2.41 | 1.142 0.515 | 0.0371 0.018 0.008 | -0.0007 -0.0003 -0.0001 | -0.0393 -0.019 -0.0084 |
| n_u | σ_{NC}^* | 0.25-0.30 | 1.003 0.451 | 0.0137 0.050 0.023 | -0.0031 -0.011 -0.005 | 0.0002 0.0008 0.0004 |
| n_u | σ_{NO}^* | 0.25-0.30 | 1.04 0.467 | 0.0214 0.080 0.038 | -0.0021 -0.008 -0.0036 | 0.0009 0.0035 0.0016 |
| $1s_{\text{N}}$ | σ_{NC}^* | 17.2 | -15.5 -9.82 | 0.0113 -0.0102 -0.0064 | --- | --- |
| $1s_{\text{N}}$ | σ_{NO}^* | 16.3 | -16.02 -10.16 | 0.0112 -0.011 -0.0069 | --- | --- |
| σ_{NC} | σ_{NO}^* | 1.37 | 1.18 0.531 | 0.0303 0.026 0.012 | --- | -0.0016 -0.0014 -0.0006 |
| σ_{NO} | σ_{NC}^* | 3.63 | 1.105 0.497 | 0.0206 0.0062 0.0028 | -0.0011 -0.0003 -0.0001 | -0.0009 -0.0003 -0.0001 |

Table V (continued)

| I | II | III | IV | V | VI | VII |
|------------------------|------------------------|------|------------------|------------------------------|-------------------------------|-------------------------------|
| Part IVa: Nitrobenzene | | | | | | |
| σ_{NC} | σ_{NC}^* | 1.89 | 1.113 0.502 | 0.0367 0.022 0.010 | -0.0306 -0.018 -0.008 | 0.0003 0.0002 0.0001 |
| σ_{NO} | σ_{NO}^* | 2.41 | 1.142 0.515 | 0.0371 0.018 0.008 | -0.0007 -0.0003 -0.0001 | -0.0393 -0.019 -0.0084 |
| $1s_{\text{N}}$ | σ_{NC}^* | 17.2 | -15.5 -9.82 | 0.0113 -0.0102 -0.0064 | --- | --- |
| $1s_{\text{N}}$ | σ_{NO}^* | 16.3 | -16.02 -10.16 | 0.0112 -0.011 -0.0069 | --- | --- |
| σ_{NC} | σ_{NO}^* | 1.37 | 1.18 0.531 | 0.0303 0.026 0.012 | --- | -0.0019 -0.0016 -0.0007 |
| σ_{NO} | σ_{NC}^* | 3.63 | 1.65 0.497 | 0.0206 0.0062 0.0028 | -0.0011 -0.0003 -0.0001 | -0.0002 -0.0004 -0.0002 |
| σ_{NO} | σ_{NO}^* | 2.61 | 1.142 0.515 | 0.0252 0.0110 0.0050 | -0.0021 -0.0009 -0.0004 | -0.0004 -0.0002 -0.0001 |

Table V (Continued)

| VIII | IX | X |
|---|--|---|
| Q_N^N : Expression = | Q_{CN}^N : Expression = | Q_{ON}^N : Expression = |
| Calculated Value (in Gauss) | Calculated Value (in Gauss) | Calculated Value (in Gauss) |
| <u>Part Ib: Pyridine</u> | | |
| $2Q_{NN}(\sigma_{NC} \rightarrow \sigma_{NC}^*) + 2Q_{NN}(n_u \rightarrow \sigma_{NC}^*)$ $+2Q_{NN}(1s_N \rightarrow \sigma_{NC}^*) + 2Q_{NN}(\sigma_{NC} \rightarrow \sigma_{NC}^*)$ = 55 (STO [†]), 24 (HO). | $Q_{CC}(\sigma_{NC} \rightarrow \sigma_{NC}^*) + Q_{CC}(n_u \rightarrow \sigma_{NC}^*)$ $+ Q_{CC}(\sigma_{NC} \rightarrow \sigma_{NC}^*)$ = -14(STO [†]), -6.4(HO). | |
| <u>Part IIb: Pyridine n-oxide</u> | | |
| VIII | IX | X |
| $2Q_{NN}(\sigma_{NC} \rightarrow \sigma_{NC}^*) + Q_{NN}(\sigma_{NO} \rightarrow \sigma_{NO}^*)$ $+2Q_{NN}(1s_N \rightarrow \sigma_{NC}^*) + Q_{NN}(1s_N \rightarrow \sigma_{NO}^*)$ $+2Q_{NN}(\sigma_{NC} \rightarrow \sigma_{NC}^*)$ = 60(STO [†]), 25(HO) | $Q_{CC}(\sigma_{NC} \rightarrow \sigma_{NC}^*) + Q_{CC}(\sigma_{NO} \rightarrow \sigma_{NO}^*)$ $+Q_{CC}(\sigma_{NC} \rightarrow \sigma_{NO}^*) + Q_{CC}(\sigma_{NO} \rightarrow \sigma_{NC}^*)$ = -15(STO [†]), -6.5(HO). | $2Q_{OO}(\sigma_{NC} \rightarrow \sigma_{NC}^*) + Q_{OO}(\sigma_{NO} \rightarrow \sigma_{NO}^*)$ $+2Q_{OO}(\sigma_{NC} \rightarrow \sigma_{NO}^*) + 2Q_{OO}(\sigma_{NO} \rightarrow \sigma_{NC}^*)$ = -10(STO [†]), -4.8(HO). |

Table V (Continued)

| VIII | IX | X |
|--|---|---|
| <u>Part IIIb: Nitrosobenzene</u> | | |
| $Q_{NN}(\sigma_{NC} \rightarrow \sigma_{NC}^*) + Q_{NN}(\sigma_{NO} \rightarrow \sigma_{NO}^*)$ $+ Q_{NN}(n_u \rightarrow \sigma_{NC}^*) + Q_{NN}(\sigma_{NO} \rightarrow \sigma_{NO}^*)$ $+ Q_{NN}(1s_N \rightarrow \sigma_{NC}^*) + Q_{NN}(1s_N \rightarrow \sigma_{NO}^*)$ $+ Q_{NN}(\sigma_{NC} \rightarrow \sigma_{NO}^*) + Q_{NN}(\sigma_{NO} \rightarrow \sigma_{NC}^*)$ $= 42(\text{STO}^\dagger), 18(\text{HO}).$ | $Q_{CC}(\sigma_{NC} \rightarrow \sigma_{NC}^*) + Q_{CC}(\sigma_{NO} \rightarrow \sigma_{NO}^*)$ $+ Q_{CC}(n_u \rightarrow \sigma_{NC}^*) + Q_{CC}(n_u \rightarrow \sigma_{NO}^*)$ $+ Q_{CC}(\sigma_{NO} \rightarrow \sigma_{NC}^*)$ $= -8.7(\text{STO}^\dagger), -3.7(\text{HO}).$ | $Q_{OO}(\sigma_{NC} \rightarrow \sigma_{NC}^*) + Q_{OO}(\sigma_{NO} \rightarrow \sigma_{NO}^*)$ $+ Q_{OO}(n_u \rightarrow \sigma_{NC}^*) + Q_{OO}(n_u \rightarrow \sigma_{NO}^*)$ $+ Q_{OO}(\sigma_{NC} \rightarrow \sigma_{NO}^*) + Q_{OO}(\sigma_{NO} \rightarrow \sigma_{NC}^*)$ $= -3.7(\text{STO}^\dagger), -1.7(\text{HO}).$ |

| | | |
|---|---|---|
| <u>Part IVb: Nitrobenzene</u> | | |
| $Q_{NN}(\sigma_{NC} \rightarrow \sigma_{NC}^*) + 2Q_{NN}(\sigma_{NO} \rightarrow \sigma_{NO}^*)$ $+ Q_{NN}(1s_N \rightarrow \sigma_{NC}^*) + 2Q_{NN}(1s_N \rightarrow \sigma_{NO}^*)$ $+ 2Q_{NN}(\sigma_{NC} \rightarrow \sigma_{NO}^*) + 2Q_{NN}(\sigma_{NO} \rightarrow \sigma_{NC}^*)$ $+ 2Q_{NN}(\sigma_{NO} \rightarrow \sigma_{NO}^*)$ $= 26(\text{STO}^\dagger), 10(\text{HO}).$ | $Q_{CC}(\sigma_{NC} \rightarrow \sigma_{NC}^*) + 2Q_{CC}(\sigma_{NO} \rightarrow \sigma_{NO}^*)$ $+ 2Q_{CC}(\sigma_{NO} \rightarrow \sigma_{NO}^*) + 2Q_{CC}(\sigma_{NO} \rightarrow \sigma_{NC}^*)$ $= -4.9(\text{STO}^\dagger), -2.1(\text{HO}).$ | $Q_{OO}(\sigma_{NC} \rightarrow \sigma_{NC}^*) + Q_{OO}(\sigma_{NO} \rightarrow \sigma_{NO}^*)$ $+ Q_{OO}(\sigma_{NC} \rightarrow \sigma_{NO}^*) + Q_{OO}(\sigma_{NO} \rightarrow \sigma_{NC}^*)$ $+ Q_{OO}(\sigma_{NO} \rightarrow \sigma_{NO}^*)$ $= -4.8(\text{STO}^\dagger), -2.2(\text{HO}).$ |

a) All integrals and densities of Columns III-VII are in atom units 1 a.u. = 27.2 e.v.

$$Q(\text{Gauss}) = 233 Q(\text{a.u.}).$$

moment integral $\langle \phi | xz | \phi' \rangle$ for the corresponding charge distribution.

All two electron, two center, homonuclear integrals were taken from the tables of Kopineck,⁷² Kotani,⁷³ and Preuss.⁷⁴ The overlap and moment integrals were calculated using a two center expansion of the atomic orbitals in elliptical coordinates. (See Roothan,⁷⁵ Rudenberg,⁷⁶ or Lothaus^{77a}).

In a similar manner the heteronuclear exchange integrals were approximated by the relation:

$$\begin{aligned} \left\langle \begin{array}{cc|cc} \alpha_\phi & \beta_\phi & \alpha_\phi & \beta_\phi \\ a_i & b_j & a_k & b_l \end{array} \right\rangle &= \frac{\left\langle \begin{array}{cc|cc} \alpha_\phi & \beta_\phi & \alpha_\phi & \beta_\phi \\ a_i & b_j & a_k & b_l \end{array} \right\rangle}{\left(\left\langle \begin{array}{cc|cc} \alpha_\phi & \alpha_\phi & \beta_\phi & \beta_\phi \\ a_i & b_j & a_i & b_j \end{array} \right\rangle \left\langle \begin{array}{cc|cc} \alpha_\phi & \alpha_\phi & \beta_\phi & \beta_\phi \\ a_k & b_l & a_k & b_l \end{array} \right\rangle \right)^{1/2}} \\ &\times \left(\left\langle \begin{array}{cc|cc} \alpha_\phi & \alpha_\phi & \alpha_\phi & \alpha_\phi \\ a_i & b_i & a_k & b_l \end{array} \right\rangle \left\langle \begin{array}{cc|cc} \beta_\phi & \beta_\phi & \beta_\phi & \beta_\phi \\ a_i & b_j & a_k & b_l \end{array} \right\rangle \right)^{1/2} \quad (16) \end{aligned}$$

The exact values for all the pyridine carbon-nitrogen integrals were calculated using the diatomic molecule integral program of Corbato and Switendick,⁷⁸ revised for use on the Bky 7094 by R. N. Kortzeborn. The exact values for the nitrogen-oxygen integrals of NO ($r_{NO} = 2.20$ a.u.) have been reported by Brion et al.⁷⁹ The differences noted between exact and approximate values of the hybrid and exchange integrals are similar in both cases. Therefore adjustment of the approximate values of all four sets of integrals were made, assuming the relative differences between exact and approximate integrals to be constant over the four sets.

In order to determine the heteronuclear coulomb integrals, the assumption was made that the quantity

$$\frac{\langle \alpha_{\phi_i} \alpha_{\phi_j} | \beta_{\phi_k} \beta_{\phi_l} \rangle - \langle \beta_{\phi_i} \beta_{\phi_j} | \beta_{\phi_k} \beta_{\phi_l} \rangle}{\langle \alpha_{\phi_i} \alpha_{\phi_j} | \alpha_{\phi_k} \alpha_{\phi_l} \rangle - \langle \beta_{\phi_i} \beta_{\phi_j} | \beta_{\phi_k} \beta_{\phi_l} \rangle} \quad (17)$$

is constant over the range of parameters involved. This ratio was determined using the exact values of the pyridine nitrogen-carbon integrals for each set (i,j,k,l) not involving $1s_n$. The values for the remaining sets of integrals were then computed. Agreement with the exact integrals for NO was quite good and the approximation was felt to be reasonable. Formulae for computing the two center coulomb integrals are available;^{73,75} however, the approximate nature of the calculation did not seem to justify their use. Coulomb integrals involving $1s_n$ were computed using Roothan's formulae⁷⁵ because the difference in orbital exponents is much larger than for any of the cases not involving $1s_n$ electrons.

All the one center two electron integrals were obtained from the tables of Brion et al.⁷⁹ or those of Mulligan.⁷⁰ Three and four center integrals were neglected. The two electron integral computations involved primarily the use of STO's. It was found that the difference between integrals calculated using STO's and those calculated using STO^+ 's was small in most cases. The significant exceptions were integrals involving the product $1s_n \cdot 2s_n$ and for those integrals, the values calculated using STO^+ 's were taken to be more accurate.

3.2.3 Evaluation of Excitation Energies and of Magnitudes of Wave Functions at the Nitrogen Nucleus

The energy of excitation was calculated for each set $x \rightarrow y$ using the equation:

$$\Delta E(x \rightarrow y) = \langle \psi(x \rightarrow y) | \mathcal{H} + \mathcal{H}' | \psi(x \rightarrow y) \rangle - \langle \psi_0 | \mathcal{H} + \mathcal{H}' | \psi_0 \rangle \quad (18)$$

where \mathcal{H} is the one electron Hamiltonian $\sum_i (-\frac{1}{2} \nabla_i^2 - \sum_x \frac{Z_x}{r_{xi}})$ and \mathcal{H}' is the two electron repulsion term $\sum_{i < j} 1/r_{ij}$. For the specific types of wave functions being considered, the expression for $\Delta E(x \rightarrow y)$ becomes

$$\begin{aligned} \Delta E(x \rightarrow y) = & \langle \sigma_{ny}^* | \mathcal{H} | \sigma_{ny}^* \rangle - \langle \sigma_x | \mathcal{H} | \sigma_x \rangle + \langle \sigma_x \sigma_x | \sigma_{ny}^* \sigma_{ny}^* \rangle - \\ & \langle \sigma_x \sigma_x | \sigma_x \sigma_x \rangle + \langle \sigma_{ny}^* \sigma_{ny}^* - \sigma_x \sigma_x | \pi_0 \pi_0 \rangle + 1/2 \langle \sigma_{ny}^* \pi_0 | \sigma_{ny}^* \pi_0 \rangle + \quad (19) \\ & 3/2 \langle \sigma_x \pi_0 | \sigma_x \pi_0 \rangle - \langle \sigma_x \sigma_{ny}^* | \sigma_x \sigma_{ny}^* \rangle \end{aligned}$$

plus small terms involving $\Sigma(x \rightarrow y)$ which were neglected. The one center integrals were again taken from the papers of Brion and of Mulligan and the two center one electron terms were computed using the formulae of Lofthus^{77b} and of Roothan.⁷⁵ The energies found for the excitations $\sigma_{nx} \rightarrow \sigma_{ny}^*$ and $1s_n \rightarrow \sigma_{ny}^*$ were used in the final calculation of the Q's. However, it was found that the energy of the orbital occupied by the lone pair electrons of pyridine and nitrosobenzene was close to, and in some cases greater than, the energy of the antibonding orbitals. The spectroscopic data available⁸⁰ indicate that there are transitions in the region of 0.25 to 0.3 a.u. that correspond to $n \rightarrow \sigma^*$ type transitions and this energy range was used for $\Delta E(n_c - \sigma_{ny}^*)$.

The quantity $\sigma_{nx}(r_N = 0) \cdot \sigma_{ny}^*(r_N = 0)$ was evaluated using both STO[†]'s and HO's. The value obtained using STO[†]'s was in general about twice as great as that obtained using the HO's. Since there is no a priori reason for choosing one set over the other, the numbers for both cases are included in Table V.

3.2.4 Discussion of Results

The largest contribution to Q_N^N for pyridine and nitrosobenzene comes from the term that corresponds to the $n \rightarrow \sigma^*$ type excitations, the contributions from the $\sigma \rightarrow \sigma^*$ type terms being only 1/3 to 1/4 as great. In pyridine N-oxide, which does not have any unpaired electrons on nitrogen, the major contribution comes from the cross excitation $\sigma_{NC} \rightarrow \sigma_{NO}^*$ because of the predicted small energy difference between the two orbitals. This does not occur in nitrobenzene and all of the contributions are of similar magnitude with the largest contribution predicted to be at most only three times the smallest. In all cases, the contributions from the 1s electrons are of comparable magnitude to the $\sigma \rightarrow \sigma^*$, but of opposite sign.

For pyridine, the contributions to Q_N^N can be grouped in two terms S^N and $2Q_{NC}^N$. S^N includes the $n_c \rightarrow \sigma^*$ and $1s_n \rightarrow \sigma^*$ contributions. Q_{NC}^N is the sum of the remaining $\sigma \rightarrow \sigma^*$ terms involving one of the carbon-nitrogen bonds. From the table it can be seen that S^N accounts for 60 to 70% of Q_N^N and $2Q_{NC}^N$ is about 30 to 40%. Stone and Maki⁶⁸ sorted out the values for several of the nitrogen parameters from the coupling constants of the radical anions of s-tetrazine, pyridazine, phthalazine, phenazine, and the radical cation of di-protopyridazine. They found that $Q_N^N = 31 \pm 2$ gauss, $S^N = 11 \pm 2$ gauss, $Q_{NC}^N = 10 \pm 2$ gauss, $Q_{NN}(1s_b \rightarrow \sigma_{nc}^*) = 5 \pm 6$ gauss, and $Q_{CN}^N = 2 \pm 2$ gauss. With the uncertainty in the 1s contribution S^N could account for as much as 50% of Q_N^N . Considering the wide range of parameter variations possible in the calculation of theoretical values, the agreement is encouraging. The percentages and magnitudes of the values calculated using HO's are closer to the experimental values than those calculated using STO's. The

percentage agreement can be improved either by an increase of $\Delta E(n \rightarrow \sigma^*)$ or a decrease of $\Delta E(\sigma \rightarrow \sigma^*)$, both of which seem reasonable. The sign predicted for the $1s_n$ contribution is in agreement with the sign predicted by Karplus and Fraenkel for the $1s_c$ contribution to the C^{13} hyperfine interaction and the experimental value quoted above gives little evidence to the contrary.

The negative sign predicted for Q_{CN}^N is in agreement with the results of Stone and Maki and with results reported in section 3.1 of this thesis. The magnitude predicted is about twice as large relative to Q_N^N as the value experimentally deduced. The relative magnitude is fairly insensitive to variation of excitation energies, but is dependent on ratios of the type:

$$\frac{\langle n_c^P \pi_n | n_c^P \pi_n \rangle - \langle C_n^P \pi_n | C_n^P \pi_n \rangle}{\langle n_c^P \pi_c | n_c^P \pi_c \rangle - \langle C_n^P \pi_c | C_n^P \pi_c \rangle}$$

The magnitudes predicted for all Q's for nitroso- and nitrobenzene are smaller than the corresponding values for pyridine and pyridine N-oxide. This is due, in the calculation, to the increased excitation energies determined for both the $\sigma_{nc} \rightarrow \sigma_{nc}^*$ and the $\sigma_{no} \rightarrow \sigma_{no}^*$ terms as well as the cross excitation terms. These changes are probably exaggerated and it seems unlikely that the smaller Q's are of any great significance. The value predicted for the parameter Q_{ON}^N is similar to that predicted for Q_{CN}^N for all cases.

The value of $Q_N^N(\phi NO)$ of 18 to 25 gauss (see section 5.5) and the values determined by Ayscough et al.⁶⁰ for $Q_N^N(\phi NHO) = 25$ gauss and $Q_N^N(\phi_2 NO) = 36$ gauss can be compared with the theoretical results

for nitrosobenzene and pyridine N-oxide. Some difference between Q_N^N (ϕNO) and Q_N^N (ϕNHO) would be expected due to the difference between the contribution of the unpaired electrons and that of the electrons in the NH bond. However, it probably is not large. Q_N^N for pyridine N-oxide has also been estimated to be ~ 50 gauss using the ESR data in liquid ammonia combined with MO calculations (see Section 3.3.3). Both theoretical and experimental results indicate that Q_N^N (pyridine N-oxide) is larger than Q_N^N (pyridine). Q_N^N (ϕNO) seems to be less than or about equal to the pyridine value. Gross and Symons⁸¹ sorted out the parameter Q_{NO}^N from data on a variety of radicals and radical ions that contained nitrogen-oxygen bonds. Assuming the $1s_n$ contribution to be ~ 6.3 gauss in all cases (estimated from $Q(1s_c)(\text{SN/gc})$, they determined values for Q_{NO}^N of about 10 to 20 gauss. Combining these data with Maki's estimations of Q_{NC}^N and of the lone pair contribution, Q_N^N (ϕNO) = ($S^N + Q_{\text{NC}}^N + Q_{\text{NO}}^N$) is estimated to be 30 ± 10 gauss. Similarly, Q_N^N (ϕNO_2) is estimated to be $\sim 35 \pm 10$ gauss in contrast to the estimate of Reiger and Fraenkel⁶² of ~ 100 gauss for Q_N^N (ϕNO_2). The experimental estimates seem to confirm the earlier suggestion that theoretical predictions that Q_N^N (ϕNO_2) and Q_N^N (ϕNO) are less than Q_N^N (pyridine) or Q_N^N (pyridine N-oxide) are not of great significance.

The experimental estimates of Q_{ON}^N include Reiger and Fraenkel's of -36 gauss, Ayscough et al. and of Gross and Symons' of -4 to ± 2 gauss, Pannell's⁸² of $\sim +37$ gauss, and the values -65 gauss (pyridine-N-oxide), -2 to $+0$ gauss (ϕNO) of this work. Pannell, Ayscough and this author (for ϕNO values) used the variable oxygen Coulomb integral model for the MO calculations in conjunction with the variation of $A(\text{N})$ with solvent in

order to determine Q_{ON}^N .

The above discrepancies among experimentally determined values for the nitrogen hyperfine coupling parameters has been explained by some authors^{60,81} as being due in part to variations in the configuration of the nitrogen atom between planar and pyramidal hybridization. This is reasonable for small deviations, but is unlikely to account for the spread of values of Q_{ON}^N or even for values of Q_N^N (ϕNO_2) ranging from 35 to 100 gauss, especially since values at both extremes were determined from ϕNO_2 data. From the theoretical point of view, it is likely that not all mechanisms, whereby pi electron density on the oxygen atom polarizes the nitrogen s electrons, have been considered in this simple model.

The factors that multiply the off diagonal spin density matrix elements ρ_{ij} ($i \neq j$) in expression (13) for $A(N)$ were not included in Table V. They are in general positive and of about the same magnitude as Q_{CN}^N and Q_{ON}^N . Terms of this order of magnitude may not be negligible in the interpretation of coupling constants, but the author feels that a much more elaborate treatment of the problem would be necessary in order to make the inclusion of such terms meaningful.

4. THEORETICAL SPIN DENSITIES FOR NITROGEN HETEROCYCLIC RADICAL ANIONS

4.1 Unsubstituted Nitrogen Heterocyclics

4.1.1 McLachlan and Restricted Self Consistent Field Approximations

A number of molecular orbital calculations were carried out using both Hückel and McLachlan approximations^{34,35} in order to see how well simple theory correlates with the experimentally determined spin densities. For the unsubstituted N-heterocyclics the two necessary parameters are δ_N which measures the difference between the carbon and nitrogen coulomb attraction integrals, and β_{CN} the carbon-nitrogen resonance integral, both in units of the carbon-carbon resonance integral. Calculations reported in the literature for excited states and radical anions of similar molecules use values of δ_N ranging from 0.2 to 1.0 and of β_{CN} from 0.8 to 1.2. Pariser and Parr⁸³ determined a semi-empirical value for $\beta_{CN} = 1.076$ by fitting calculations to the electronic spectra of benzene and s-triazine. Using a value of $\lambda = 1$ for the McLachlan parameter, spin densities were calculated for $0.5 < \delta_N < 1.0$ and $0.8 < \beta_{CN} < 1.2$. The Pariser-Parr value for β_{CN} seemed to give the best overall results, with the best value of $\delta_N = 0.80$. It was observed that the difference in the Hückel and McLachlan spin densities corresponded to an over-estimation of the importance of the splitting in the lower "doubly occupied" orbitals. Since the McLachlan parameter λ is fairly arbitrary, λ was reduced to 0.75. This improves the agreement between theory and experiment. In fact, any of the experimental spin densities can be reproduced quite well with only small variations from the "best" set of parameters. Theoretical McLachlan spin densities along with those calculated from experimental coupling constants using

the experimentally determined Q values are listed in Table VI. The agreement is excellent.

A number of other SCF calculations have appeared in the literature treating pyridine, pyrazine and pyrimidine. Nishimoto⁸⁴ lists wave functions for pyridine, pyrazine and s-triazine calculated using an LCAO MO SCF framework in the form proposed by Pople⁸⁵ with $\beta_{CN} = 1.076$, core integrals estimated from ionization potentials, and two center coulomb repulsion integrals based on an inverse separation approximation. Spin densities for the pyridine radical anion can be calculated from the lowest unoccupied orbital of the set using the so-called virtual orbital (VO) approximation. Nagakura⁶⁰ has used these wave functions as a basis set for a configuration interaction approximation to the orbitals for the pyridine radical anion. The CI calculation has very little effect on the spin density distribution, although it does improve energy calculations. Miller et al.⁸⁶ have calculated spin densities for the pyridine and pyrimidine radical anions using both the VO approximation and an open shell (OS) calculation based on SCF orbitals determined for the neutral molecules. Their neutral molecule calculation differs from that of Nishimoto in the inclusion of penetration integrals in the estimation of diagonal matrix elements, theoretical calculation of two center coulomb integrals using Slater type orbitals with adjustable exponent (semiemperically determined), and an exponential expression for β adjusted to fit the Pariser-Parr values for $\beta_{CC}(1.39 \text{ \AA})$ and $\beta_{CN}(1.36 \text{ \AA})$. Bond distances were determined as a function of bond order and iterated to self-consistency for the neutral molecule. Hinchliffe⁸⁷ has calculated spin densities for various radicals including the pyrazine radical anion. He reports values obtained both from open shell SCF and open shell SCF plus CI approximations using core

Table VI. Experimental and Theoretical Spin Densities in N-Heterocyclic Radical Anions

| Radical Anion | Position | Expt. (a) | Theory | | | | |
|---------------|---------------------|-----------|-------------|----------|-------------------------|-------------------------|------------------------|
| | | | McLach. (b) | USCF (c) | $\underline{v_0}^{(d)}$ | $\underline{v_0}^{(e)}$ | $\underline{os}^{(e)}$ |
| Pyridine | N | 0.247 | 0.275 | 0.263 | 0.273 | 0.228 | 0.206 |
| | 2 | 0.145 | 0.153 | 0.142 | 0.114 | 0.120 | 0.079 |
| | 3 | 0.033 | 0.007 | 0.019 | 0.074 | 0.071 | 0.082 |
| | 4 | 0.395 | 0.403 | 0.416 | 0.346 | 0.390 | 0.476 |
| Pyrazine | N | 0.278 | 0.291 | 0.297 | 0.285 | 0.336 | 0.379 |
| | 2 | 0.111 | 0.105 | 0.100 | 0.102 | 0.082 | 0.061 |
| Pyrimidine | N | 0.143 | 0.151 | 0.137 | | 0.181 | 0.187 |
| | 2 | -0.029 | -0.028 | -0.015 | | 0.000 | 0.000 |
| | 4 | 0.398 | 0.402 | 0.408 | | 0.318 | 0.313 |
| | 5 | -0.053 | -0.078 | -0.071 | | 0.000 | 0.000 |
| 4-Picoline | N | 0.227 | 0.263 | | | | |
| | 2 | 0.155 | 0.160 | | | | |
| | 3 | 0.024 | -0.004 | | | | |
| | 4(CH ₃) | 0.415 | 0.433 | | | | |
| 3,5-Lutidine | N | 0.287 | 0.282 | | | | |
| | 2 | 0.130 | 0.163 | | | | |
| | 3(CH ₃) | 0.044 | 0.012 | | | | |
| | 4 | 0.364 | 0.367 | | | | |

Table VI. (Continued)

| Radical Anion | Position | Expt. (a) | Theory | | |
|-------------------------|---------------------|------------|------------------------|----------------------|---------------------|
| | | | McLach. (b) | USCF | |
| Pyridine N-oxide | OX } N } | 0.363 | { 0.065 | 0.057 ^(g) | .155 ^(h) |
| | | | { 0.298 | 0.266 | .226 |
| | 2 | 0.124 | 0.126 | 0.126 | .129 |
| | 3 | 0.019 | 0.015 | 0.012 | .001 |
| | 4 | 0.351 | 0.360 | 0.398 | .358 |
| 4-Picoline N-oxide | OX } N } | 0.350±.012 | { 0.058 | | |
| | | | { 0.284 | | |
| | 2 | 0.136 | 0.135 | | |
| | 3 | 0.008±.002 | -0.002 | | |
| | 4(CH ₃) | 0.362±.010 | 0.392 | | |
| 2,6-Lutidine N-oxide | OX } N } | 0.276±.010 | { 0.054 ⁽ⁱ⁾ | 0.036 ^(j) | |
| | | | { 0.261 | 0.253 | |
| | 2(CH ₃) | 0.160±.005 | 0.134 | 0.148 | |
| | 3 | 0.019 | 0.023 | 0.017 | |
| | 4 | 0.366 | 0.370 | 0.378 | |

a) Experimental spin densities are calculated from the coupling constants using $Q^H = -24.5$ gauss, $Q_N^N = 27.3$ gauss and $Q_{CN}^N = -1.7$ gauss along with the restriction that ρ total = 1. $Q_{CH_3}^{CF_3} = 25$ gauss was used for the N-oxides.

b) See text for discussion of parameters used.

c) Calculation for unsubstituted N-heterocyclics done with $\delta w_N = 1.63$. See text for further discussion of method.

d) References 60 and 84.

e) Reference 86

f) Reference 87

g) Calculated using $\delta w_O = 8.33$; $\delta w_N = 2.1$, $\beta_{NO} = 1.2$.

h) Calculated using $\delta w_O = 7.9$, $\delta w_N = 2.5$, $\beta_{NO} = 1.2$.

i) Calculated using $\delta_O = 1.5$.

j) Calculated using $\delta_O = 2.0$.

integrals estimated from ionization potentials, β values and two center coulomb integrals as proposed by Pariser and Parr,⁸³ and starting orbitals calculated by Hückel theory with $\delta_N = 0.5$ and $\beta_{CN} = 0.8$. The various SCF spin densities are also included in Table VI.

There are some relevant observations that can be made about the MO calculations. First it should be pointed out that spin densities calculated from closed shell SCF wave functions using VO's can be closely reproduced by Hückel orbitals calculated with core integrals related to those used in the SCF calculation. Configuration interaction seems to have very little effect on spin density distribution in a closed shell approximation, while Hinchliffe's calculation seems to indicate that the correction is in the wrong direction in an open shell basis. Similarly the open shell calculation of Miller et al. compared with VO's calculated using the same parameters yields a correction in the wrong direction for both radical anions considered.

4.1.2 Unrestricted Self Consistent Field Approximation

The success of McLachlan's approximate USCF (USCF) calculations in the treatment of heteroatom containing radical anions encouraged further investigation of the USCF treatment of such systems. The method of USCF calculations using LCAO-MO basis functions has been discussed by a number of authors.^{36,88-90} The distinguishing feature is that it allows electrons of different spin to occupy different spatial orbitals, thus accounting for the effects of spin correlation. Applying this method to a basis set consisting of pi atomic orbitals, ϕ_r , two sets of spin molecular orbitals (SMO's) can be formed:

$$\pi_i = \sum_r a_{ri} \phi_r \quad \pi_j = \sum_r b_{rj} \bar{\phi}_r \quad (20)$$

The coefficients a_{ri} and b_{rj} are determined by solving the matrix equations:

$$\mathcal{F} \cdot \vec{a}_i = e_i \cdot \mathcal{S} \cdot \vec{a}_i \quad \text{and} \quad \mathcal{F} \cdot \vec{b}_j = e_j \cdot \mathcal{S} \cdot \vec{b}_j \quad (21)$$

\vec{a}_i and \vec{b}_j are column vectors having components a_{ri} and b_{rj} . \vec{a}_i^* and \vec{b}_j^* are the corresponding row vectors. \mathcal{S} is the overlap matrix which will be taken as the unit matrix in the following development. This is consistent with the usual zero differential overlap approximation made in MO calculations for pi systems.²⁶ The elements of \mathcal{F} and $\bar{\mathcal{F}}$ are determined by the following equations:

$$F_{rs} = H_{rs} - P_{rs} \gamma_{rs} + \delta_{rs} \sum_{t \neq r} (P_{tt} + Q_{tt}) \gamma_{rt} \quad (22a)$$

$$\bar{F}_{rs} = H_{rs} - Q_{rs} \gamma_{rs} + \delta_{rs} \sum_{t=r} (P_{tt} + Q_{tt}) \gamma_{rt} \quad (22b)$$

where:

$$\mathcal{P} = \sum_{i \text{ occ}} \vec{a}_i \cdot \vec{a}_i^* \quad , \quad \mathcal{Q} = \sum_{j \text{ occ}} b_j \cdot b_j^*$$

$$H_{rs} = \langle \phi_r | \mathcal{H}_{\text{core}} | \phi_s \rangle$$

$$\gamma_{rs} = \langle \phi_r \phi_r | \phi_s \phi_s \rangle$$

$$\delta_{rs} = 1, r = s, \quad \delta_{rs} = 0, r \neq s$$

\mathcal{P} and \mathcal{Q} are the pi electron density matrices for electrons having spin of + 1/2 and - 1/2, respectively. $\mathcal{H}_{\text{core}}$ is the effective one electron Hamiltonian:

$$H_{\text{core}} = -1/2 \nabla^2 - \sum_t Z_t / r_t + \text{terms accounting for interaction with uncharged nuclei and the sigma core.}$$

The sum over t includes all nuclei contributing pi electrons and Z_t is the number of pi electrons contributed by atom t .

Single determinant wave functions having the form of antisymmetrized products of unrestricted molecular orbitals (ASP-USCF-MO) are eigenfunctions of the spin operator S_z , but not of the operator S^2 . The ASP-USCF-MO wave function can be expressed as a sum of single determinant wave functions that are eigenfunctions of S^2 . For a wave function having $S_z = 1/2$, the major components of the summation are those corresponding to doublet and quartet states ($S^2 = 3/4$, and $S^2 = 15/4$). A wave function corresponding to a nearly pure doublet state can be projected out of the ASPUSCF-MO using a quartet state annihilation operator. Amos and Snyder^{29,91} have derived expressions for the electron density matrices ρ' and ρ'' corresponding to the projected doublet state wave function.

A program was written (see appendix II) to solve the \mathcal{F} equations by iteration starting with ρ and \mathcal{J} computed from Hückel orbitals and to compute spin densities for the projected doublet states using the equations of Amos and Snyder.

In this initial venture into USCF studies of heteroatom radical anions it seemed practical to use simple and time tested semiempirical values for the various integrals in the equations for the F matrices.

H_{rr} was assumed to have the form:

$$H_{rr} = \delta w_r - \sum_{t \neq r} Z_t \gamma_{rt} \quad (23)$$

where δw_r is the difference in electron affinity between core atom r and aromatic carbon core atom. H_{rs} was set equal to β_{rs} and the values of Pariser and Parr⁸³ were taken for β_{rs} and γ_{rs} . The value of δw_r was taken to be a variable parameter, although experimental electron affinities and ionization potentials were consulted as a first guess. The nitrogen heterocyclic calculations were carried out for $0.75 \leq \delta w_N \leq 1.6$ (δw_N in units of β_{CC}).

The initial HMO calculations were done using the relation proposed by McWeeney⁹² to correlate Hückel type calculations with closed shell SCF calculations. This allows a value for δ_N to be determined from the values assumed for δw_N , Z_N , and γ_{NN} :

$$\delta_N = \delta w_N - 1/2Z_N(\gamma_{NN} - \gamma_{CC}) \quad (24)$$

For the nitrogen heterocyclics; $\delta_N = \delta w_N - 0.37$.

The best overall results were found for $\delta w_N = 1.63$. The spin densities computed for this value are included in Table VI. It can be seen that the general agreement is only slightly better than that for the best set of McLachlan calculations. However the McLachlan calculation involved more adjustable parameters. Varying δw_N from the "best overall" value it is found that the experimental pyrazine spin densities can be predicted exactly using $\delta w_N = 1.88$. Similar agreement is found in the McLachlan approximation using $\delta_N = 0.87$. Using $\delta w_N = 1.68$ for pyridine or $\delta w_N = 1.55$ for pyrimidine, the USCF spin densities predict the experimental values closer than is possible using the three variable parameters in the McLachlan calculation.

Considering the simple approximations made for the F matrix elements and the use of only one variable parameter, the success of these USCF

calculations is encouraging. There are many possible variations to and extensions of this simple treatment; most of which have been included in closed shell SCF calculations or the USCF treatment of hydrocarbon radicals. The term H_{rs} could be treated more rigorously with the inclusion of penetration integrals and a more accurate treatment of the interaction with the charged core atoms represented by the term $Z_t \gamma_{rt}$.^{26,86} Self consistent bond orders with β_{rs} a function of the bond order and computation of γ_{rt} using exact formulae or semiempirical approximations such as those of Nishimoto and Mataga²⁴ are also possibilities. Successful calculations of electronic properties have been reported by authors using various combinations of these approximations.

Another factor to be considered is the validity of the McConnell or Karplus and Fraenkel equations for relating experimental coupling constants to the computed spin densities. Amos and Snyder⁹¹ carried out USCF calculations for many hydrocarbon radicals and radical ions. They found that the computed spin densities were able to predict the proton coupling constants more consistently using either of two modifications of McConnell's equation. Colpa and Bolton^{93a} proposed that the coupling constant should be dependent on charge density as well as spin density and arrived at an equation of the form:

$$A(H) = (Q + K(q_C - 1)) \rho_C \quad (25)$$

where Q and K are constants and q_C is the total pi electron density on the carbon atom. Theoretical values of Q and K were determined by extending McConnell's treatment to include second order effects in the perturbed wave function. Bolton^{93b} has since pointed out errors in the treatment and has redetermined the charge dependence from which he finds

the form of Eq. (25) to be valid. Giacometti et al.⁹⁴ suggested that the proton coupling constant should be a function of the off diagonal spin density terms $\rho_{CC'}$ in the following manner:

$$A(H) = Q\rho_C + K \sum_{C'} \rho_{CC'} \quad (26)$$

where again Q and K are constants and the sum is over all core atoms bonded to the carbon atom in question. An expression of this form can be derived by including the pi orbitals of adjacent atoms in the simple McConnell treatment of the CH fragment.

As was mentioned earlier, there has been much discussion as to the usefulness of wave functions that are not eigenfunctions of S^2 for determining electronic properties. In order to demonstrate the effects of electron spin correlation and the effects of the presence of higher spin states on the spin properties of nitrogen heterocyclic radical anions, the spin densities computed for pyrazine, pyridine, and pyrimidine radical anions (with $\delta w_N = 1.6$) using Hückel, ASP-USCF-MO and projected doublet state wave functions are shown in Table VII. The spin densities computed before annihilation of the quartet component corresponds to an over-estimation of the importance of spin correlation. This is as expected, since the electrons should be more highly spin correlated in the higher spin states. A similar effect was noted in the McLachlan approximation and was corrected by adjusting the value of λ .

4.2 Methyl-Substituted Pyridines: McLachlan Approximations

It can be seen from Table I that methyl group substitution brings about some changes in the spin density distribution of the pyridine framework. Since the McLachlan theory gives a good description of the

Table VII. Effects of spin correlation and high spin components on spin densities calculated for N-heterocyclic radical anions.

| Radical Anion | Position | Expt. (a) | Theory (b) | | |
|---------------|----------|-----------|------------|--------|--------|
| | | | HMO | USCFBA | USCFAA |
| Pyridine | N | .247 | .162 | .294 | .268 |
| | 2 | .145 | .227 | .154 | .139 |
| | 3 | .033 | .027 | -.029 | .020 |
| | 4 | .395 | .326 | .454 | .415 |
| Pyrimidine | N | .143 | .082 | .156 | .141 |
| | 2 | -.029 | .000 | -.038 | -.016 |
| | 4,6 | .398 | .418 | .450 | .402 |
| | 5 | -.053 | .000 | -.174 | -.070 |
| Pyrazine | N | .278 | .175 | .328 | .302 |
| | 2 | .111 | .162 | .086 | .099 |

a) See Table VI.

b) USCF wave functions correspond to $\delta w_N = 1.6$

USCFBA, USCFAA spin densities before and after annihilation of quartet state components respectively.

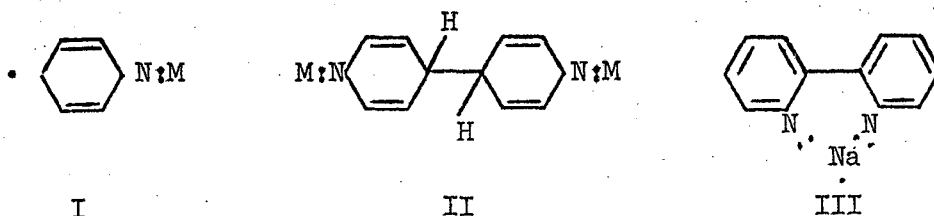
HMO wave functions calculated using $\delta_N = \delta w_N - 0.37 = 1.23$.

unsubstituted radical anions, it is logical to try to include the effects of the methyl groups in this type of calculation. A number of models were tested. For the simple inductive model the parameter δ_C for the carbon atom to which the methyl group is attached was varied over the range $-0.1 \leq \delta_C \leq 0.4$. For the hyperconjugation model without inductive effect the parameters of Coulson and Crawford:⁹⁵ $\beta_{CC'} = 0.76$, $\beta_{C'H} = 2.00$, $\delta_{C'} = -0.1$ and $\delta_H = -0.5$ were used. Here methyl group carbon atom is designated by C' and H is the pi type orbital formed from the hydrogen 1s orbitals. To include the inductive effect in the hyperconjugation model δ_C was varied from -0.1 to -0.5. It was found that the best agreement was obtained when the changes in spin density due to the methyl group were predicted using the hyperconjugation model with $\delta_C = -0.2$. The calculated spin densities are included in Table VI.

The calculation of methyl proton hyperfine splittings is still the subject of some controversy. McLachlan⁹⁶ has suggested that $A(\text{CH}_3)$ is proportional to the spin density on the pi system carbon atom to which the methyl group is bonded. Using valence bond calculations he predicted the proportionality constant to be on the order of 28 gauss. Values ranging from 15 to 30 gauss have been found necessary to explain the observed coupling constants. Levy⁹⁷ derived equations for calculating methyl and methylene group coupling constants from spin densities computed using the hyperconjugation model. Methyl coupling constants were calculated using Levy's equations over the ranges of parameters discussed above. The quantity $Q^{\text{CH}_3} = A(\text{CH}_3)/\rho_t$ was computed for each case. $A(\text{CH}_3)$ is the calculated coupling constant and ρ_t is the total spin density associated with the methyl group: $\rho_t = \rho_C + \rho_{C'} + \rho_H$. Levy's theory

predicts that Q_{CH_3} should be nearly the same for all the substituted pyridine radical anions with an average value of 25 gauss. The corresponding Q 's calculated for the radical cations are predicted to be much larger (on the order of 50 gauss). It has often been found experimentally that for methyl substituted radical cations and radical anions different values of Q_{CH_3} are necessary to explain the observed coupling constants. The variation in Q_{CH_3} might be explained by the fact that the value predicted by Levy's equations is strongly dependent on the amount of spin density in the hydrogen pi orbital. The spin density calculated using the hyperconjugation model is dependent on the shape of the wave function which is quite different for the pyridine radical cation and anion. An experimental value for Q_{CH_3} can be found using the previously determined values of Q_{N}^{N} , Q_{CN}^{N} , and Q_{CH}^{H} to compute the spin densities in the radical anions. Data for the 4-picoline radical anion give $Q_{\text{CH}_3} = 27.3$ gauss; whereas, the 3,5-lutidine radical anion gives $Q_{\text{CH}_3} = 24.1$ gauss. Although the range is greater than that predicted by simple theory, the average of 25.7 gauss is in good agreement with the theoretical value. The discrepancy could in fact be an indication of deviation from the relations assumed in Eqs. (3) and (5).

The variations observed in the 3,5-lutidine radical anion coupling constants in electrolytic and chemical reduction systems remain to be considered. It has been proposed^{11a,98} that the dimerization of pyridine observed in alkali metal/ether systems involves complexes such as I and II. Although the dimerization of 3,5-lutidine is made sterically unfavorable by the the presence of the methyl groups, it is not unlikely that a complex like I would form in the presence



of an alkali metal cation. Further evidence of a nitrogen lone pair electron / alkali metal interaction has been reported by Zahlan et al.⁹⁹ They observed the ESR spectrum of a sodium 2,2'-dipyridyl complex which they suggested has the structure III. This type of interaction would certainly perturb the spin density distribution and would also change the value of Q_N^N . Donation of the lone pair electron to a nitrogen alkali metal bond would in simple theory have the effect of increasing δ_N . With this variation, McLachlan theory does predict changes in spin density in the appropriate directions.

On the other hand, the system pyrazine/alkaline metal/ether has been extensively studied by a number of workers.^{45a,b, 59b, 100} It is found that the pyrazine radical anion coupling constants are independent of cation, temperature, and choice of solvent. Line width alteration and other theoretical and experimental considerations have led to the proposal that the cation is above (or below) the plane of the radical anion rather than in the plane of the anion as is suggested for pyridine and 2,2'-dipyridyl. Calculations by Atherton¹⁰¹ indicate that the interaction is predominantly with the pi-electrons rather than with the nitrogen lone pair electrons. If this is the case, the effect on Q_N^N and on the spin density distribution would be considerably smaller.

4.3 Pyridine N-Oxides

4.3.1 McLachlan Approximation

The calculation of spin densities in the N-oxide radical anions involves the evaluation of a number of parameters. In order to set reasonable limits on the values of δ_N and δ_O Eq. (24) was used. Using the valence state ionization potentials for values of δw_A of Pritchard and Skinner¹⁰² and values of γ_{AA} calculated by Orloff and Sinanoglu,¹⁰³ the following estimates for δ_N and δ_O were made.

$$\delta_N(Z_N = 1) = 0.8$$

$$\delta_N(Z_N = 2) = 2.0$$

$$\delta_O(Z_O = 1) = 1.75$$

$$\delta_O(Z_O = 2) = 3.5$$

In the MO calculations, it was assumed that the oxygen atom donates two electrons to the pi system. This effect is partially cancelled by the donation of nitrogen lone pair electrons to the oxygen in the σ bond formation and δ_N and δ_O would be expected to lie between the extremes of $Z = 1$ and $Z = 2$.

Nishimoto and Forester¹⁰⁴ have worked out equations relating the quantities β_{CC} , β_{CN} , and β_{CO} to the pi bond order. Assuming that the quantity β_{XY} can be approximated by an average of β_{XX} and β_{YY} , a similar relation for the dependence of β_{NO} on the pi bond order was worked out, with the result that β_{NO} should lie between 1.1 and 1.2 for pi bond orders of 1/4 to 1/2.

The pyridine N-oxide radical anion spin densities were determined for the following ranges of the semiempirical parameters: $0.75 \leq \delta_N \leq 2.0$,

$1.5 \leq \delta_O \leq 2.5$, $0.8 \leq \beta_{NO} \leq 1.4$ with $\beta_{CN} = 1.0$ and 1.076 . Corresponding calculations were carried out for the methyl substituted pyridine N-oxides using the methyl group parameters determined for methyl substituted pyridines.

At values of $\beta_{NO} \geq 1.4$ a low lying unoccupied orbital with a node passing through the N-O bond drops below the orbital occupied by the unpaired electron thus placing an upper limit on the value of β_{NO} . It was necessary to approach this limit in order to account for the large spin density observed in the N-O entity, therefore β_{NO} was set equal to 1.2. With $\beta_{CN} = 1.076$, the spin densities in the 4 positions were much too large, so a value of 1.00 was used. The choice of δ_N and δ_O was somewhat less well defined. Several sets of $\{\delta_N, \delta_O\}$ in the ranges $1.0 \leq \delta_N \leq 1.5$ and $1.5 \leq \delta_O \leq 2.0$ predicted reasonable spin densities. The best description of the pyridine N-oxide and the 4-picoline N-oxide radical anions corresponded to $\delta_N = 1.1$ and $\delta_O = 1.5$ but the agreement for the 2,6-lutidine N-oxide radical anion was considerably improved by increasing δ_O to 2.0. The value of Q_{CH_3} for methyl substituted pyridine N-oxides was taken to be 25 gauss. This is in accord with the application of Levy's hyperconjugation model to these compounds. The theoretical and experimental spin densities are listed in Table VI.

Previous MO studies of the aromatic amine N-oxides are limited. Jaffe¹⁰⁵ compared the reactivities of the ring positions in pyridine and pyridine N-oxide using HMO wave functions. He determined the parameters δ_N and δ_O semiempirically using Hammett substituent constants. Barnes¹⁰⁶ carried out similar calculations treating β_{NO} as a variable parameter. The final choice of a value for β_{NO} was based on the best calculation of the

pyridine N-oxide dipole moment. Tsoucaris¹⁰⁷ reported calculations of charge density distributions, dipole moments, bond orders, basicities, IR spectra and chemical reactivities for pyridine N-oxide, a number of -NH₂ and -NO₂ derivatives, and some fused ring amine N-oxides. The values of the parameters assumed in the above amine N-oxide calculations are collected in Table VIII. All the calculations were moderately successful in rationalizing the chemical behavior of pyridine-N-oxide and in predicting the dipole moment. Barnes calculated the charge density in the alpha position (carbon atom No. 2) to be greater than that in the beta position (carbon atom No. 3). The calculations of Tsoucaris and neutral molecule calculations using the parameters from this work predict that the reverse is true. NMR data¹⁰⁸ indicate that the beta charge density is in fact greater than the alpha charge density.

4.3.2 Unrestricted Self Consistent Field Approximation

USCF calculations were also carried out for the unsubstituted pyridine N-oxide radical anion. Three ways to account for the three electrons donated to the pi system by the N-O entity were considered. The values of Z_N , Z_O , γ_{NN} , γ_{OO} , δw_N , and δw_O for each case are listed below.

$$\begin{aligned} \text{Case 1: } Z_N &= 1, Z_O = 2, \gamma_{NN} = -5.1, \gamma_{OO} = -7.88 \\ \delta w_N &= 1.25 \text{ or } 2.50, \delta w_O = 6.25 \text{ or } 8.40 \end{aligned}$$

$$\begin{aligned} \text{Case 2: } Z_N &= 2, Z_O = 1, \gamma_{NN} = -6.9, \gamma_{OO} = -6.43 \\ \delta w_N &= 4.2 \text{ or } 6.25, \delta w_O = 1.67 \text{ or } 2.50 \end{aligned}$$

$$\begin{aligned} \text{Case 3: } Z_N &= 1.5, Z_O = 1.5, \gamma_{NN} = -6.0, \gamma_{OO} = -7.15 \\ \delta w_N &= 2.9 \text{ or } 5.0, \delta w_O = 3.35 \text{ or } 5.4 \end{aligned}$$

The values of β_{CC} and β_{CN} were again those of Pariser and Parr and each calculation was done for $\beta_{NO} = 1.0$ and $\beta_{NO} = 1.2$. The integrals γ_{rt} were

Table VIII. Survey of parameters used in MO calculations for pyridine N-oxide

| δ_0 | δ_N | β_{NO} | β_{CN} | Reference |
|------------|------------|--------------|--------------|--------------------------|
| 1.0 | 2.0 | 1.0 | 1.0 | Jaffe ¹⁰⁵ |
| 1.0 | 0.6 | 0.75 | 1.0 | Barnes ¹⁰⁶ |
| 1.2 | 0.8 | 1.0 | 1.0 | Tsoucaris ¹⁰⁷ |
| 1.5 | 1.1 | 1.2 | 1.0 | This work |

determined using the spherical charge approximation²⁶ extrapolated to the appropriate values of γ_{rr} and γ_{tt} as listed above. The set of calculations resulted in a variety of predicted spin density distributions which are given in Appendix III. It was noted immediately that case 2 where $Z_N = 2$ gives unreasonable results. The values predicted for ρ_3 are much greater than for ρ_2 . The spin densities computed for case 1 ($Z_N = 1$) with $\delta w_N = 2.5$ and $\delta w_0 = 8.4$ or case 3 ($Z_N = 1.5$) with $\delta w_N = 5.0$ and $\delta w_0 = 5.4$, however, are promising. Distributions interpolated between the calculated points with the restriction that ρ_2^U (the USCF doublet state spin density) = ρ_2^e (the experimentally determined spin density) are included in Table VI. The decision to fit the calculated spin densities to the alpha position was arbitrary, but it gives a starting point for examination of the effects of parameter variation. It is notable that the sum δw_N plus δw_0 is equal to 10.4 for each of the sets of parameters satisfying the restriction $\rho_2^U = \rho_2^e$. In fact it appears that this restriction can be satisfied using any set of values for δw_N and δw_0 satisfying the constraints: $\delta w_N < \delta w_0$ and $\delta w_N + \delta w_0 = 10.4$

with only small variations in β_{NO} necessary (Table IX). Using the set $\{\delta w_N = 2.1, \delta w_O = 8.3, \beta_{NO} = 1.2\}$, the value calculated for ρ_3^U is in better agreement with the experimental value than in the other cases, but ρ_4^U is too large. Using the set $\{\delta w_N = 2.5, \delta w_O = 7.9, \beta_{NO} = 1.2\}$, ρ_4^U is much too small. Using $\{\delta w_N = 5.0, \delta w_O = 5.4, \beta_{NO} = 1.0\}$, the values of ρ_4^U and ρ_3^U are a compromise of the values determined using the previous two sets of parameters while if β_{NO} is increased to 1.2, ρ_3^U and ρ_4^U have values corresponding to the best values found for the previous two sets but the value of ρ_2^U is too small. The distribution of the remaining electron spin density between the oxygen and nitrogen atoms is very sensitive to changes in δw_N and δw_O , and somewhat less dependent on changes in β_{NO} . For this reason it would be necessary to have solid estimates of the spin density distribution in the NO entity before a meaningful decision can be made regarding which is the best set of parameters.

4.3.3 Theoretical Spin Densities Used to Determine the Parameters

Q_N^N (Pyridine N-oxide) and Q_{ON}^N

Part of the interest in the calculation of spin densities for the N-oxide radical anions resulted from an interest in the nitrogen hyperfine coupling parameters. The nitrogen coupling constant for pyridine N-oxide can be written:

$$A(N) = (S'_N + 2Q_{NC}^N + Q_{NO}^N) \rho_N + Q_{ON}^N \rho_O + Q_{CN}^N (\rho_C + \rho_{C'}) \quad (27)$$

where S'_N represents only the $1s_N$ contribution. The quantity $(S'_N + 2Q_{NC}^N + Q_{NO}^N)$ is replaced by the symbol Q_N^N (pyridine N-oxide) since the individual quantities are not separable.

Table IX. Comparison of experimental and USCF spin densities for the Pyridine N-Oxide Radical Anion with selected parameter values.

| Position | expt. (a) | Theory | | | |
|--------------------------|--------------|--------|------|------|------|
| | | 1 | 2 | 3 | 4 |
| 0 | .363 | .057 | .155 | .075 | .107 |
| N | | .266 | .226 | .296 | .316 |
| 2 | .124 | .126 | .129 | .122 | .100 |
| 3 | .019 | .012 | .001 | .004 | .011 |
| 4 | .351 | .398 | .358 | .378 | .355 |
| USCF Variable Parameters | δw_0 | 8.33 | 7.9 | 5.4 | 5.4 |
| | δw_N | 2.1 | 2.5 | 5.0 | 5.0 |
| | β_{NO} | 1.2 | 1.2 | 1.0 | 1.2 |

a) See Table VI.

Q_N^N and Q_{ON}^N were determined using the experimental values of $A(N)$ listed in Table I, the values of ρ_N and ρ_O predicted in the McLachlan type calculations (see Table VI), the experimental values of $\rho_{2,3,4}$ listed in Table VI, and the value of Q_{CN}^N already determined. The values obtained are: $Q_N^N = \pm 50 \pm 8$ gauss and $Q_{ON}^N \pm 65 \pm 25$ gauss. The large uncertainty is in part due to the uncertainty in the 4-picoline N-oxide coupling constants and to the fact that the three equations for $A(N)$ are nearly linearly dependent. In addition, the results of the USCF calculation indicate that the ratio ρ_N/ρ_O is not well determined in the theoretical calculations. It would be of considerable value to determine coupling constants for N-oxides not so closely related to pyridine so that the linear dependence of the $A(N)$ equations could be removed and better Q values could be determined.

5. NITROSOBENZENES

5.1 Assignment of the Ortho Proton Coupling Constants

The microwave spectrum of ϕNO^{109} indicates that the neutral molecule is planar with the ONC angle equal to about 116° . Many organic molecules undergo one-electron reduction without significant change of conformation and it can be argued that resonance stabilization of the added electron increases the tendency of pi conjugated substituents to be coplanar with the aromatic ring. Additional evidence is available in infrared studies of nitrobenzene derivatives and the corresponding radical anions.¹¹⁰ No shift in the frequency of the symmetric or asymmetric NO_2 vibrations was observed for any of the compounds in going from the neutral molecule to its radical anion. If any large conformation change has occurred, frequency changes would be expected.¹¹¹

If the radical anion of ϕNO is on the average planar and if the rotation of the NO group about the C-N bond is slower than $\sim 10^7$ cps, the ESR spectrum observed would correspond to that of an unsymmetrical molecule. The number of unique proton coupling constants observed with good resolution does indeed correspond to the unsymmetrical situation although two of these coupling constants are almost equivalent. There are, however, conflicting reports in the literature as to the assignment of the three largest proton coupling constants to specific ring positions. Levy and Myers^{1b,61} assigned the larger two coupling constants of $3.94 \pm .15$ gauss to the ortho protons and the small coupling constant of 2.97 gauss to the para proton. Their assignment was based on McLachlan type MO calculations including either the " α " or the " β " effect. The " α " effect was first

proposed by Reiger and Fraenkel¹¹² to account for the asymmetries observed in substituted benzaldehydes and interprets the effect of the proximity of an oxygen atom by including a small negative value for δ_{C-cis} (C-cis is the ortho carbon atom closest to the oxygen atom). Stone and Maki¹¹³ used the " α " effect and also proposed the use of a small non-neighbor resonance integral $\beta_{C-cis,0}$ in additional studies of aromatic aldehydes. Using $\delta_{C-cis} = -0.07$ or $\beta_{C-cis,0} = 0.05$, a difference of about 0.3 gauss in the ortho proton coupling constants was predicted and a separation of ~1 gauss between the ortho proton coupling constants seemed unlikely. Russell and co-workers⁵⁰ prepared a number of selectively deuterated ϕNO 's and concluded from the ESR spectra of their corresponding radical anions that the large proton coupling constant, unresolved in their spectra, was due to one ortho and one para proton having nearly equivalent coupling constants and that the smaller doublet splitting was due to the remaining ortho proton.

Additional data from the ESR spectra of the radical anions of para substituted nitrosobenzenes, including p-chloro- ϕNO ^{50,62} and p-nitrosotoluene (Table II), show a splitting of ~1 gauss between the ortho proton coupling constants that further confirms the conclusions of Russell et al.

Stone and Maki observed that the " α " and " β " effects predict changes in spin density of comparable magnitude but opposite sign in ring positions that would be equivalent in the absence of hindered rotation. Calculations for the nitrosobenzene radical anion show similar results with the " α " effect predicting that $A(H-trans)$ is larger than $A(H-cis)$. Since the two models for including the effects of hindered rotation in an HMO framework are not entirely equivalent, it would be of interest to determine which of the two is the more relevant. Using the coupling constant data from

Table II, an assignment of each of the three larger proton coupling constants to specific positions in the ring relative to the oxygen atom can be made.

The coupling constants for ϕNO and p-NOT radical anions in liquid ammonia indicate that the methyl group has very little effect on the basic ϕNO electron distribution. This is consistent with the ultra-violet spectra^{65,114} of the neutral molecules which show absorptions at nearly equal frequencies with the same extinction coefficients. The melting point, absence of a tendency to form dimers (prominent in ϕNO and NOT), and very weak UV spectra of 2-nitroso-m-xylene⁶⁵ indicate a definite steric effect and it has been proposed that the NO group is forced out of the plane of the benzene ring. The ESR spectrum of the 2-nitroso-m-xylene radical anion shows that the two methyl groups are equivalent. The appearance of symmetry implies that the nitroso group is either positioned symmetrically or that it moves rapidly between equivalent positions. From these considerations, it is clear that there is no strong methyl group-oxygen interaction that would stabilize an asymmetric configuration for times longer than 10^{-7} sec. The physical and spectroscopic properties of o-NOT⁶⁵ are very similar to those of ϕNO which indicate that substitution of a single methyl group in the ortho position causes no major perturbation.

The ESR spectrum of the radical anion produced from o-NOT can be completely assigned to a single species. Steric considerations indicate that the configuration with the methyl group trans to the oxygen would be highly favored. The coupling constant for the ortho proton is very close in value to the larger of the two coupling constants assigned to

ortho protons in ϕNO and p- NO_2 . The remaining proton coupling constants are also similar to those in ϕNO and p- NO_2 ; therefore, it seems reasonable to assign the larger ortho coupling constant to the proton cis to the oxygen atom. This is consistent with the assignment predicted by the "β" effect, and with assignments made for similar asymmetries observed in the proton coupling constants of iminoxy radicals.⁵²

The similarity of the 2-nitroso-m-xylene coupling constants with those of the remaining ϕNO 's was surprising. If the NO group is indeed twisted out of the plane of the ring, there should be significant de-coupling and MO theory predicts that the odd electron would tend to reside in the NO entity. This is observed in nitrobenzenes where $A(\text{N})$ is about 50% greater for the 2-nitro-m-xylene radical anion than for the nitrobenzene radical anion and the ring proton coupling constants are about 30% less. However, substitution of two methyl groups ortho to the nitroxyl group ($-\text{NH}(=\text{O})$) in the mono-phenylnitroxide radical results in only a small decrease in the nitrogen coupling constant and in a negligible decrease in the para proton coupling constant. The methyl coupling constant is about 30% smaller than the corresponding proton coupling constant which may or may not indicate a decrease in the ortho position spin density.

Other authors (ref.110 and references therein), have mentioned that the angle of twist (θ) necessary to account for the observed spin density distributions using a resonance integral proportional to $\cos \theta$ does not agree in all cases with the angles used in semi-empirical treatments of UV and IR data. There are apparently differing mechanisms for out of plane distortions and other perturbations caused by steric hindrance to which ESR measurements are sensitive.

5.2 Theoretical Spin Densities: McLachlan Approximation Including Alpha and Beta Effects

Reiger and Fraenkel⁶⁷ noted that there were several sets of the parameters $\{\delta_N, \delta_O, \beta_{CN}, \beta_{NO}\}$ that gave equally good results in the calculation of nitrobenzene radical anion spin densities. Similar results have been obtained for the nitrosobenzene radical anion with the distribution of the spin density in the NO entity being dependent on the exact choice of parameters.

The first step was to determine more generally the values of $d\rho_i = \rho_i(\delta_{C-cis}, \beta_{C-cis,0} = 0) - \rho_i(\delta_{C-cis} \text{ or } \beta_{C-cis,0} \neq 0)$ to be expected when the "α" or "β" effect is included in a McLachlan type calculation. For different sets of values of $\delta_N, \delta_O, \beta_{NC},$ and β_{NO} that give a reasonable prediction of the average experimental spin densities, the $d\rho_i$'s were nearly constant. For $\delta_{C-cis} = -0.30$, the values of $d\rho_i$ are: $d\rho_{ox} \sim .015$, $d\rho_N \sim .015$, $d\rho_{cis} \sim +.025$, $d\rho_{trans} \sim -.025$, $d\rho_{para} \sim -.005$, and $d\rho_{meta} \sim \pm .01$. For $\beta_{C-cis,0} = 0.2$, the values of $d\rho_i$ are: $d\rho_{ox} \sim .015$, $d\rho_N \sim .020$, $d\rho_{cis} \sim -.028$, $d\rho_{trans} \sim +.025$, $d\rho_{para} \sim .015$, and $d\rho_{meta} \sim \pm .01$.

For the purpose of determining the appropriate set(s) of the parameters $\{\delta_N, \delta_O, \beta_{CN}, \beta_{NO}\}$, experimental spin densities were determined for the hypothetical symmetrical molecule from the coupling constants of nitrosobenzene radical anion in liquid ammonia, using $Q_{CH}^H = -24.5$ and taking the ρ_O^{sym} to be the average of the two experimental ortho spin densities. When the values of $\delta_N, \delta_O, \beta_{CN}, \beta_{NO}$ are determined for the symmetrical case, δ_{C-cis} or $\beta_{C-cis,0}$ can be included giving the correct ring spin densities for the unsymmetrical case.

McLachlan calculations with $\lambda = 1$ were carried out for parameters in the following ranges: $0.6 \leq \delta_O \leq 1.40$, $0.5 \leq \delta_N \leq 1.00$, $1.00 \leq \beta_{NO} \leq 2.0$,

$0.9 < \beta_{\text{CN}} < 1.2$. It was found that for any combination of β_{CN} , β_{NO} within the approximate limits $1.0 \leq \beta_{\text{CN}} \leq 1.2$ and $1.4 \leq \beta_{\text{NO}} \leq 1.6$, there is a unique set of values $\{\delta_{\text{N}}, \delta_{\text{O}}\}$ that predicts the experimental ring position spin densities quite well. The overall variations in δ_{N} and δ_{O} , $0.87 \leq \delta_{\text{O}} \leq 1.45$ and $0.5 < \delta_{\text{N}} < 1.0$, are two to three times as large as the variations in β_{NO} or β_{CN} . Results of this calculation for several selected values of β_{NO} and β_{CN} are given in Appendix IV. It can be seen that experimental knowledge of the distribution of spin density in the NO entity would allow a rather precise choice of a value for β_{CN} . However, for any particular value of β_{CN} , simultaneous variation of β_{NO} , with δ_{N} and δ_{O} under the constraint of maintaining constant spin densities in the ring, has much less effect on the NO density distribution. Even so, the concern is with a difference of only 0.2 units in β_{NO} which is probably trivial compared to variations in the parameters necessary to account for different types of spectroscopic data.

Calculations were carried out for the methyl substituted ϕNO radical anions that were studied, using the methyl group parameters determined for the methyl substituted pyridines and the same sets of values $\{\delta_{\text{N}}, \delta_{\text{O}}, \beta_{\text{CN}}, \beta_{\text{NO}}\}$ as for the unsubstituted ϕNO . The results are included in Appendix IV. It can be seen that the changes predicted for each methyl substituted nitrosobenzene are independent of the choice of basic ϕNO parameters. The proportionality constant, Q_{CH_3} , was determined in the manner described for the methyl substituted pyridines (Section 4.2) and was found to be 24.2 ± 0.2 gauss. The experimental spin densities for the radical anions of ϕNO , o,p-NOT, and NOX along with the theoretical spin densities predicted by including the "α" or the "β" effect in McLachlan type calculations

with $\beta_{NO} = 1.5$ and $\beta_{CN} = 1.1$ are shown in Table X. The spin densities calculated for the methyl nitrosobenzenes generally give good agreement with the experimental observations. For p-NOT, the methyl coupling constant is predicted to be close to the corresponding proton coupling constant as is observed. A very small increase in the ortho position spin densities and an increase in $A(N)$ are also predicted and observed. The o-NOT calculations give additional evidence for preference of the "β" effect over the "α" effect. A single methyl group in the ortho position produces some splitting of the ortho position spin densities in the symmetrical molecule calculations. Inclusion of δ_{C-cis} tends to bring the ortho position spin densities back together, while inclusion of $\beta_{C-cis,0}$ increases the separation. This is consistent with the fact that the observed ortho position coupling constants for o-NOT are separated by nearly twice the amount that the corresponding coupling constants for the ϕNO radical anion are separated. Even accounting for variations in Q_{CH_3} this increase is significant. The expected change in $A(N)$ is unclear due to the uncertainties in Q_{N}^N and Q_{ON}^N and the fact that equal magnitude changes are predicted for ρ_{ox} and ρ_N by the o-NOT and the NOX calculations. Since both molecules show a decrease in $A(N)$ that is much larger than predicted for any reasonable Q values, it may be that the change in $A(N)$ caused by ortho methyl groups is due to a distortion of the nitroso group rather than to inductive or hyperconjugative effects. The poorest agreement noted is for the methyl coupling constants in nitrosoxylene. The observed coupling constant corresponds more closely to the smaller of the ortho

Table X. Experimental and theoretical spin densities for nitrosobenzene type radical anions

| Radical Anion | Model | ρ_{ox} | ρ_N | $\rho_o(cis)$ | $\rho_o(trans)$ | $\rho_m(cis)^{(e)}$ | $\rho_m(trans)$ | ρ_p |
|-------------------|-----------|-------------|----------|---------------|-----------------|---------------------|-----------------|----------------------|
| Nitroso-benzene | expt. (a) | -- | -- | .163±.006 | .121 | .043±.004 | | .163±.006 |
| | Alpha (b) | .302 | .342 | .120 | .164 | -.033 | -.053 | .167 |
| | Beta (c) | .304 | .341 | .162 | .120 | -.050 | -.035 | .157 |
| | Q (d) | .414 | .226 | .120 | .120 | -.037 | -.037 | .161 |
| p-Nitroso-toluene | expt. | -- | -- | .161 | .124 | -.046 | -.046 | .172 ^{*(f)} |
| | Alpha | .304 | .350 | .122 | .161 | -.036 | -.051 | .168* |
| | Beta | .294 | .355 | .164 | .122 | -.052 | -.038 | .156* |
| | Q | .415 | .246 | .126 | .126 | -.043 | -.043 | .156* |
| o-Nitroso-toluene | expt. | -- | -- | .165 | .091* | -.050 | -.040 | .165 |
| | Alpha | .299 | .345 | .133 | .156* | -.038 | -.045 | .167 |
| | Beta | .290 | .351 | .172 | .112* | -.053 | -.027 | .154 |
| | Q | .405 | .236 | .144 | .105* | -.046 | -.024 | .161 |
| | expt. (g) | -- | -- | .131* | | -.047 | | .172 |
| | | .296 | .347 | .146* | | -.040 | | .167 |
| | Q | .396 | .244 | .129* | | -.034 | | .165 |

a) Exptl. spin densities determined for coupling constants measured in l NH₃ using Eq. (3) with $Q_{CH}^H = -24.5$ gauss.

b) Calc'd. using McLachlan approximation with $\lambda = 1.0$, $\delta_{ox} = 1.2$, $\delta_N = 0.7$, $\beta_{NO} = 1.5$, $\beta_{CN} = 1.1$ and $\delta_{C-cis} = -.2$.

c) Same as (b) with $\delta_{C-cis,0} = 0.12$.

d) Calculated using McLachlan approximation with $\lambda = 1.0$, $\delta_{ox} = 0.8$, $\delta_N = 0.8$, $\beta_{NO} = 1.5$, $\beta_{CN} = 1.1$.

e) Sign and assignment of ρ_m are based on MO calculations.

f) Starred quantities represent methyl group spin densities. Experimental methyl spin densities determined using $Q_{CH_3} = 24.2$ gauss, theoretical spin density $\rho_t = \rho_C + \rho_{C'} + \rho_H$ with $\rho_{C'}$, ρ_H determined using hyperconjugation parameters $\delta_H = -0.5$, $\delta_{C'} = -0.1$, $\delta_C = -0.2$, $\beta_{CC'} = 0.76$, $\beta_{C'H} = 2.00$.

g) Same as (b) with $\delta_{C-cis} = 0.0$.

proton coupling constants in the nitrosobenzene radical anion than to the average coupling constant predicted in the absence of hindered rotation effects, while the meta and para position spin densities are in good agreement with experiment.

An additional discrepancy is that for values of $\beta_{C-cis,0}$ or δ_{C-cis} large enough to predict the observed separation of ortho coupling constants, the meta position splitting is predicted to be more than twice observed value. It should also be noted that the values of δ_{C-cis} and $\beta_{C-cis,0}$ assumed in the above calculations are much larger than can be rationalized by simple considerations.

5.3 The "Q" Effect: Theoretical Calculation of the Parameters

$$\underline{Q_{CH}^H \text{ and } Q_{OH}^H}$$

It has been proposed that reactions involving the N-O group of iminoxy radicals occur through 6-membered ring intermediates formed by $H_{cis} \cdots O$ bonding.¹¹⁵ A third mechanism for accounting for the observed asymmetries in ESR spectra of radicals containing an X=O group that exhibits hindered rotation can be formulated by considering the effect of additional polarization of the hydrogen 1s electrons by electron spin density in the oxygen pi orbital. A rough calculation was done to determine the effect of such an interaction. The method used was completely analogous to that described in Section 3.2.

A set of sigma molecular orbitals $\{\phi_i\}$ can be formed from the CH bonding and antibonding orbitals, $(\sigma_{CH} \text{ and } \sigma_{CH}^*)$, and an oxygen lone pair orbital, ox_h , using the one electron Hamiltonian: $-1/2 \nabla_k^2 - \sum_x Z_x/r_{xk}$. Since the CH bond orbitals are nearly eigenfunctions of this Hamiltonian, the basis set was combined according to perturbation theory. The matrix

elements $\langle \phi_i | \frac{1}{r_{\text{core}}} | \phi_j \rangle$ were again calculated using the formulae of Roothan⁷⁵ and of Lofthus^{77b} assuming sp^2 hybridization for the oxygen and carbon atoms, internuclear distances $r_{\text{CH}} = 2.0$ a.u. and $r_{\text{OH}} = 4.5$ a.u. and an angle of 30° between the OH axis and the direction of the orbital ox_h . The resulting approximate wave functions, $\phi_i = b_{ih} 1s_h + b_{ic} c_h + b_{io} ox_h$, are:

$$\begin{aligned} \phi_1 &= 0.26 1s_h + 0.52 c_h + 0.66 ox_h \\ \phi_2 &= 0.40 1s_h + 0.40 c_h - 0.73 ox_h \\ \phi_3 &= 1.16 1s_h - 1.16 c_h + 0.16 ox_h \end{aligned} \quad (28)$$

The sigma system being considered consists of four electrons with the zero order wave function written as an antisymmetrized product of the pi and sigma molecular orbitals as follows:

$$\psi_0 = \|\phi_1 \bar{\phi}_1 \phi_2 \bar{\phi}_2 \pi_0\| \quad (29)$$

There are two single sigma excitations allowed in this basis set:

$\phi_1 \rightarrow \phi_3$ and $\phi_2 \rightarrow \phi_3$. The appropriate doublet states have the same form as those of Eq. (11).

Sample calculations showed that the amount of mixing of the three components in the expressions for ϕ_i could be varied considerably without great changes in the resulting predictions. However the energies of each of the orbitals is a significant factor. Considering the difficulties already noted in predicting reasonable energy levels using limited basis sets and simple Hamiltonians, the values of $Q_{\text{OHC}}^{\text{H}}$ and $Q_{\text{CHO}}^{\text{H}}$ were first expressed in terms of ΔE_{13} and ΔE_{23} as follows:

$$Q_{\text{CHO}}^{\text{H}} \sim \frac{-5.1 \text{ to } -7.1}{\Delta E_{23}} \left(1 + \frac{\Delta E_{23}}{E_{13}} \right) \text{ gauss} \quad (30)$$

$$Q_{\text{OHC}}^{\text{H}} \sim \frac{-5.1 \text{ to } -7.1}{\Delta E_{23}} \left(1 - \frac{\Delta E_{23}}{E_{13}} \right) \text{ gauss}$$

It can be seen from Eq. (28) that ϕ_3 is predominantly the C-H antibonding orbital while ϕ_1 and ϕ_2 are mixtures of ox_h and σ_{CH} . The mixing of ox_h and σ_{CH} will push ϕ_2 closer to ϕ_3 and ϕ_1 farther away. The quantity $\Delta E_{23}/\Delta E_{13}$ is thus less than 1 giving $Q_{\text{OHC}}^{\text{H}}$ and $Q_{\text{CHO}}^{\text{H}}$ the same sign. Simple calculations of excitation energies using $\Delta E_{ij} = \langle \phi_j | \mathcal{H} | \phi_j \rangle - \langle \phi_i | \mathcal{H} | \phi_j \rangle$ show that $\Delta E_{23} \sim 0.5$ to 0.7 a.u. and $\Delta E_{13} \sim 1.5$ a.u. that gives values of $Q_{\text{CHO}}^{\text{H}} \sim -16$ gauss and $Q_{\text{OHC}}^{\text{H}} \sim -7$ gauss. MO calculations (Table X) indicate that ρ_o is $\sim \frac{1}{2} \rho_{\text{ox}}$ making the contributions of ρ_o and ρ_{ox} to the total coupling constant nearly equal. From these rough estimations, it appears that the proposed mechanism of hydrogen ls electron polarization by the oxygen pi electron density ("Q" effect) is indeed a very reasonable one.

5.4 Theoretical Spin Densities: McLachlan Approximation

Assuming "Q" Effect

One major difference between the " α " and " β " effects and the "Q" effect is that the former invoke a significant perturbation of the spin density distribution when hindered rotation is present; whereas, the latter effect can be employed assuming an essentially symmetrical spin density distribution.

In view of this difference additional McLachlan type calculations were carried out for the nitrosobenzene radical anion in order to find the necessary combination(s) of $\{\delta_{\text{N}}, \delta_{\text{O}}, \beta_{\text{NO}}, \beta_{\text{CN}}\}$ to predict the

experimental spin densities assuming ρ_o to be that measured for the trans ortho position, i.e., the ortho proton having the small coupling constant. It was again found that for each set of values (β_{NO}, β_{NC}) there is a unique set of values for (δ_N, δ_O) that predicts exactly the ortho and para spin densities. These calculations are included in Appendix IV. The agreement for the meta position spin density is not as close as in the previous set of calculations, but it is still quite good. The corresponding calculations were carried out for the methyl substituted ϕNO 's with the results shown in Appendix IV. Table X includes the "Q" effect calculations for $\beta_{NO} = 1.5$ and $\beta_{CN} = 1.1$.

The changes predicted due to methyl substitution are the same as those predicted in the previous calculations. The point to be noted is that the predicted methyl coupling constant in NOX is now consistent with experiment contrary to the previous predictions. There is also a large increase in ρ_{ox} partly at the expense of ρ_{ortho} and partly at the expense of ρ_N . The ratio ρ_{ox}/ρ_N is again more strongly a function of β_{CN} than of β_{NO} .

The small inequivalence of the meta proton coupling constant observed in some cases is not treated in the basic Q effect; however, more sophisticated MO calculations that allow inclusion of geometry in the basic matrix elements do indeed predict a small amount of asymmetry in the spin density (See Section 5.6). It is also likely that the non-neighbor resonance integrals do contribute to the asymmetry of the wave functions.

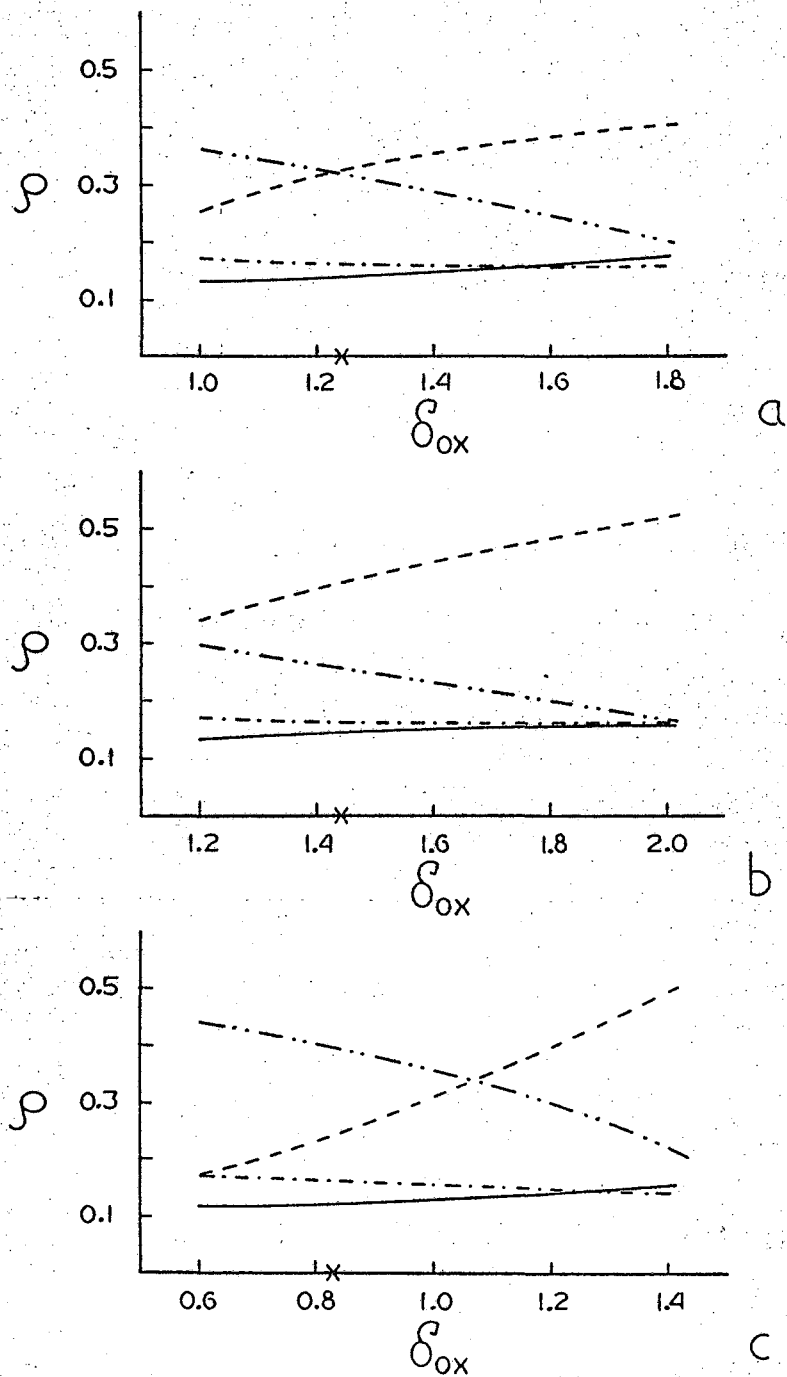
5.5 Solvent Effects

The coupling constants that are compiled in Table II for the radical anion of ϕNO were measured in a variety of solvents and show significant

variations both in $A(N)$ and $A(H_{o,p})$. The effect of a change in solvent characteristics on the coupling constants of radicals and radical ions was first included in a MO framework by Gendell, Freed, and Fraenkel¹¹⁶ in studies of aromatic quinones. They proposed that the interaction was predominantly between the solvent and the functional group and could be accounted for by varying the oxygen coulomb parameter δ_o . This technique has also been applied to nitroxide radicals and to radical anions of nitrobenzene and its derivatives with reasonable success.^{62,67}

The dependence of ρ_{ox} , ρ_N , ρ_o , and ρ_p on the value of δ_o were determined for several of the sets of parameters determined for the ϕNO radical anion. The shape of each of the curves (ρ_i vs δ_o) was independent of the choice of parameters. The ρ_N and ρ_{ox} curves slope in opposite directions and the value of δ_o at which the two cross does depend on the values of δ_N , β_{NO} , and β_{CN} . The same is true of the curves for ρ_o and ρ_p . Three sets of curves are shown in Fig. 14. The higher values of δ_o correspond to the water/alcohol end of the solvent scale in accord with convention and other authors. The predicted decrease in $A(H_p)$ and increase in $A(H_o)$ for increasing δ_{ox} are consistent with experimental observations. Assuming that Ayscough's assignment of the coupling constant 3.76 gauss to one ortho and one para position is correct and that the trans ortho proton still has the smaller coupling constant, the increase observed for $A(H_{cis})$ is about 1/2 that of $A(H_{trans})$ over the range of solvents. This is consistent with the predictions of the Q effect, since the value computed for ρ_{ox} decreases about 5 times as rapidly as that computed for ρ_o increases.

Several authors^{62,82} have used coupling constants measured in quite



XBL 679-4945

Fig. 14. Solvent effect on spin density distribution in nitrosobenzene radical anion calculated using variable δ_{ox} , (a) average α or β effect model with $\delta_N = 0.8$, $\beta_{NO} = 1.6$, $\beta_{CN} = 1.1$; (b) same as (a) with $\delta_N = 0.5$, $\beta_{NO} = 1.15$, $\beta_{CN} = 1.0$; (c) Q effect model with $\delta_N = 0.8$, $\beta_{NO} = 1.5$, $\beta_{CN} = 1.1$. The asterisk indicates value of δ_{ox} that corresponds to the $\ln NH_3$ data in each case. --- ρ_N , -.-.- ρ_{ox} , — ρ_o , -.-.- ρ_p .

different solvents together with spin densities determined using a variable δ_0 to determine hyperfine coupling parameters. Although the accuracy of the values of the parameters determined in this manner is questionable, a knowledge of what the predictions are, correlated with other data as they become available will certainly provide a test of the validity of the theory underlying such a determination. In particular, for the nitrosobenzene radical anion, a bilinear relation, $A(N) = Q_N^N \rho_N + Q_{ON}^N \rho_O$ is assumed with the parameters Q_N^N and Q_{ON}^N being independent of the solvent. It is also assumed that the change in spin density distribution in various solvents can be accurately described by varying δ_{ox} . Values of $Q_N^N \sim 24$ gauss, $Q_{ON}^N \sim -2$ gauss are determined using α or β effect spin density calculations while values of $Q_N^N \sim 18$ gauss and $Q_{ON}^N \sim +9$ gauss are determined using the Q effect model.

5.6 Theoretical Spin Densities: Unrestricted Self Consistent Field Approximations

The UCSF method of calculating spin density distributions includes differences between rotational or other conformational isomers in the γ_{rt} dependence of the integrals γ_{rt} that appear in the F matrices. The symmetry of the spin density distribution is quite sensitive to small asymmetries in the values of γ_{rt} . Calculations using the USCF framework described in Section 4.1.2 were carried out for the nitrosobenzene radical anion assuming the geometry shown in Fig. 13. The values of γ_{rt} were determined again using the spherical charge approximation extrapolated to $\gamma_{CC} = -4.40$, $\gamma_{NN} = -5.15$ and $\gamma_{OO} = -6.45$. The parameters $\delta w_O, \delta w_N, \beta_{NO}$, and β_{CN} were varied over the following ranges: $1.67 \leq \delta w_O \leq 5.0$, $0.85 \leq \delta w_N \leq 1.6$,

$1.2 \leq \beta_{NO} \leq 1.6$, and $0.8 \leq \beta_{CN} \leq 1.2$. The variation in each of the parameters that allowed prediction of the experimental spin densities is $\sim \pm 0.15$ units, similar to ranges noted in the McLachlan type calculations. Results for 4 sets of parameters chosen to fit the experimental values of $\rho_{trans}^e = 0.12$ and $\rho_p^e = 0.16$ are shown in Table XI. The variation in N-O spin density distribution is smaller than that in the corresponding McLachlan calculation. The total density in the NO group is not constant in the USCF calculations. The changes are absorbed by the spin density in the carbon atom to which the NO group is bonded. The density in this position is in any case predicted by the USCF calculations to be ~ 0.07 to 0.1 in contrast to the small constant value ~ 0.02 determined in the McLachlan calculations. The meta position spin densities are similar for each of the four cases. The magnitudes are somewhat smaller than those observed, but the magnitude of the separation predicted is close to that observed. Also to be noted is that the trans position is predicted to have a larger spin density than the cis, contrary to the experimental assignment of coupling constants. The lower value of ρ_{cis} does not, however, eliminate the possibility of the Q effect accounting for the larger cis coupling constant.

The additional set of spin densities included in Table XI was fitted to the coupling constants as observed without regard to specific assignment of cis and trans coupling constants. The agreement is surprisingly good in regard to the magnitudes; however, the trans coupling constant is again predicted to be larger. This phenomenon was found for any of the sets of parameters used. The discrepancy between experiment and theory can in part be rationalized by the fact that non-neighbor resonance integrals

Table XI. Comparison of experimental and USCF spin densities for the nitrosobenzene radical anion.

| Position | Expt. (a) | Theory | | | | |
|--------------------------------|--------------|--------|-------|-------|-------|-------|
| | | 1 | 2 | 3 | 4 | 5 |
| ox | --- | .325 | .395 | .345 | .390 | .164 |
| N | --- | .250 | .220 | .200 | .165 | .480 |
| cis | .163 | .095 | .100 | .097 | .105 | .136 |
| trans | .121 | .120 | .120 | .120 | .120 | .161 |
| ortho | | | | | | |
| cis | .043 | -.019 | -.019 | -.016 | -.016 | -.035 |
| trans | .043 | -.034 | -.034 | -.034 | -.033 | -.052 |
| p | .163 | .160 | .160 | .160 | .160 | .155 |
| USCF variable parameters | δw_O | 2.97 | 2.68 | 2.84 | 2.64 | 5.0 |
| | δw_N | 1.05 | 1.15 | 1.20 | 1.35 | 1.6 |
| | β_{NO} | 1.4 | 1.4 | 1.6 | 1.6 | 1.4 |
| | β_{CN} | 1.0 | 1.2 | 1.0 | 1.2 | 1.2 |

a) See Table X.

were neglected in the determination of the terms F_{rs} and \bar{F}_{rs} while non-neighbor repulsion integrals were included. These integrals are of opposite sign. It is the " β " effect in the McLachlan calculations that predicts the observed direction of splitting in the ortho spin densities, and this effect essentially corrects for neglect of non-neighbor interactions. Inclusion of the non-neighbor resonance integrals in the USCF calculation of spin densities is likely to partially cancel the asymmetries in the spin density distribution predicted in the above calculations, leaving the Q effect to account for the difference in coupling constants.

The above discussion points out the necessity for greater care in making approximations to the F matrices in the USCF type calculations. The deficiencies may not be obvious in cases where the symmetry of the matrices allows cancellation of errors (one of the reasons for the success of Hückel calculations). These deficiencies however make themselves known in the present case, and it seems likely that the situation would repeat itself without proper caution.

ACKNOWLEDGMENTS

My appreciation and thanks go to Professor R. J. Myers for his advice, clever suggestions, and patience throughout the course of this work, to Professor F. R. Jensen for many helpful discussions, to Dr. R. N. Kortzeborn for the loan of several computer programs, and to my husband, Stanley M. Williamson, for much typing, technical editing, and constant faith and encouragement.

This work was supported under the auspices of the United States Atomic Energy Commission.

APPENDIX I

Atomic Orbitals Used in Calculation
of Spin Polarization Parameters

A. General forms of 1s, 2s, and 2p orbitals

$$1s_a(\text{STO}) = 1s_a(\text{STO}^+) = 1s_a(\text{HO}) = \left[(\zeta_{a1})^{3/2} / \pi^{1/2} \right] e^{-\zeta_{a1} r}$$

$$2s_a(\text{STO}) = \left[(\zeta_{a2})^{5/2} / (3\pi)^{1/2} \right] r e^{-\zeta_{a2} r}$$

$$2s_a(\text{SHO}) = \left[(\zeta_{a2})^{3/2} / \pi^{1/2} \right] e^{-\zeta_{a2} r} (\zeta_{a2} r - 1)$$

$$2s_a(\text{STO}^+) = (1 - S_{1a,2a}^2)^{-1/2} (2s_a(\text{STO}) - S_{1a,2a} 1s_a(\text{STO}))$$

$$S_{1a,2a} = \langle 1s_a(\text{STO}) | 2s_a(\text{STO}) \rangle$$

$$P_{\sigma a} = \left[(\zeta_{a2})^{5/2} / \pi^{1/2} \right] r e^{-\zeta_{a2} r} \cos \theta$$

$$\left. \begin{array}{l} P_{\pi a} \\ P_{\pi' a} \end{array} \right\} \left[(\zeta_{a2})^{5/2} / \pi^{1/2} \right] r e^{-\zeta_{a2} r} \sin \theta \left\{ \begin{array}{l} \cos \phi \\ \sin \phi \end{array} \right.$$

B. Value of orbital exponents¹ and overlap integrals

| a | ζ_{a1} | ζ_{a2} | $S_{1a,2a}$ |
|---|--------------|--------------|-------------|
| H | 1.0 | -- | -- |
| C | 5.7 | 1.625 | 0.2205 |
| N | 6.7 | 1.95 | 0.2279 |
| O | 7.7 | 2.275 | 0.2334 |

1. Orbital exponents determined using Slater's rules.

APPENDIX II

Program USCFMO

USCFMO is a Fortran IV program written for the CDC 6600 computer. The function of the program is to calculate energy levels and wave functions for systems containing any number of electrons of spin $+1/2$ and $-1/2$ (within the limits of the program dimension) using the unrestricted SCF LCAO MO formalism. There is also provision for computing spin densities which correspond to projected doublet state wave functions for cases where the number of electrons with spin $+1/2$ is one greater than the number of electrons with spin $-1/2$.

The subroutine FCALC calculates the USCF Hamiltonian matrix elements. Variations to the FCALC routine may be substituted according to the approximations desired for the various terms of the Hamiltonian. HDIAG is a JACVAT program for diagonalizing symmetrical matrices written by Dr. R. N. Kortzeborn. ANIH is the subroutine that computes the electron density matrices corresponding to wave functions having the quartet spin states annihilated. The formulae used are those of Snyder and Amos.⁹¹

The input variables are described below:

ANAME(I) is the problem label and is printed at the beginning of the output for each calculation. ANAME may have up to 72 characters.

N is the total number atomic orbitals being considered. N must be less than 50.

NA is the number of electrons having $S_z = +1/2$. NA must be less than 50.

NB is the number of electrons having $S_z = -1/2$. NB must be less than 50.

NIT prescribes the maximum number of iterations that the program will execute.

H(I,J) is the one electron Hamiltonian matrix element between atomic orbitals I and J.

G(I,J) is the two electron Hamiltonian matrix element between atomic orbitals I and J.

Z(I) is the number of electrons donated to the system from the atom containing atomic orbital I.

SPIN is the total z component of the electron spin for the system.

The data deck for each problem consists of the following set of cards:

| <u>Variable</u> | <u>Format</u> |
|--|---------------|
| ANAME(I), I = 1,8 | 7A10, A2 |
| N, NA, NB, NIT | 4I4 |
| H deck: one card for each non zero H(I,J) with variables: | |
| I, J, H(I,J) | 2I4, F64.10 |
| Blank card | |
| G Deck: one card for each non zero G(I,J) with variables: | |
| I, J, H(I,J) | 2I4, F64.10 |
| Z(I), I = 1,N | 12F6.3* |
| SPIN | F12.6 |

The calculations may be stacked directly and the program will repeat itself as many times as necessary.

* The format statement for Z(I) limits the value of N to 12, for larger values of N, an appropriate change in the statement is necessary.

```

PROGRAM USCFCM(INPUT, OUTPUT)
CCCCMCM H(50, 50), hh(50, 50), G(50, 50), A(50, 50),
1 B(50, 50), Z(50), ALPHA(50, 50), BETA(50, 50),
2 KHU(50,50), ANAME(8), P(50,50), Q(50,50), U(50,50),
3 ASAP(50,50), ASAQ(50,50), ASAKHU(50), AAP(50,50), AAQ(50,50),
4 AARHU(50), AARA(50), SORHU(50),
5 PQ(50,50), WP(50,50), PqP(50,50), QPQ(50,50), PqPq(50,50),
6 QPQP(50,50), PqQP(50,50), QPQP(50,50)
10 CC 11 I = 1, 50
    CL 11 J = 1, 50
    H(I,J) = 0.0
    hh(I,J) = 0.0
11 G(I,J) = 0.0
    READ 12, (ANAME(I), I=1,8)
12 FORMAT (7A10, A2)
    READ 13, N, NA, NB, NIT
13 FCRMAT (414)
    IF(N) 14, 55, 14
14 PRINT 15, (ANAME(I), I = 1, 8)
15CFORMAT ( 48H1 UNRESTRICTED SCF LCAD MO CALCULATION OF
1 7A10, A2)
    PRINT 16
16 FCRMAT ( 1H0, 15X, 42HNON-ZERO ELEMENTS IN ONE-ELECTRON H-MATRIX)
17 READ 18, I, J, H(I,J)
18 FCRMAT (214, F04.10)
    IF(I) 19, 21, 19
19 H(J, I) = H(I, J)
    PRINT 20, I, J, H(I, J)
20 FCRMAT ( 20X, 2HH(, 12, 1H,, 12, 4H) = , F9.5 )
    GL TO 17
21 PRINT 22
22 FCRMAT ( 1H0, 15X, 40HTWO-ELECTRON COULOMB REPULSION INTEGRALS)
23 READ 18, I, J, G(I,J)
    IF(I) 24,26,24
24 G(J,I) = G(I,J)
    PRINT 25, I, J, G(I,J)
25 FCRMAT ( 20X, 2HG(, 12, 1H,, 12, 4H) = , F9.5)
    GL TO 23
26 PRINT 27
27CFORMAT ( 1H0, 15X, 53HNUMBER OF ELECTRONS DONATED BY PI SYSTEM BY
1 ITH ATOM )
    READ 28, (Z(I), I = 1, N)
28 FCRMAT (12F0.3)
    PRINT 29, ((I, Z(I)), I = 1,N)
29 FCRMAT (10X, 12, F0.3, 11(2X, 12, F6.3))
    READ 9, SPIN, QMC
5 FCRMAT (2F12.0)
    NDIM = 50
30 DC 31 I = 1, N
    CL 31 J = 1, N
    IDEL = I
    JDEL = J
31 hh(I,J) = H(I,J) - ADEL(IDEL,JDEL)*(Z(I)*G(I,J) - 10.53)/2.0
    CALL HDIAG(hh, NDIM, N, 0, A)
    CALL HCRD(hh, A, N)
    PRINT 01
61C FCRMAT (1H0, 15X, 74HHUCKEL ORBITAL ENERGIES WITH ENERGY ZERO SUC
1H THAT E(CARBON 2PZ) IS ZERO )
    PRINT 02, ((I, hh(I,I)), I = 1, N)
62 FCRMAT ( 20X, 2HE( , 12, 4h) = , F9.5 )
    DC 32 I = 1, N

```

```

      DO 32 J = 1, N
32  B(I,J) = A(I,J)
      KIT = 1
35  CALL PANDQ (A, B, KIT, NA, NB, N, P, Q, RHQ)
      PRINT 63
63C  FORMAT (1H0, 15X, 70HALPHA SPIN ORBITAL DENSITY MATRIX FROM HUCK
      1EL WAVE FUNCTIONS )
69  FCRMAT ( 10X, 12F10.4 )
      DO 64 I = 1, N
      PRINT 69, (P(I,J), J = 1, N)
64  CONTINUE
      PRINT 65
65C  FORMAT (1H0, 15X, 70HBETA SPIN ORBITAL DENSITY MATRIX FROM HUCKE
      1L WAVE FUNCTIONS )
      DO 66 I=1, N
      PRINT 69, (Q(I,J), J = 1, N)
66  CONTINUE
      PRINT 36, KIT
36  FORMAT ( 15X, 43HELECTRON SPIN DENSITY IN ITH ATOMIC ORBITAL
      1 20X, 16ITERATION NUMBER , 13 )
      PRINT 37, ((I, RHO(I, KIT)), I = 1, N )
27C  FCRMAT ( 1H0, 20X, 4HRHO( , 12, 4H) = , F9.5, 10X, 4RRHO( ,
      1 12, 4H) = , F9.5/)
      DO 41 K = 2, NIT
      KIT = K
      CALL FCALC(H, G, Z, P, Q, N, ALPHA, BETA)
      CALL HDIAG( ALPHA, NDIM, N, O, A)
      CALL HCRD (ALPHA, A, N)
      CALL HDIAG(BETA, NDIM, N, O, B)
      CALL HCRD(BETA, B, N)
      CALL PANDQ( A, B, KIT, NA, NB, N, P, Q, RHQ)
      PRINT 36, KIT
      PRINT 37, ((I, RHO(I, KIT)), I = 1, N )
      CALL TCST(RHO, KIT, N, TESTM)
      IF(TESTM - 0.005) 42, 42, 41
41  CONTINUE
42  DO 49 I = 1, N
49  SDRHC(I) = RHO(I, KIT)
      PRINT 71
71C  FORMAT (1H0, 15X, 88HUSCF ORBITAL ENERGIES FOR ALPHA AND BETA S
      1PIN BEFORE ANIHILATION OF QUARTET COMPONENTS )
      PRINT 72, ((I, ALPHA(I, I), I, BETA(I, I)), I = 1, N)
72C  FORMAT ( 20X, 7HEALPHA( , 12, 4H) = , F9.5, 20X, 6HEBETA( ,
      1 12, 4H) = , F9.5 )
      PRINT 73
73C  FORMAT (1H0, 15X, 78HALPHA SPIN ORBITAL DENSITY MATRIX FROM USC
      1F WAVE FUNCTIONS BEFORE ANIHILATION )
      DO 74 I = 1, N
      PRINT 69, (P(I,J), J = 1, N)
74  CONTINUE
      PRINT 75
75C  FCRMAT (1H0, 15X, 78HBETA SPIN ORBITAL DENSITY MATRIX FROM USCF
      1WAVE FUNCTIONS BEFORE ANIHILATION )
      DO 76 I = 1, N
      PRINT 69, (Q(I,J), J = 1, N)
76  CONTINUE
      PRINT 37, ((I, SDRHC(I)), I = 1, N)
      CALL ANIH ( NA, NB, N, SPIN)
      PRINT 43
43C  FORMAT (1H0, 15X, 86HSPIN DENSITY IN THE I-TH ATOMIC ORBITAL AF
      1TER HALF ANNIHILATION OF QUARTET COMPONENTS )
      PRINT 37, ((I, ASDRHC(I)), I = 1, N)

```

```
      PRINT 81
81C FCRMAT (1H0, 15X, 76HALPHA SPIN ORBITAL DENSITY MATRIX FROM USCF
      WAVE FUNCTIONS AFTER ANIHILATION )
      DC 82 I = 1, N
      PRINT 69, (AAP(I,J), J = 1, N)
82 CONTINUE
      PRINT 83
83C FCRMAT (1H0, 15X, 76HBETA SPIN ORBITAL DENSITY MATRIX FROM USCF W
      WAVE FUNCTIONS AFTER ANIHILATION )
      DC 84 I = 1, N
      PRINT 69, (AAJ(I,J), J = 1, N)
84 CONTINUE
      PRINT 44
44C FCRMAT (1H0, 15X, 86HSPIN DENSITY IN THE I-TH ATOMIC ORBITAL AF
      TER TOTAL ANNIHILATION OF QUARTET COMPONENTS )
      PRINT 37, ((I, AAKHC(I)), I = 1,N)
52 GO TO 10
55 PRINT 56
56 FCRMAT ( 1H0, 10X, 18HEND OF DATA DECK )
      CALL EXIT
      ENC
```

```
      FUNCTION ADEL (I,J)
      IF (I - J) 601, 602, 601
601 ADEL = 0.0
      RETURN
602 ADEL = 1.0
      RETURN
      ENC
```

```
      SUBROUTINE FCALC( H, G, Z, P, Q, N, ALPHA, BETA)
      DIMENSION H(50,50), G(50,50), P(50,50), Q(50,50), ALPHA(50,50),
      1 BETA(50,50), GAM(50), Z(50)
      DC 501 I = 1, N
      DC 501 J = 1, N
      II=I
      JJ=J
      IF (II - JJ) 502,503,502
502 ALPHA(I,J) = H(I,J) - P(I,J)*G(I,J)
      BETA(I,J) = H(I,J) - Q(I,J)*G(I,J)
      GO TO 501
503 GAM(I) = 0.0
      DC 505 L = 1, N
      LL=L
      IF (II - LL) 504,505,504
504 GAM(I) = GAM(I) + (P(L,L) + Q(L,L) - Z(L))*G(I,L)
505 CONTINUE
      ALPHA(I,I) = H(I,I) + Q(I,I)*G(I,I) + GAM(I)
      BETA(I,I) = H(I,I) + P(I,I)*G(I,I) + GAM(I)
501 CONTINUE
      RETURN
      ENC
```

```
      SUBROUTINE PANDQ(A, B, K, NA, NB, N, P, Q, RHO)
      DIMENSION A(50,50), B(50,50), P(50,50), Q(50,50), RHO(50,50)
      DC 301 I = 1, N
      DC 301 J = 1, N
      P(I,J) = 0.0
      Q(I,J) = 0.0
      DC 302 L = 1, NA
3C2 P(I,J) = P(I,J) + A(I,L)*A(J,L)
      DC 303 M = 1, NB
3C3 Q(I,J) = Q(I,J) + B(I,M)*B(J,M)
      II = I
      JJ = J
      IF (II - JJ) 304,305, 304
3C4 P(J,I) = P(I,J)
      Q(J,I) = Q(I,J)
      GO TO 301
3C5 RHC(I,K) = P(I,I) - Q(I,I)
3C1 CONTINUE
      RETURN
      END
```

```
      SUBROUTINE HURD(H, U, N)
      DIMENSION H(50,50), U(50,50)
      NEND = N - 1
      DC 201 I = 1, NEND
      IDU = I + 1
      DC 201 J = IDU, N
      IF (H(I,I) - H(J,J)) 201, 201, 202
2C2 HTEMP = H(I,I)
      H(I,I) = H(J,J)
      H(J,J) = HTEMP
      DC 201 L = 1, N
      UTEMP = U(L,I)
      U(L,I) = U(L,J)
      U(L,J) = UTEMP
2C1 CONTINUE
      RETURN
      END
```

```
      SUBROUTINE TEST (RHO, KIT, N, TESTM)
      DIMENSION RHO(50,50), DR( 50,50)
      DC 401 I = 1, N
4C1 DR(I,KIT) = ABSF(RHO(I,KIT) - RHO(I,KIT -1))
      DC 403 J = 2, N
      IF (DR(I, KIT) - DR(J,KIT)) 402, 403, 403
4C2 DTEMP = DR(I,KIT)
      DR(I,KIT) = DR(J,KIT)
      DR(J,KIT) = DTEMP
4C3 CONTINUE
4C4 TESTM = DR(I,KIT)
      RETURN
      END
```

```
      SUBROUTINE HDIAG (A, NDIM, N, IEGEN, EIVR)
C     THIS IS JACVAT
      DIMENSION A(NDIM,NDIM), EIVR(NDIM,NDIM)
      IF(N-1) 2,2,1
      2 EIVR(1,1)=1.0
      RETURN
      1 IF(IEGEN) 102,99,102
      99 DO 101 J=1,N
      DO 100 I=1,N
C     100 EIVR(I,J)=0.0
C     101 EIVR(J,J)=1.0

C     FIND THE ABSOLUTELY LARGEST ELEMENT OF A
C     102 ATCP=0.
      DO 111 I=1,N
      DO 111 J=1,N
      IF(ATCP-ABS(A(I,J)))104,111,111
C     104 ATCP=ABS(A(I,J))
      111 CCNTINCE
      IF(ATCP)109,109,113
C     109 RETURN

C     CALCULATE THE STOPPING CRITERION -- DSTOP
C     113 AVGF=FLOAT(N*(N-1))*0.55
      U=C.0
      DO 114 JJ=2,N
      DO 114 II=2,JJ
      S=A(II-1,JJ)/ATCP
C     114 U=S*S+U
      DSTOP=(1.E-06)*U

C     CALCULATE THE THRESHOLD, THRSH
C     THRSH = SQRT(U/AVGF)*ATOP

C     START A SWEEP
C     115 IFLAG=0
      DO 130 JCUL=2,N
      JCCL1=JCUL-1
      DO 130 IRUW=1,JCUL1
      AIJ=A(IRUW,JCUL)

C     COMPARE THE OFF-DIAGONAL ELEMENT WITH THRSH
C     IF(ABS(AIJ)-THRSH)130,130,117
C     117 AII=A(IRUW,IRUW)
      AJJ=A(JCUL,JCUL)
      S=AJJ-AII

C     CHECK TO SEE IF THE CHOSEN ROTATION IS LESS THAN THE ROUNDING ERROR.
C     IF SO , THEN DO NOT ROTATE.
C     IF(ABS(AIJ)-1.E-09*ABS(S))130,130,118
C     118 IFLAG=1

C     IF THE ROTATION IS VERY CLOSE TO 45 DEGREES, SET SIN AND COS
C     TO 1/(ROOT 2).
C
```

```
IF (1.E-10*ABS(AIJ)-ABS(S))116,119,119
115 S=.707106781
C=S
GC TO 120
C
C CALCULATION OF SIN AND COS FOR ROTATION THAT IS NOT VERY CLOSE
C TO 45 DEGREES
C
116 T=AIJ/S
S=C.25/SQRT(0.25+T*T)
C
C COS = C , SIN= S
C
C G=SQRT(0.5+S)
S=2.*T*S/C
C
C CALCULATION OF THE NEW ELEMENTS OF MATRIX A
C
120 DC 121 I=1,IR0W
T=A(I,IR0W)
U=A(I,JC0L)
A(I,IR0W)=C*T-S*U
121 A(I,JC0L)=S*T+C*U
I2=IR0W+2
IF(I2-JC0L)127,127,123
127 CONTINUE
DO 122 I=I2,JC0L
T=A(I-1,JC0L)
U=A(IR0W,I-1)
A(I-1,JC0L)=S*U+C*T
122 A(IR0W,I-1)=C*U-S*T
123 A(JC0L,JC0L)=S*A(IJ+C*AJJ)
A(IR0W,IR0W)=C*A(IR0W,IR0W)-S*(C*AIJ-S*AJJ)
DO 124 J=JC0L,N
T=A(IR0W,J)
U=A(JC0L,J)
A(IR0W,J)=C*T-S*U
124 A(JC0L,J)=S*T+C*U
C
C ROTATION COMPLETED.
C SEE IF EIGENVECTORS ARE WANTED BY USER
C
IF(IEGEN) 126,131,126
131 DO 125 I=1,N
T=EIVR(I,IR0W)
EIVR(I,IR0W)=C*T-EIVR(I,JC0L)*S
125 EIVR(I,JC0L)=S*T+EIVR(I,JC0L)*C
C
C CALCULATE THE NEW NORM D AND COMPARE WITH DSTOP
C
126 CONTINUE
S=AIJ/AT0P
D=L-S*S
IF(D-DSTOP)1200,129,129
C
C RECALCULATE DSTOP AND THRSH TO DISCARD ROUNDING ERRORS
C
1260 D=C.
DO 128 JJ=2,N
DC 128 II=2,JJ
S=A(II-1,II)/AT0P
128 D=S*S+D
```



```
USTCP=(1.E-06)*U
129 THRSR=SQRT(U/AVGF)*ATUP
13C CONTINUE
    IF(IFLAG)115,134,115
134 RETURN
    END
```

```
      SUBROUTINE ANIH ( NA, NB, N, SPIN )
      COMMON H(50, 50), HH(50, 50), G(50, 50), A(50, 50),
1         B(50, 50), Z(50), ALPHA(50, 50), BETA(50, 50),
2         RHO(50,50), ANAME(8), P(50,50), Q(50,50), U(50,50),
3         ASAP(50,50), ASAQ(50,50), ASARHO(50), AAP(50,50), AAQ(50,50),
4         AARHO(50), AARA(50), SDRHO(50),
5         PQ(50,50), QP(50,50), PQP(50,50), QPQ(50,50), PQPQ(50,50),
6         QPQP(50,50), PQPQP(50,50), QPQPQ(50,50)
      CALL MULT (P, Q, N, PQ)
      CALL MULT (Q, P, N, QP)
      CALL MULT (PQ, P, N, PQP)
      CALL MULT (QP, Q, N, QPQ)
      CALL MULT (PQP, Q, N, PQPQ)
      CALL MULT (QPQ, P, N, QPQP)
      CALL MULT (PQPQ, P, N, PQPQP)
      CALL MULT (QPQP, Q, N, QPQPQ)
      CALL TRAC(PQ, N, TRPQ)
      CALL TRAC(QPQP, N, TRPQPQ)
      EN = FLUAT(N)
      BNA = FLUAT(NA)
      ENB = FLUAT(NB)
      C XND = (SPIN + 1.0)*(SPIN + 2.0) - 0.25*(BNA - BNB)**2
      1 - 0.5*(BNA + BNB) + TRPQ
      DO 701 I = 1, N
      II = I
      DO 701 J = 1, N
      JJ = J
      ASAP(I,J) = P(I,J) - (PQP(I,J) - 0.5*(PQ(I,J) + QP(I,J)))/XND
      ASAQ(I,J) = Q(I,J) - (QPQ(I,J) - 0.5*(PQ(I,J) + QP(I,J)))/XND
      IF(II-JJ) 701, 703, 7C1
7C3 ASARHO(I) = ASAP(I,I) - ASAQ(I,I)
7C1 CONTINUE
      AN = BNB - 2.0*(SPIN + 1.0)
      C ANORM = AN**2 + (2.0 - 2.0*AN - BN)*TRPQ + BNA*BNB
      1 + 2.0*(TRPQ**2 - TRPQPQ)
      C FCGP = (AN**2 + (3.0 - BN - 2.0*AN)*TRPQ + BNA*BNB - BNB
      1 + 2.0*(TRPQ**2 - TRPQPQ))/ANORM
      PCQP = (BNA - TRPQ)/ANORM
      FCGQP = (BN - 4.0*TRPQ - 3.0 + 2.0*AN)/ANORM
      FCGAPQ = (2*TRPQ - BNA + 1.0 - AN)/ANORM
      C QCOQ = (AN**2 + (3.0 - BN - 2.0*AN)*TRPQ + BNA*BNB - BNA
      1 + 2.0*(TRPQ**2 - TRPQPQ))/ANORM
      CLCP = (BNB - TRPQ)/ANORM
      CCOQPQ = FCGQP
      CCGAPQ = (2.0*TRPQ - BNB + 1.0 - AN)/ANORM
      DO 704 I = 1, N
      II = I
      DO 704 J = 1, N
      JJ = J
```

```
C AAP(I,J) = PCOP*P(I,J) + PCOQ*Q(I,J) + QPQ(I,J)/ANORM
1   + PCOPQ*PQP(I,J) + PCOAPQ*(PQ(I,J) + QP(I,J))
2   - 2.0*(PQPQ(I,J) + QPQP(I,J) - 2.0*PQPQP(I,J))/ANORM
C AAQ(I,J) = QCOQ*Q(I,J) + QCOP*P(I,J) + PQP(I,J)/ANORM
1   + QCOQPQ*QPQ(I,J) + QCOAPQ*(PQ(I,J) + QP(I,J))
2   - 2.0*(PQPQ(I,J) + QPQP(I,J) - 2.0*QPQPQ(I,J))/ANORM
IF (II-JJ) 704, 706, 704
7C6 AARHO(I) = AAP(I,I) - AAQ(I,I)
7C4 CONTINUE
C XNORM = (SPIN + 1.0)*(SPIN + 2.0) - 0.25*(BNA - BNB)**2
1   - 0.5*BN + TRPQ
CO 707 I = 1, N
7C7 AAKA(I) = P(I,I) - Q(I,I) - 2.0*(PQP(I,I) - QPQ(I,I))/XNORM
RETURN
END
```

```
SUBROUTINE MULT(X, Y, N, XY)
DIMENSION X(50,50), Y(50,50), XY(50,50)
DO 801 I = 1, N
DO 801 J = 1, N
XY(I,J) = 0.000
DO 801 L = 1, N
8C1 XY(I,J) = XY(I,J) + X(I,L)*Y(L,J)
RETURN
END
```

```
SUBROUTINE TRAC(X, N, TRX)
DIMENSION X(50,50)
TRX = 0.0
DO 901 I = 1, N
9C1 TRX = TRX + X(I,I)
RETURN
END
```

APPENDIX III

USCF Calculation of Spin Densities in the
Pyridine-N-Oxide Radical Anion: Parameter Variation

| Parameters | | | Positions | | | | |
|------------|--|--------------|-------------|----------|----------|----------|----------|
| Z_N | $\left. \begin{matrix} \delta_O \\ \delta_N \end{matrix} \right\}$ | β_{NO} | ρ_{ox} | ρ_N | ρ_2 | ρ_3 | ρ_4 |
| 1.0 | 6.25 | 1.0 | .312 | .325 | -.002 | .054 | .257 |
| | 1.25 | 1.2 | .350 | .327 | -.018 | .061 | .238 |
| | 6.25 | 1.0 | .534 | .211 | .024 | .019 | .168 |
| | 2.50 | 1.2 | .546 | .225 | .012 | .023 | .159 |
| | 8.33 | 1.0 | .043 | .337 | .076 | .038 | .390 |
| | 1.25 | 1.2 | .062 | .349 | .060 | .046 | .379 |
| | 8.33 | 1.0 | .038 | .214 | .173 | -.008 | .418 |
| | 2.50 | 1.2 | .055 | .226 | .159 | -.004 | .408 |
| 2.0 | 1.67 | 1.0 | .032 | .223 | -.066 | .208 | .460 |
| | 4.17 | 1.2 | .036 | .181 | -.061 | .218 | .469 |
| | 1.67 | 1.0 | .179 | .478 | -.029 | .070 | .262 |
| | 6.25 | 1.2 | .208 | .451 | -.041 | .080 | .263 |
| | 2.50 | 1.0 | .022 | .261 | -.069 | .200 | .453 |
| | 4.17 | 1.2 | .026 | .222 | -.065 | .210 | .463 |
| | 2.50 | 1.0 | .096 | .531 | -.014 | .062 | .276 |
| | 6.25 | 1.2 | .122 | .512 | -.026 | .071 | .276 |
| 1.5 | 3.33 | 1.0 | .244 | .354 | -.064 | .114 | .300 |
| | 2.90 | 1.2 | .261 | .328 | -.073 | .126 | .304 |
| | 3.33 | 1.0 | .675 | .192 | -.015 | .027 | .110 |
| | 5.00 | 1.2 | .654 | .212 | -.021 | .031 | .115 |

APPENDIX III - Continued

| Parameters | | Positions | | | | | |
|------------|---|--------------|-------------|----------|----------|----------|----------|
| Z_N | $\left. \begin{array}{l} \delta_0 \\ \delta_N \end{array} \right\}$ | β_{NO} | ρ_{ox} | ρ_N | ρ_2 | ρ_3 | ρ_4 |
| 1.5 | | | | | | | |
| | 5.40 | 1.0 | --- | --- | --- | --- | --- |
| | 2.90 | 1.2 | .068 | .441 | -.038 | .107 | .352 |
| | 5.40 | 1.0 | .075 | .296 | .122 | .004 | .378 |
| | 5.00 | 1.2 | .107 | .316 | .100 | .011 | .355 |

APPENDIX IV

McLachlan Approximate Spin Densities for Nitrosobenzene
Type Radical Anions: Parameter Variations

| Parameters | | Radical Anions (a) | Positions (b) | | | | |
|--------------|------------|--------------------|---------------|----------|-----------------|------------------|----------|
| β_{NO} | δ_O | | ρ_{ox} | ρ_N | ρ_O | ρ_m | ρ_p |
| β_{CN} | δ_N | A | .238 | .393 | .139 | -.042 | .166 |
| | | B | .241 | .411 | .142 | -.047 | .163* |
| | 1.45 | C | .231 | .403 | .145* | -.038 | .170 |
| | 0.50 | D | .235 | .398 | [.159 .122*] | [-.049 -.029] | .167 |
| 1.5 | | | | | | | |
| | | A | .359 | .286 | .120 | -.036 | .157 |
| 1.0 | 0.95 | B | .362 | .304 | .124 | -.041 | .153* |
| | 0.70 | C | .348 | .301 | .126* | -.032 | .161 |
| | | D | .354 | .293 | [.141 .104*] | [-.043 -.022] | .158 |
| | | | | | | | |
| | | A | .312 | .337 | .140 | -.044 | .160 |
| | 1.10 | B | .313 | .355 | .143 | -.048 | .157* |
| | 0.62 | C | .298 | .350 | .146* | -.040 | .166 |
| | | D | .306 | .344 | [.160 .124*] | [-.050 -.032] | .162 |
| 1.4 | | | | | | | |
| | | A | .419 | .221 | .120 | -.037 | .159 |
| 1.1 | 0.70 | B | .420 | .239 | .125 | -.042 | .156* |
| | 0.70 | C | .400 | .238 | .128* | -.033 | .166 |
| | | D | .410 | .230 | [.143 .104*] | [-.045 -.023] | .161 |
| | | | | | | | |
| | | A | .308 | .335 | .141 | -.044 | .163 |
| 1.5 | 1.20 | B | .310 | .352 | .144 | -.048 | .159* |
| 1.1 | 0.70 | C | .296 | .347 | .146* | -.040 | .167 |
| | | D | .303 | .341 | [.161 .125*] | [-.050 -.032] | .164 |

Appendix IV (continued)

| Parameters | | Radical Anions | Positions | | | | | |
|--------------|------------|----------------|-------------|----------|-----------------|------------------|----------|-------|
| β_{NO} | δ_O | | ρ_{ox} | ρ_N | ρ_O | ρ_m | ρ_p | |
| 1.5 | 0.80 | A | .414 | .226 | .120 | -.037 | .161 | |
| | | B | .415 | .246 | .126 | -.043 | .156* | |
| | | 1.1 | C | .396 | .244 | .129* | -.034 | .165 |
| | | D | .405 | .236 | [.144 .105*] | [-.046 -.024] | .161 | |
| 1.6 | 0.80 | A | .317 | .321 | .139 | -.043 | .164 | |
| | | 1.25 | B | .320 | .338 | .143 | -.048 | .160* |
| | | C | .305 | .334 | .145* | -.039 | .168 | |
| | | D | .312 | .328 | [.160 .123*] | [-.050 -.030] | .165 | |
| 1.1 | 0.94 | A | .402 | .246 | .123 | -.038 | .157 | |
| | | B | .405 | .263 | .128 | -.043 | .154* | |
| | | C | .388 | .260 | .130* | -.033 | .174 | |
| | | D | .395 | .253 | [.145 .107*] | [-.045 -.022] | .159 | |
| 1.4 | 0.87 | A | .380 | .250 | .139 | -.043 | .167 | |
| | | B | .378 | .268 | .144 | -.048 | .165* | |
| | | 1.2 | C | .357 | .266 | .148* | -.040 | .174 |
| | | D | .369 | .258 | [.161 .123*] | [-.050 -.031] | .170 | |
| 1.5 | 1.08 | A | .372 | .291 | .141 | -.046 | .157 | |
| | | B | .372 | .308 | .145 | -.050 | .153* | |
| | | 1.2 | C | .352 | .305 | .148* | -.042 | .163 |
| | | D | .363 | .298 | [.162 .124*] | [-.052 -.034] | .159 | |

Appendix IV (continued)

| Parameters | | Radical Anions | Positions | | | | |
|--------------|------------|----------------|-------------|----------|----------------|-----------------|----------|
| β_{NO} | δ_O | | ρ_{ox} | ρ_N | ρ_O | ρ_m | ρ_p |
| β_{CN} | δ_N | A | .463 | .159 | .120 | -.036 | .165 |
| 1.5 | 0.60 | B | .464 | .175 | .125 | -.042 | .164* |
| 1.2 | 0.90 | C | .441 | .175 | .128* | -.033 | .174 |
| | | D | .452 | .167 | [.144 .102* | [-.045 -.022 | .169 |
| | | A | .378 | .278 | .140 | -.045 | .158 |
| 1.6 | 1.12 | B | .379 | .295 | .144 | -.049 | .155* |
| 1.2 | 1.00 | C | .360 | .292 | .147* | -.041 | .165 |
| | | D | .370 | .285 | [.161 .124* | [-.051 -.033 | .161 |

(a) A = Nitrosobenzene, B = p-Nitrosotoluene, C = 2-Nitroso-m-xylene
D = O-Nitrosotoluene

(b) starred quantities denote ρ_t for a methyl group: $\rho_t = \rho_C + \rho_C' + \rho_H$

REFERENCES

1. (a) D. H. Levy and R. J. Myers, *J. Chem. Phys.* 41, 1062 (1964);
(b) D. H. Levy, Ph.D. Thesis, The Electron Spin Resonance Studies of Radical Anions in Liquid Ammonia, Lawrence Radiation Laboratory Report, UCRL-11864, January 1965.
2. For more general and complete information on ESR studies the following books and reviews are useful:
 - (a) A. Carrington and A. D. McLachlan, Introduction to Magnetic Resonance, (Harper and Row, Publishers, New York, 1967).
 - (b) S. A. Al'tshuler and B. N. Kozyrev, Electron Paramagnetic Resonance, (Academic Press, New York, 1964).
 - (c) D. E. Ingram, Free Radicals as Studied by Electron Spin Resonance, (Butterworth Scientific Publications, London, 1958).
 - (d) A. Carrington, *Quart. Rev.*, 17, 67 (1963).
 - (e) D. Kivelson and C. Thomson, *Ann. Rev. Phys. Chem.*, 15, 197 (1964).
 - (f) A. G. Shulman, *ibid.* 13, 325 (1962).
 - (g) S. I. Weissman, *ibid.* 12, 151 (1961).
 - (h) R. Bersohn, *ibid.* 11, 369 (1960).
 - (i) G. K. Fraenkel and B. Segal, *ibid.* 10, 435 (1959).
3. D. Lipkin, D. E. Paul, J. Townsend, and S. I. Weissman, *Science*, 117, 534 (1953); S. I. Weissman, J. Townsend, G. E. Pake, and D. E. Paul, *J. Chem. Phys.* 21, 2227 (1953); T. L. Chu, G. E. Pake, D. E. Paul, J. Townsend, and S. I. Weissman, *J. Phys. Chem.* 57, 504 (1953).
4. G. Fraenkel and B. Venkataraman, *J. Am. Chem. Soc.* 77, 2707 (1955); G. Fraenkel and B. Venkataraman, *J. Chem. Phys.* 23, 588 (1955); *ibid.*, 24, 737 (1956).

5. (a) E. DeBoer and S. I. Weissman, *J. Am. Chem. Soc.* 80, 4549 (1958).
(b) T. R. Tuttle, Jr., and S. I. Weissman, *J. Am. Chem. Soc.* 80, 5342 (1958).
6. D. E. G. Austen, P. H. Given, D. J. F. Ingram and M. F. Peover, *Nature*, 182, 1784 (1958).
7. A. H. Maki and D. H. Geske, *J. Chem. Phys.* 30, 1356 (1959); *Anal. Chem.* 31, 1450 (1959); D. H. Geske and A. H. Maki, *J. Am. Chem. Soc.* 82, 2671 (1960).
8. L. H. Piette, P. Ludwig and R. N. Adams, *J. Am. Chem. Soc.* 83, 3909 (1961).
9. P. H. Rieger, I. Bernal, W. H. Reimuth and G. K. Fraenkel, *J. Am. Chem. Soc.* 85, 683 (1963).
10. A. Carrington and J. dos Santos-Viega, *Mol. Phys.* 5, 21 (1962).
11. (a) R. L. Ward, *J. Am. Chem. Soc.* 83, 3623 (1961).
(b) *ibid.* 84, 332 (1962).
12. K. H. Hausser, A. Habich, and V. Franzen, *Z. Naturforsch.* 16a, 836 (1961).
13. J. C. M. Henning, *J. Chem. Phys.* 44, 2139 (1966).
14. I. Bernal, P. H. Reiger and G. K. Fraenkel, *J. Chem. Phys.* 37, 2811 (1962).
15. E. Brunner and F. Foerr, *Ber. Bunsenges. Physik. Chem.* 68, 468 (1964).
16. P. B. Ayscough and F. P. Sargent, *Proc. Chem. Soc.* 1963, 94.
17. W. T. Dixon and R. O. C. Norman, *Proc. Chem. Soc.* 1963, 97.
18. P. K. Kolker and W. A. Waters, *Proc. Chem. Soc.* 1963, 55; *J. Chem. Soc. (London)* 1964, 1136.
19. M. H. L. Pryce, *Proc. Phys. Soc.* A63, 25 (1950).
20. A. Abragam and M. H. L. Pryce, *Proce. Roy. Soc.* 205A, 135 (1951).

21. B. Bleaney and K. W. H. Stevens, Rep. Prog. Phys. 16, 108 (1953).
22. G. E. Pake, Paramagnetic Resonance, (Benjamin, New York, 1962). Chap. 3.
23. A. J. Stone, Proc. Roy. Soc. 271A, 424 (1963).
24. J. S. Griffiths, Mol. Phys. 3, 79 (1960).
25. S. I. Weissman, J. Chem. Phys. 22, 1135 (1954).
26. R. G. Parr, Quantum Theory of Molecular Electronic Structure, (W. A. Benjamin, Inc., New York, 1963) Chap. 3 and reprints section.
27. J. Malrieu, J. Chem. Phys. 46, 1954 (1967).
28. G. Giacometti and G. Orlandi, Theoret. Chim. Acta. 3, 337 (1965).
29. T. Amos and L. C. Snyder, J. Chem. Phys. 41, 1773 (1964), and references cited therein.
30. a) H. M. McConnell, J. Chem. Phys. 24, 764 (1956).
b) H. M. McConnell and D. B. Chesnut, *ibid.* 28, 107 (1958).
31. S. I. Weissman, J. Chem. Phys. 25, 890 (1956).
32. A. D. McLachlan, H. H. Dearman, and R. Lefebvre, J. Chem. Phys. 33, 65 (1960).
33. M. Karplus and G. K. Fraenkel, J. Chem. Phys. 35, 1312 (1961).
34. A. Streitwieser, Molecular Orbital Theory, (John Wiley and Sons, Inc., New York, 1961).
35. A. D. McLachlan, Mol. Phys. 3, 233 (1960).
36. C. C. J. Roothaan, Rev. Mod. Phys. 32, 179 (1960).
37. O. W. Adams and P. G. Lykos, J. Chem. Phys. 34, 1444 (1961).
38. T. Amos and L. C. Snyder, J. Chem. Phys. 42, 3670 (1965).
39. A. Carrington and H. C. Longuet-Higgins, Mol. Phys. 5, 447 (1962).
40. J. C. M. Henning and C. de Waard, Phys. Letters 3, 139 (1962).
41. E. DeBoer and E. L. Mackor, J. Chem. Phys. 38, 1450 (1963).

42. G. A. Russell et al. *Advan. Chem. Ser.* 51, 112 (1965).
43. F. C. Adams and S. I. Weissman, *J. Am. Chem. Soc.* 80, 2057 (1958).
44. N. M. Atherton and S. I. Weissman, *J. Am. Chem. Soc.* 83, 1330 (1961).
45. (a) N. M. Atherton and A. E. Goggins, *Trans. Farad. Soc.* 61, 1399 (1965).
(b) *ibid.* 62, 1702 (1966).
46. R. Chang and C. S. Johnson, *J. Chem. Phys.* 46, 2314 (1967).
47. J. M. Fritsch, T. P. Layloff, and R. N. Adams, *J. Am. Chem. Soc.* 87, 1724 (1965).
48. A. H. Maki and D. H. Geske, *J. Am. Chem. Soc.* 83, 1852 (1961);
A. H. Maki, *J. Chem. Phys.* 35, 761 (1961).
49. R. Chang and S. S. Johnson, Jr., *J. Chem. Phys.* 41, 3272 (1964).
50. E. J. Geels, R. Konaka, and G. A. Russell, *Chem. Comms.* 1965, 13.
51. G. A. Russell and E. J. Geels, *J. Am. Chem. Soc.* 87, 122 (1965).
52. W. M. Fox and W. A. Waters, *J. Chem. Soc.* 1965, 4628.
53. T. J. Katz and H. L. Strauss, *J. Chem. Phys.* 32, 1873 (1960);
T. J. Katz and C. Talcott, *J. Am. Chem. Soc.* 88, 4732 (1966).
54. K. Kuwata, T. Ogawa, and K. Hirota, *Bull. Chem. Soc. Japan* 34, 291 (1961).
55. V. V. Voevodski, S. P. Solodovnikov, and V. M. Chibrikin, *Doklady Akad. Nauk. S.S.S.R.* 129, 1082 (1959).
56. S. P. Solodovnikov, *J. Struct. Chem.* 2, 282 (1961).
57. K. Markau and W. Maier, *Z. Naturforsch.* 16a, 1116 (1961).
58. J. W. Dodd, F. J. Horton, and N. S. Hush, *Proc. Chem. Soc. (London)* 1962, 61 (1962).

59. (a) N. M. Atherton, F. Gerson, and J. N. Murrell, *Mol. Phys.* 5, 509 (1962).
(b) C. A. McDowell and K. F. G. Paulus, *Can. J. Chem.* 43, 224 (1965).
60. M. Itoh, T. Okamoto, and S. Nagakura, *Bull. Chem. Soc. Japan* 36, 1665 (1963).
61. D. H. Levy and R. J. Myers, *J. Chem. Phys.* 42, 3731 (1965).
62. P. B. Ayscough, F. P. Sargent, and R. Wilson, *J. Chem. Soc. (B)* 1966, 903; *ibid.* 907.
63. C. J. W. Gutch and W. A. Waters, *Proc. Chem. Soc.* 1964, 230.
64. A. I. Vogel, Practical Organic Chemistry, 3rd. Ed. (John Wiley and Sons, Inc., New York, 1957).
65. W. J. Mijs, S. E. Hoekstra, R. M. Ulmann, and E. Havinga, *Rec. Trav. Chim.* 77, 746 (1958).
66. M. Ishikawa and K. Tokuyama, *Ann. Rept. Shionogi Research Lab.*, (1963), p. 37-39; See C. A. 50, 14752c.
67. P. Réiger and G. K. Fraenkel, *J. Chem. Phys.* 39, 609 (1963).
68. E. J. Stone and A. H. Maki, *J. Chem. Phys.* 39, 1635 (1963).
69. D. H. Geske and G. R. Padmanabhan, *J. Am. Chem. Soc.* 87, 1651 (1965).
70. J. F. Mulligan, *J. Chem. Phys.*, 19, 347 (1951).
71. A. L. Sklar, *J. Chem. Phys.*, 7, 990 (1939).
72. H. J. Kopineck, *Z. Naturforsch.* 5a, 420 (1950).
73. M. Kotani, A. Ameniya, G. Ishiguro, and T. Kimura, Tables of Molecular Integrals, (Maruzen Co., Ltd., Tokyo, Japan, 1955).
74. H. Preuss, Integraltafel zur Quanten Chemie, (Springer-Verlag, Berlin, 1956).

75. C. C. J. Roothann, J. Chem. Phys. 19, 1445 (1951).
76. K. Rudenberg, J. Chem. Phys. 19, 1459 (1951).
77. (a) A. Lofthus, Mol. Phys., 5, 105 (1962).
(b) A. Lofthus, Mol. Phys., 6, 115 (1963).
78. I.B.M. SHARE program, Diatomic Integral Program, programmed by F. J. Corbato and A. C. Switendick, M.I.T. Computation Center.
79. H. Brion, C. Moser, and M. Yamazaki, J. Chem. Phys. 30, 673 (1959).
80. E. Tannenbaum, E. M. Coffin, and A. J. Harrison, J. Chem. Phys. 21, 311 (1953); D. P. Stevenson, G. M. Coppinger, and J. W. Forbes, J. Am. Chem. Soc. 83, 4350 (1961).
81. J. M. Gross and M. C. R. Symons, J. Chem. Soc. (A), 451 (1966).
82. J. Pannell, Mol. Phys., 7, 599 (1964).
83. R. Pariser and R. G. Parr, J. Chem. Phys. 21, 466, 767 (1953).
84. N. Mataga and K. Nishimoto, Z. fur Physik. Chem. N.F. 13, 140 (1957).
85. J. A. Pople, Trans. Farad. Soc. 49, 1375 (1953).
86. R. L. Miller, P. G. Lykos, and H. N. Schmeising, J. Am. Chem. Soc. 84, 4623 (1962).
87. A. Hinchliffe, Theoret. Chim. Acta (Ber.) 5, 208 (1966).
88. A. T. Amos and G. G. Hall, Proc. Roy. Soc. (London), A263, 483 (1961).
89. G. Berthier, J. Chim. Phys., 51, 363 (1954); 52, 141 (1955).
90. J. Pople and R. Nesbet, J. Chem. Phys., 22, 571 (1954).
91. L. C. Snyder and T. Amos, J. Chem. Phys. 42, 3670 (1965).
92. R. McWeeny, Proc. Royal Soc. A 237, 355 (1956).
93. (a) J. P. Colpa and J. R. Bolton, Mol. Phys. 6, 273 (1963).
(b) J. R. Bolton, Private communication to Ref. 91.
94. G. Giacometti, C. L. Nordio, M. V. Pavan, Theoret. Chem. Acta, 1, 404 (1963).

95. C. A. Coulson and V. A. Crawford, J. Chem. Soc. 1953, 2052 (1953).
96. A. D. McLachlan, Mol. Phys. 1, 233 (1958).
97. D. H. Levy, Mol. Phys. 10, 233 (1966).
98. E. Klingsberg, ed., Pyridine and Its Derivatives, Pt. I, (Interscience Publishers, Inc., New York, 1960), p. 53.
99. A. Zahlan, F. W. Heineken, M. Bruin, and F. Bruin, J. Chem. Phys. 37, 683 (1962).
100. J. dos Santos-Viega and A. F. Neiva-Correia, Mol. Phys. 9, 395 (1965).
101. N. M. Atherton, *ibid.*, 1707 (1966).
102. H. O. Pritchard and H. A. Skinner, Chem. Rev. 55, 745 (1955).
103. M. K. Orloff and O. Sinanoglu, J. Chem. Phys. 43, 49 (1965).
104. K. Nishimoto and L. Forester, Theoret. Chim. Acta (Ber.) 4, 155 (1966).
105. H. H. Jaffe, J. Am. Chem. Soc. 76, 3527 (1954).
106. R. A. Barnes, J. Am. Chem. Soc. 81, 1935 (1959).
107. G. Tsoucaris, J. Chim. Phys. 58, 41 (1961).
108. A. R. Katritsky and J. M. Lagowsky, J. Chem. Soc. 1961, 43.
109. Y. Hanyu and J. E. Boggs, J. Chem. Phys. 43, 3454 (1955).
110. Y. Nakai, Bull. Chem. Soc., Japan 39, 1372 (1966).
111. A. Van Veen, P. E. Verkade, and B. M. Wepster, Rec. Trav. Chem. 76, 801 (1957).
112. P. H. Rieger and G. K. Fraenkel, J. Chem. Phys. 37, 2811 (1962).
113. E. W. Stone and A. H. Maki, J. Chem. Phys. 38, 1999 (1963).
114. K. Tabei and S. Nagakura, Bull. Chem. Soc. Japan, 38, 965 (1965).
115. B. C. Gilbert, R. O. C. Norman, and D. C. Price, Proc. Chem. Soc. 1964, 234.
116. J. Gendell, J. H. Freed, and G. K. Fraenkel, J. Chem. Phys. 37, 2832 (1962).

This report was prepared as an account of Government sponsored work. Neither the United States, nor the Commission, nor any person acting on behalf of the Commission:

- A. Makes any warranty or representation, expressed or implied, with respect to the accuracy, completeness, or usefulness of the information contained in this report, or that the use of any information, apparatus, method, or process disclosed in this report may not infringe privately owned rights; or
- B. Assumes any liabilities with respect to the use of, or for damages resulting from the use of any information, apparatus, method, or process disclosed in this report.

As used in the above, "person acting on behalf of the Commission" includes any employee or contractor of the Commission, or employee of such contractor, to the extent that such employee or contractor of the Commission, or employee of such contractor prepares, disseminates, or provides access to, any information pursuant to his employment or contract with the Commission, or his employment with such contractor.

